Universidade Federal do Rio Grande do Sul

Instituto de Ciências Básicas da Saúde

Departamento de Bioquímica Professor Tuiskon Dick

Programa de Pós-Graduação em Ciências Biológicas: Bioquímica

Marcelo Sartori Grunwald

A interação diferencial da proteína de choque térmico de 70kDa com o receptor dos produtos finais de glicação avançada e toll-like 4 – uma relação com suas diferentes conformações e com o estado redox

Porto Alegre

2017

Universidade Federal do Rio Grande do Sul

Instituto de Ciências Básicas da Saúde

Departamento de Bioquímica Professor Tuiskon Dick

Programa de Pós-Graduação em Ciências Biológicas: Bioquímica

Tese apresentada ao Programa de Pós-graduação em Ciências Biológicas: Bioquímica da Universidade federal do Rio Grande do Sul, como requisito para obtenção do título de doutor em Ciências Biológicas: Bioquímica sob a orientação do Prof. Dr. José Cláudio Fonseca Moreira.

Porto Alegre

2017

CIP - Catalogação na Publicação

Grunwald, Marcelo
A interação diferencial da proteína de choque térmico de 70kDa com o receptor dos produtos finais de glicação avançada e toll-like 4 – uma relação com suas diferentes conformações e com o estado redox / Marcelo Grunwald. -- 2017.
88 f.

Orientador: José Cláudio Fonseca Moreira.

Tese (Doutorado) -- Universidade Federal do Rio Grande do Sul, Instituto de Ciências Básicas da Saúde, Programa de Pós-Graduação em Ciências Biológicas: Bioquímica, Porto Alegre, BR-RS, 2017.

1. HSP70. 2. RAGE. 3. TLR4. 4. Docking molecular. 5. Energia de interação. I. Fonseca Moreira, José Cláudio, orient. II. Título.

Elaborada pelo Sistema de Geração Automática de Ficha Catalográfica da UFRGS com os dados fornecidos pelo(a) autor(a).

Lista de Abreviaturas

ADP: adenosina difosfato

AGE: produto final de glicação avançada

APCs: células apresentadoras de antígenos

ATP: adenosina trifosfato

CAT: catalase

CD: cluster differentiation

DAMPs: damage associated molecular patterns

HMGB1: high mobility group box 1 protein

HSP70: heat shock protein 70

IFN-γ: interferon gama

IL: interleucinas

LPS: lipopolissacarídeo

MAPK: mitogen-activated protein kinase

MHC: major histocompability complex

MyD88: molécula adaptadora fator de diferenciação mielóide 88

NDB: nucleotide-binding domain

NF-κB: fator nuclear kappa B

oxHSP70: heat shock protein 70 oxidada

PAMPs: padrões moleculares associados à patógenos

PRRs: receptores de reconhecimento de padrões

RAGE: receptor dos produtos finais de glicação avançada

SBD: substrate-binding domain

SOD: superóxido dismutase

TLR2: receptor tipo toll 2

TLR4: receptor tipo toll 4

TNF-α: fator de necrose tumoral α

Resumo

A expressão da HSP70 intracelular está associada a efeitos citoprotetores contra uma variada gama de estímulos estressores e situações onde é comum que proteínas sofram ação de agentes oxidantes. A HSP70 foi recentemente detectada no meio extracelular, e sua presença tem sido associada a situações patológicas, nas quais ela exerce efeitos modulatórios sobre células do sistema imunológico. Para investigar a possível associação entre HSP70 oxidada e efeitos citoprotetores ou morte celular, macrófagos da linhagem RAW 264.7 foram incubados com HSP70 e HSP70 oxidada. Observamos que a oxidação da HSP70 alterou a estrutura da proteína; e que os macrófagos tratados com HSP70 oxidada apresentaram menor proliferação, maior produção de espécies reativas de oxigênio, menor atividade fagocítica e menor liberação de TNF-α. Estes resultados indicam que a oxidação da HSP70 extracelular modifica suas propriedades sinalizadoras, causando alterações na modulação das funções e da viabilidade dos macrófagos. Uma vez que estes resultados não concordam com as vias de sinalização ativadas classicamente por HSP70, via receptor TLR4, observamos uma nova interação com o receptor dos produtos finais de glicação avançada em um modelo de cultura de células A549 através de sondas fluorescentes. A quantificação do experimento mostrou um maior número de interações quando as células são tratadas com HSP70 na sua conformação ligada à ATP em comparação com o tratamento com HSP70 na sua conformação ligada à ADP; e, através de sucessivos experimentos de *docking* molecular propusemos um modelo putativo para a interação. Além disso, mostramos que na conformação ligada à ADP, a HSP70 interage preferencialmente com TLR4, de forma similar ao peptídeo MD-2, necessário para o reconhecimento de LPS, sugerindo que a chaperona atue como uma molécula acessória ou como citocina, dependendo do receptor e da situação patológica ou fisiológica.

Abstract

Expression of intracellular HSP70 is associated to cytoprotective effects against a wide range extent of stressful stimuli and conditions where is common to proteins to suffer the action of oxidative agents. HSP70 was recently detected in the extracellular medium and its presence in serum is commonly associated with pathological situations, where it exerts modulatory effects on cells of the immune system. To investigate the possible association between oxidized HSP70 and cytoprotection or cell death, we incubated RAW 264.7 macrophages with oxidized HSP70. We observed that the Oxidation of HSP70 altered its protein structure; and that macrophages treated with oxidized HSP70 presented lower proliferation, higher reactive oxygen species production, lower phagocytic activity and TNF-α release. These results indicate that oxidation of extracellular HSP70 modify its signaling properties, causing alterations on its modulatory effects on macrophage function and viability. As these results do not concur with the signaling pathways classically activated by HSP70, via TLR4, we observed a new interaction with the receptor for advanced glycation end products through fluorescent probes in a A549 cell culture model. Quantification of the experiment showed a higher number of interactions when cells are treated with HSP70 bound to ATP when compared to the treatment with HSP70 in the conformation ADP-bound; and, by successive molecular *docking* experiments, we proposed a putative model for such interaction. Moreover, we showed that on its ADP-bound conformation, HSP70 binds preferentially to TLR4, in a similar way as the peptide MD-2, necessary for the recognizing of LPS, suggesting that the chaperone could act as an accessory molecule or as a cytokine, depending on the receptor and physiological or pathological situation.

Sumário

Parte 1

1. Introdução

1.1. As proteínas de choque térmico – uma visão geral

As proteínas de choque térmico (*heat shock proteins – HSPs*) foram descritas em 1962 quando o pesquisador italiano Ferrucio Ritossa expos acidentalmente células de glândulas salivares de *Drosophila melanogaster* à uma situação de estresse térmico (Ritossa 1962). Classicamente conhecidas pela função de chaperonas moleculares dependentes de ATP, as proteínas de choque térmico transportam diversas proteínas intracelulares em células sob estresse ou em condições normais, auxiliando no correto dobramento e estabilização de peptídeos danificados. As proteínas de choque térmico são constituintes de uma família proteica extremamente conservada durante o curso da evolução, presentes em bactérias a mamíferos. As HSPs variam em tamanho, de 7 a 110 kDa, e podem ser encontradas em qualquer compartimento celular, incluindo núcleo, citoplasma e mitocôndrias. As nomenclaturas mais comuns para as proteínas de choque térmico fazem uso do seu peso molecular, como por exemplo em HSP70, na qual 70 corresponde ao peso molecular em kDa.

Algumas proteínas de choque térmico são expressas constitutivamente, como por exemplo a HSP90, enquanto outras possuem sua expressão aumentada rapidamente em resposta a um estresse celular. Durante os anos subsequentes à sua descoberta, diferentes estudos associaram a proteína a diversas formas de injúria, nas quais sua expressão é encontrada aumentada, como por exemplo, a indução da expressão de HSPs se mostrou associada à proteção de animais contra a síndrome da angústia respiratória aguda, choque séptico e lesões da isquemia-reperfusão (Ryan, Flanagan et al. 1992, Villar, Edelson et al. 1993, Yang and Lin 1999), processos inflamatórios, estresse oxidativo, exposição a metais pesados e agentes oxidantes (Wong, Ryan et al. 1997), sendo a elas atribuídas uma nova função de citoproteção, além da função de chaperona. Além disso, a superexpressão específica de HSP70 levou a proteção do

epitélio respiratório contra a morte celular mediada por hipóxia, peroxidação lipídica e depleção intracelular de ATP (Wong, Menendez et al. 1998).

Esse efeito citoprotetor observado é, principalmente, atribuído à capacidade que as proteínas de choque térmico têm de estabilizar estruturas proteicas através de interações reversíveis do tipo chaperona (Ribeiro, Villar et al. 1994). Observações clínicas mostram também que a expressão de HSP70 é induzida em pacientes com choque séptico, trauma ou síndrome da angústia respiratória aguda (Kindas-Mugge, Hammerle et al. 1993, Kindas-Mugge, Pohl et al. 1996).

Juntos esses dados demonstram uma função fundamental da HSP70: proteção a nível celular e tecidual contra processos patofisiológicos bastante frequentes nas unidades de terapia intensiva, sendo que a desregulação da resposta anti-inflamatória é uma característica comum a eles.

1.2 O papel da HSP70 extracelular

As proteínas de choque térmico encontram-se distribuídas em diversos compartimentos celulares, incluindo o citosol, núcleo e organelas membranosas, como a mitocôndria e o retículo endoplasmático; recentemente, achados científicos demonstraram sua presença no meio extracelular, particularmente após o estabelecimento de diversas condições patológicas (Campisi, Leem et al. 2003). Estudos realizados nos últimos anos mostraram que as HSPs podem ser produzidas e liberadas ativamente pelas células, possuindo a capacidade de interagir com outras células quando no meio extracelular. Primeiramente, acreditava-se que essa liberação para o meio extracelular ocorria somente em células necróticas após algum evento de estresse com consequente dano celular. Entretanto, a secreção de HSP70 ocorre na ausência da morte celular, através de um mecanismo não clássico. Aparentemente, essa proteína é translocada para a membrana celular e é então liberada por um processo ativo associado à membrana, o qual pode ser por exocitose ou evaginação inversa (Vega, Rodriguez-Silva et al. 2008). Após a translocação para a membrana plasmática e liberação para o meio extracelular, a

HSP70 é capaz de exercer efeitos modulatórios sobre células do sistema imunológico (Asea, Kabingu et al. 2000, Asea, Rehli et al. 2002, Gross, Holler et al. 2008), como por exemplo macrófagos, células dendríticas e células natural-killer através de um processo mediado por receptores. Além disso, a presença de HSP70 no meio extracelular ou no soro está associada a condições patológicas como processos inflamatórios, infecções virais e bacterianas, e processos tumorigênicos (Sherman and Multhoff 2007).

Em humanos, sabe-se que a HSP70 extracelular é liberada na circulação sistêmica pelo tecido cerebral e pelo tecido hepatoesplênico (Febbraio, Ott et al. 2002, Lancaster, Moller et al. 2004) mas não pelo tecido muscular (Febbraio, Steensberg et al. 2002). O exercício físico leva a uma indução da liberação da HSP70 extracelular, fato descrito primeiramente em um experimento no qual os participantes praticaram caminhada em esteira por 60 minutos a 70% da capacidade máxima de oxigênio (Walsh, Koukoulas et al. 2001). Depois disso, o aumento na expressão da HSP70 tem sido observado após a prática de exercícios prolongados e parece ser dependente da duração e da intensidade do exercício (Fehrenbach, Niess et al. 2005). Níveis aumentados de HSP70 extracelular têm sido observados na circulação de pessoas sedentárias após 1 hora de exercício moderado e intenso, junto com um aumento na quimiotaxia de neutrófilos e macrófagos e da capacidade microbicida dos neutrófilos (Ortega, Giraldo et al. 2006, Ortega, Hinchado et al. 2009), sugerindo que a HSP70 extracelular possui um importante papel na inflamação induzida pelo exercício e na modulação da resposta imunológica inata.

As proteínas de choque térmico extracelulares possuem a capacidade de iniciarem tanto a resposta imunológica inata quanto a resposta imunológica adquirida (Srivastava 2002, Johnson and Fleshner 2006). HSPs derivadas de patógenos ou HSPs derivadas das células do hospedeiro podem diretamente ativar ou aumentar a atividade de diversas células do sistema imunológico inato de produzir citocinas e quimiocinas (Tsan and Gao 2009). Essas proteínas possuem a

capacidade de promover a maturação e migração das células apresentadoras de antígenos (APCs), e subsequente interação com as células T (APC-T), iniciando assim uma resposta imunológica adaptiva. As HSPs podem ainda ligar a peptídeos antigênicos derivados de tumores ou de vírus, tanto que elas têm sido aplicadas como adjuvantes no desenvolvimento de vacinas.

De acordo com a teoria "sinal de perigo" ou "sinal de alerta" (*do inglês "danger signal theory"*), as células do sistema imunológico são ativadas por sinais de alerta derivados de células sob estresse ou por proteínas danificadas (Matzinger 2002). É aceito que a HSP70 extracelular se encaixa no critério de um sinal de alerta, pois ela possui a capacidade de desencadear a produção de citocinas pró-inflamatórias pelas APCs e uma resposta imune antígeno específico. Além de apresentar antígenos a células T durante situações de "alerta" metabólico, estando também relacionadas com a patogênese de diversas doenças autoimunes (Millar, Garza et al. 2003, Chen and Cao 2010).

Em um de nossos trabalhos relacionados à HSP70, nós avaliamos a relação entre o imunoconteúdo da HSP70 sérica e o estado oxidante na sepse. Pacientes com sepse severa foram monitorados por 28 dias após serem diagnosticados ou até o desfecho clínico. O soro desses pacientes apresentou elevados níveis de HSP70. Analisando os parâmetros oxidativos, foi possível observar que aqueles pacientes com pronunciado dano oxidativo também apresentaram maiores níveis de HSP70 sérica; enquanto que os pacientes sépticos com parâmetros oxidativos semelhantes aos controles apresentaram menores níveis de HSP70 sérica. Pacientes com maiores níveis de HSP70 no soro também apresentaram maior taxa de mortalidade, levando-nos à conclusão de que os níveis de HSP70 no soro estão sendo modulados de acordo com o estado oxidante do paciente, e de que níveis elevados de HSP70

no soro estão associados à elevada mortalidade na sepse (Gelain, de Bittencourt Pasquali et al. 2011) – **Anexo I**.

Sabemos que o soro de pacientes sépticos é capaz de induzir a ativação de macrófagos e a produção de interleucina-10; também sabemos que o índice fagocítico desses macrófagos está correlacionado com a severidade e com a mortalidade da doença (Peck, Andrades et al. 2009). Modelos murinos de sepse letal são caracterizados por apresentarem elevados níveis de carbonilação proteica e por apresentarem um desbalanço no sistema enzimático SOD/CAT quando comparados com o grupo não-letal, indicando que o estresse oxidativo é exacerbado no modelo letal (Andrades, Ritter et al. 2005). Assim, é bastante provável que diversas proteínas sejam oxidadas por espécies reativas e, consequentemente, tenham suas funções alteradas.

Porém, os trabalhos realizados até o momento não elucidam completamente os mecanismos ativados pela HSP70, sendo que eles diferem de acordo com o contexto celular e com o momento patológico; além disso, os mecanismos celulares responsáveis pelo reconhecimento, ou seja, os receptores que atuam na interação específica com a HSP70 extracelular também permanecem parcialmente conhecidos. Na maioria dos processos inflamatórios graves, ocorre uma perda no balanço entre elementos oxidantes e as defesas antioxidantes do organismo, caracterizando uma situação de estresse oxidativo. Sob essas condições, muitas proteínas sofrem a ação de espécies reativas de oxigênio, como o peróxido de hidrogênio (H_20_2), sendo oxidadas, alterando ou perdendo parcial ou totalmente suas funções. A HSP70 pode ser incluída entre elas; em teoria, as cisteínas dessa proteína podem formar ligações dissulfeto intramoleculares, intermoleculares com cisteínas de outras HSP70 ou até mesmo com outras proteínas, dando origem a diferentes e desconhecidos complexos. Além disso, a ligação de peptídeos antigênicos pela HSP70 é mais efetiva sob condições oxidantes quando comparada com condições redutoras; sendo que este fato é provavelmente causado pelo ganho de estruturas

secundárias (maior proporção de estruturas alfa hélices e beta-pregueadas em relação às estruturas aleatórias) em meio oxidante (Callahan, Chaillot et al. 2002). Juntos estes dados sugerem que esta proteína tenha um papel específico no que diz respeito ao fluxo de informações dentro do sistema imunológico durante uma situação de estresse.

1.3 Sinalização celular por RAGE e TLR4

Recentemente foi demonstrado que a HSP70 extracelular realiza uma ligação de alta afinidade com a membrana plasmática das APCs (células apresentadoras de antígeno), induz um rápido fluxo da [Ca^{2+}] intracelular, ativa o fator de transcrição NF-Kβ e causa um aumento na expressão das citocinas pró-inflamatórias TNF-α, IL-1β e IL-6, através de um processo dependente de CD-14 (Asea, Kraeft et al. 2000, He, Chen et al. 2000, Asea, Rehli et al. 2002), utilizando tanto o receptor Toll-like 2 (TLR2) quanto o receptor Toll-like 4 (TLR4).

A primeira linha de defesa contra agentes infecciosos, incluindo infecções virais e bacterianas, são as células do sistema imunológico inato, as quais apresentam receptores de reconhecimento de padrões (PRRs). Os PRRs tais como os Toll-like e CD14 são expressos como proteínas solúveis ou como proteínas de membrana que reconhecem estruturas molecular invariantes, chamadas de padrões moleculares associados ao patógeno (PAMPs).

Dentre as células do sistema imunológico que apresentam a capacidade de ligação à HSP70, encontram-se as células natural-killer (NK) (Gross, Schmidt-Wolf et al. 2003), APCs dendríticas (Asea, Rehli et al. 2002), macrófagos e monócitos periféricos (Asea, Kabingu et al. 2000, Asea, Kraeft et al. 2000), e linfócitos B (Arnold-Schild, Hanau et al. 1999). Sabe-se, atualmente, que essa interação é mediada pelos receptores TLR2 e TLR4 com seu cofator CD14 (Asea, Rehli et al. 2002), o receptor scavenger CD36 (Delneste, Magistrelli et al. 2002), e a molécula co-estimuladora CD40 (Becker 2002).

A ligação da HSP70 com TLR2 e TLR4 está associada à liberação e translocação nuclear do NF-kB. A ativação desse fator de transcrição é dependente de MyD88 quando apenas TLR2 ou apenas TLR4 reconhecem e ligam HSP70, e é independente de MyD88 quando a ligação e sinalização de TLR2 e TLR4 ocorre sinergisticamente. Além da ativação de NF-kB, essa rota de sinalização é caracterizada pela liberação de TNF-α, IL-1β, IL-6 e IL-12. Já a interação CD40-HSP70 parece ser mais importante nos linfócitos B, nas quais a ligação a transdução da sinalização ocorre pela fosforilação de p38, a qual pode levar a uma liberação de TNF-α e IFN-γ (Asea 2003).

Apesar de importantes, esses dados acerca da ligação e da sinalização desencadeada pela HSP70 extracelular não respondem todas as perguntas. Sabemos que células imunocompetentes têm a capacidade de ligar à HSP70 e que esta ligação resulta na sinalização do tipo chaperoquina (termo cunhado para atribuir características de citocinas a chaperonas, especialmente à HSP70), bastante importante na sobrevivência do hospedeiro à patógenos microbianos, mas não esclarece a relação dessa proteína com outros processos patológicos e com o agravamento destes (Asea 2003, Asea 2008).

No ano de 2010, Juan e colaboradores realizaram um experimento de varredura de supostos novos ligantes do receptor dos produtos finais de glicação avançada através de um experimento ELISA-like (Ruan, Li et al. 2010). Dentre os possíveis ligantes levantados no processo estava a HSP70. O RAGE é conhecido por ser um receptor multiligante, pertencente à família das imunoglobulinas (**figura 1**) transmembrana que atua como um receptor reconhecedor de padrões (*PRR, do inglês pattern recognition receptor*) do sistema imunológico inato. Este receptor foi inicialmente descrito com base na sua afinidade por produtos de glicação avançada (*AGEs, advanced glicatyon end products*) e posteriormente descobriu-se que ele é capaz de interagir uma gama de peptídeos endógenos não-glicados, tanto solúveis como ligados à

membrana, peptídeos envolvidos na defesa contra danos tecidual, infecções e processos inflamatórios; destacam-se a proteína HMGB1, as proteínas da família S100/calgranulinas e o LPS (Bucciarelli, Wendt et al. 2002). O aumento na expressão e ativação de RAGE afeta uma diversidade de condições patológicas, incluindo a diabetes e inflamação. A ligação de RAGE induz a ativação de múltiplas rotas de sinalização, que variam de acordo com o ligante, tipo celular e ambiente tissular e podem mediar respostas celulares distintas, como por exemplo a ativação de NF-kB e de MAPK estão entre as principais rotas ativadas por RAGE. Por fim, as rotas mencionadas podem ter como resultado a produção e liberação de citocinas pró-inflamatórias, ativação de proteases e o estabelecimento de situações de estresse oxidativo (Schmidt, Hofmann et al. 2000).

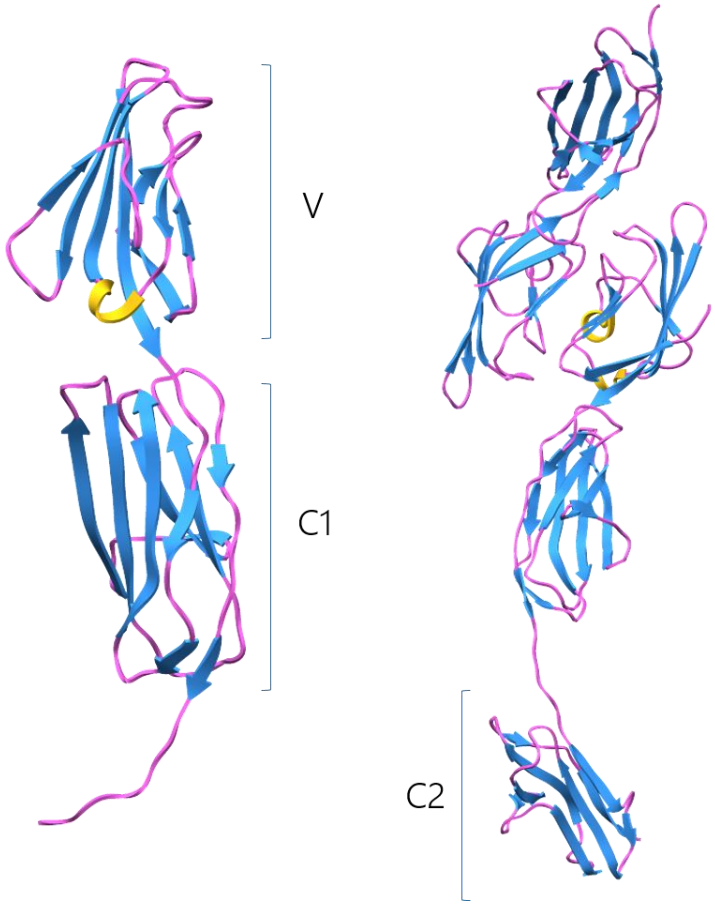

Figura 1. Representação da estrutura de RAGE com detalhe para suas diferentes regiões. À esquerda representação da forma solúvel e à direita representação da mais provável de ser encontrada na

membrana, formando oligômeros com outras moléculas do receptor. V = região variável (IgV), C1 = região constante 1 (IgC1) e C2 = região constante 2 (IgC2). PDB 3CJJ.

1.4 A estrutura tridimensional da HSP70

As proteínas de choque térmico possuem sua estrutura extremamente conservada, estão presentes em diferentes organismos, de bactérias a mamíferos. Em destaque, a HSP70 apresenta sua sequência de aminoácidos com aproximadamente 700 resíduos que formam uma proteína de 70-kDa composta por dois domínios distintos: um domínio N-terminal ligante de nucleotídeos (nucleotide binding domain-NBD), que apresenta atividade de ATPase, e um domínio C-terminal ligante de substrato/peptídeos (substrate binding domain-SBD), que por sua vez apresenta dois subdomínios, um bolso ligante de peptídeo formado predominantemente por estruturas B-pregueada, e uma tampa formada por alfa-hélices (**figura 2**).

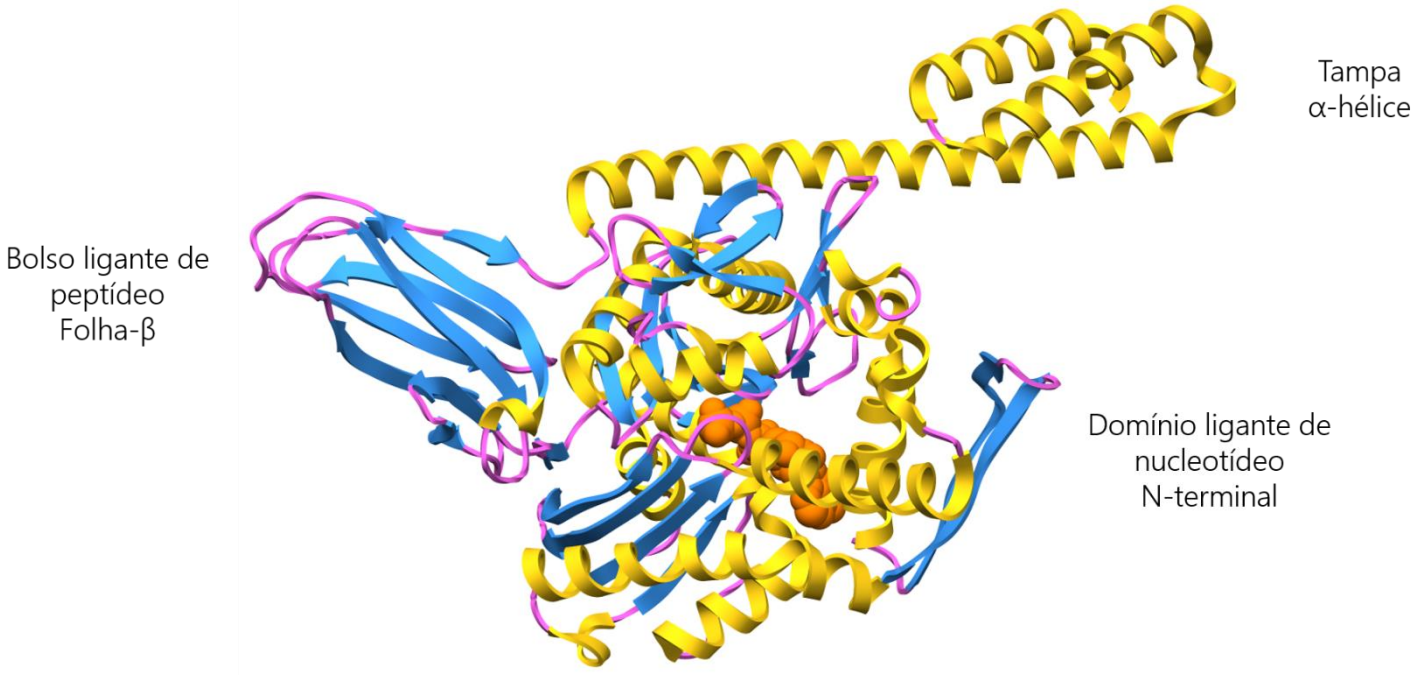

Figura 2. Visão geral da estrutura da HSP70 com detalhe para seus diferentes domínios. Estrutura colorida por estruturas secundárias, alfa-hélices representadas em amarelo, folhas beta em azul e alças em roxo. Molécula de ATP representada em laranja.

Quando a chaperona está ligada a uma molécula de ATP, a tampa está aberta, permitindo que o substrato adentre no bolso ligante de peptídeo. A molécula de ATP é então hidrolisada a ADP, a tampa se fecha fortemente sobre o substrato. Para que este seja liberado, a molécula de ADP deve ser substituída por uma de ATP, o que resulta na abertura da tampa de alfa-hélices. Quando um novo substrato peptídico é apresentado, o ATP é novamente hidrolisado, dando continuidade ao ciclo da chaperona (Sousa 2012) (**figura 3**).

Diversos estudos realizaram tentativas de atribuir os efeitos de citocina da HSP70 extracelular para o NBD ou para o SBD. A proteína recombinante oriunda de diferentes fontes é capaz de interagir e se ligar a diferentes sítios do receptor CD40 e através de diferentes porções; por exemplo, a HSP70 recombinante humana interage com o receptor através do domínio NBD, enquanto que a proteína homóloga de *Escherichia coli* (conhecida como DnaK) interage através do domínio SBD (Becker 2002). Em outro estudo hepatócitos tratados com um peptídeo truncado – correspondente ao SBD – apresentaram parâmetros de ativação aumentados quando comparados com as células tratadas com o peptídeo correspondente ao NBD (Galloway, Shin et al. 2008). Ademais, os efeitos celulares observados são aumentados quando os tratamentos são feitos com a proteína íntegra em comparação com somente um ou outro domínio. Essas diferenças podem ser atribuídas a interação diferencial da HSP70 com receptores distintos e em situações distintas, mas qualquer tentativa de elucidação é dificultada pela falta de dados estruturais a nível atômico, que descrevam a complexação da proteína com qualquer um dos seus possíveis receptores.

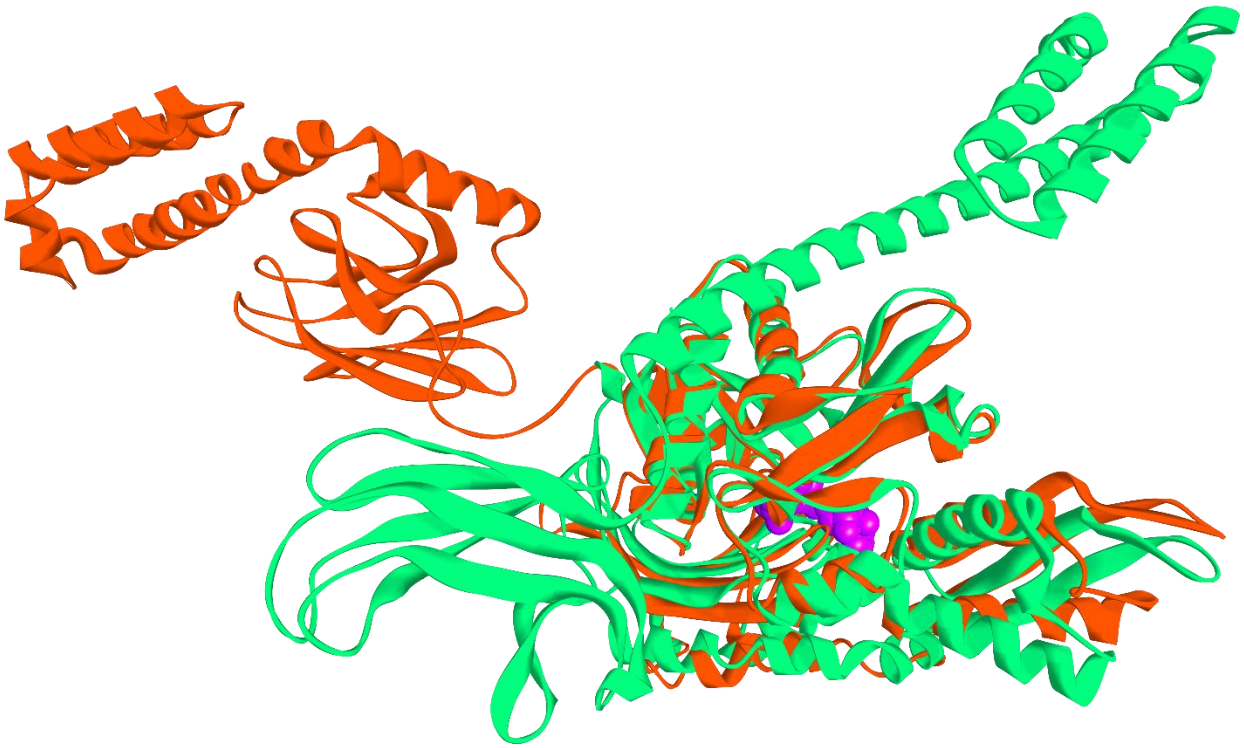

Figura 3. Visão geral do ciclo ATP/ADP e do impacto na mudança conformacional da HSP70. A estrutura em verde representa a HSP70 complexada a uma molécula de ATP, com a tampa fechada sobre o domínio ligante de peptídeos. A estrutura em laranja representa a HSp70 complexada a uma molécula de ADP, mais relaxa e aberta.

1.5 Modelos tridimensionais, atracamento molecular e análise de modos normais

Uma das formas mais racionais de se trabalhar com experimentos complexos acerca da estrutura de uma proteína e da interação física entre duas proteínas é realizar etapas prévias baseadas em modelos in silico, isto poupa tempo e principalmente recursos financeiros. Quando se trabalha com modelos tridimensionais é possível utilizar aqueles obtidos por determinação experimental, como cristalografia de raios-x e ressonância magnética nuclear, ou, na falta destes, utilizar modelos gerados por métodos preditivos com base na conservação estrutural de proteínas já conhecidas, ou estruturas molde. Ambos métodos resultam nos conhecidos arquivos PDB (*do inglês protein data bank*) que nada mais são do que representações

tridimensionais de uma determinada molécula dada pela posição geométrica do conjunto de átomos em um sistema de coordenadas cartesianas (x, y e z) ou de coordenadas internas, com informações sobre as ligações atômicas, seus comprimentos e ângulos. De modo geral, todas as estruturas obtidas por métodos físicos são depositadas em um banco de dados e disponibilizadas para a comunidade científica; estas estruturas podem ser utilizadas diretamente ou indiretamente, como moldes para a determinação de uma molécula de estrutura desconhecida.

Uma das aplicações mais comuns para as estruturas tridimensionais é o cálculo de atracamento ou encaixe molecular (em inglês conhecido como *molecular docking*, ou simplesmente *docking*, termo este que será utilizado nesta tese pois acreditamos que ambas traduções não satisfazem em questão de significado), que permite compreender boa parte dos mecanismos e processos celulares, uma vez que estes dependem da interação entre duas macromoléculas, sejam elas peptídeos e ácidos nucleicos, complexos agonista/antagonista ou substrato/inibidor. Neste trabalho utilizamos essa ferramenta para avaliar a possibilidade de interação entre a proteína ligante extracelular HSP70 e os receptores de membrana RAGE e TLR4. Este método é baseado na complementaridade de características físico-químicas e estruturais das moléculas que interagem, sendo que as interações intermoleculares formadas no processo definem a afinidade e especificidade da interação, como por exemplo ligações de hidrogênio, interações de van der Waals, iônicas, hidrofóbicas, entre outras. Dessa forma é possível calcular a contribuição individual de cada interação e, baseado no somatório das forças, estimar uma energia de ligação para o complexo formado, possibilitando a avaliação e comparação de complexos mais ou menos possíveis de serem formados ou de diferentes formas de formar um mesmo complexo, isso é, diferentes conformações para a mesma situação.

O método mais conhecido e amplamente utilizado para estudar o comportamento em função do tempo dos complexos formados por atracamento é a dinâmica molecular. Infelizmente,

complexos grandes são vítimas das limitações da metodologia: resultam em simulações computacionalmente custosas e permitem analisar movimentos atômicos na escala de nanosegundos apenas. Em contrapartida, a análise de modos normais permite estudar o complexo como uma oscilação harmônica e consequentemente, determinar todas as possíveis deformações sofridas em torno de um ponto de equilíbrio. Os modos de baixa frequência correspondem aos movimentos de caráter coletivo e estão relacionados com moções biológica e funcionalmente importantes.

2. Objetivos

2.1 Objetivo geral

A presente tese tem como objetivo evidenciar e caracterizar através de um ensaio in *vitro* os efeitos da proteína de choque térmico HSP70 oxidada sobre a modulação da ativação de macrófagos e, através de ensaios *in silico,* a interação dessa proteína com os seus possíveis receptores.

2.2 Objetivos específicos

(i). Mostrar as alterações estruturais ocasionadas pela ação do agente oxidante peróxido de hidrogênio sobre a HSP70;

(ii). Estudar os efeitos modulatórios da HSP70 sobre a ativação de macrófagos RAW 264.7;

(iii). Demonstrar a possibilidade de ligação entre as diferentes conformações de HSP70 e RAGE.

(iv). Qualificar e quantificar a interação entre as diferentes conformações de HSP70 e RAGE em modelo de cultura de células A549.

(v). Observar e caracterizar os modos de interação entre as diferentes conformações de HSP70 e o receptor TLR4.

(vi). Comparar as interações através dos complexos HSP70-RAGE e HSP70-TLR4 obtidos por *docking* molecular.

Parte 2

3. Resultados

Os resultados estão apresentados na forma de artigos publicados nos capítulos 1 e 2, e na forma de metodologia/resultados no capítulo 3

Capítulo 1

Artigo publicado na revista Cell Stress & Chaperones

“The oxidation of HSP70 is associated with functional impairment and lack of stimulatory capacity”

Cell Stress and Chaperones
DOI 10.1007/s12192-014-0516-5

ORIGINAL PAPER

The oxidation of HSP70 is associated with functional impairment and lack of stimulatory capacity

Marcelo Sartori Grunwald · André Simões Pires · Alfeu Zanotto-Filho · Juciano Gasparotto · Daniel Pens Gelain · Diogo Ribeiro Demartini · Cinthia Maria Schöler · Paulo Ivo Homem de Bittencourt Jr · José Cláudio Fonseca Moreira

Received: 4 October 2013 / Revised: 25 April 2014 / Accepted: 27 April 2014

Abstract Expression of intracellular HSP70 is associated with cytoprotective effects against a wide range of stressful stimuli, such as inflammation, oxidative stress, hypoxia, endotoxins, infections, and fever. This cytoprotective effect is mainly attributed to their ability to stabilize protein structures through chaperone-like reversible interactions. HSP70 was recently detected in the extracellular medium, and its presence in serum is commonly associated with pathological situations, where it exerts modulatory effects on cells of the immune system. Previously, we have described the relationship between serum HSP70 levels, oxidant status, and clinical outcome of septic patients; the group of patients with higher prooxidant status and higher serum HSP70 had also higher mortality. To investigate the possible association between oxidized HSP70 and cytoprotection or cell death, we incubated RAW 264.7 macrophages with oxidized HSP70 and evaluated nitrite production, cell proliferation, cell viability, TNF-α release, and phagocytic activity. We also evaluated structural modifications caused by oxidation in purified HSP70. Oxidation of HSP70 altered its protein structure; besides, the modulatory effect of oxidized HSP70 on RAW264.7 cells was different from that of native HSP70. Macrophages treated with oxidized HSP70 presented lower proliferation and viability, lower phagocytic activity, and lower TNF-α release. These results indicate that oxidation of extracellular HSP70 modified its signaling properties, causing alterations on its modulatory effects on macrophage function and viability.

Keywords HSP70 · Inflammation · Oxidative modifications · Macrophage activation

Introduction

Heat shock proteins (HSPs) were first described in 1962 when Ferrucio Ritossa accidentally exposed salivary gland cells to a heat shock (Ritossa 1962). They function as ATP-dependent molecular chaperones, transporting intracellular proteins in cells under stress and assisting the correct folding and stabilization of damaged proteins. Since then, these proteins have been associated with many other stressful stimuli, including inflammation and oxidative stress (Jaattela 1999; Lindquist and Craig 1988), gaining a new cytoprotective function. Up-regulation of intracellular HSP70 results in protective effects against hypoxia, excess oxygen radicals, endotoxins, and infections (Wong et al. 1997; Wong et al. 1998; Villar et al. 1994; Ryan et al. 1992). This cytoprotective effect is attributed to their ability to stabilize protein structures through chaperone-like reversible interactions (Ribeiro et al. 1994). Members of the heat shock superfamily have a highly conserved structure, being present from bacteria to mammals. HSP70 has an amino acid sequence constituted approximately by 700 residues that form a 70-kDa protein with two different domains: the nucleotide binding domain (NBD) and the

M. S. Grunwald (✉) · A. S. Pires · A. Zanotto-Filho · J. Gasparotto · D. P. Gelain · J. C. F. Moreira
Departamento de Bioquímica, Instituto de Ciências Básicas da Saúde, Universidade Federal do Rio Grande do Sul, Rua Ramiro Barcelos, 2600, Porto Alegre, Rio Grande do Sul CEP 90035-003, Brazil
e-mail: marcelo.sartori@yahoo.com.br

D. R. Demartini
Centro de Biotecnologia, Universidade Federal do Rio Grande do Sul, Porto Alegre, Rio Grande do Sul, Brazil

C. M. Schöler · P. I. H. de Bittencourt Jr
Departamento de Fisiologia, Instituto de Ciências Básicas da Saúde, Universidade Federal do Rio Grande do Sul, Porto Alegre, Rio Grande do Sul, Brazil

Published online: 10 May 2014

substrate binding domain (SBD). HSPs are distributed in diverse cell compartments, including the cytosol, nucleus, and membrane organelles. HSP70 has been observed to be translocated to the plasma membrane and released to extracellular environments, where they exert modulatory effects in cells of the immune system (Asea 2007; Asea et al. 2000, 2002); in addition, serum HSP70 is associated with stress conditions such as inflammation, bacterial or viral infections, and oncological diseases (Pittet et al. 2002; Pockley et al. 2003; Barreto et al. 2003).

In humans, extracellular HSP70 (eHSP70) is known to be released into the systemic circulation by the brain and hepatosplanchnic tissue (Lancaster et al. 2004; Walsh et al. 2001) but not by the contracting muscles (Febbraio et al. 2002) although physical exercise induces eHSP70 release, as it was first described in an experiment where subjects followed a 60-min treadmill at 70 % of maximal oxygen uptake (Walsh et al. 2001). After that, the upregulation of eHSP70 has been observed after prolonged exercise, which appears to rely on the duration and intensity of the exercise (Fehrenbach et al. 2005). Increased levels of eHSP70 have been reported in the circulation of sedentary people after 1 h of moderate and intensive exercise along with increased neutrophil microbicide capacity and chemotaxis (Ortega et al. 2006; Ortega et al. 2009), suggesting that eHSP70 plays an important role in exercise-induced inflammation and modulation of the innate immune response.

Extracellular HSPs can initiate both innate and adaptive immunity (Johnson and Fleshner 2006; Srivastava 2002). HSPs derived from pathogens or host cells can directly activate or enhance the activity of various innate immune cells to produce cytokines and chemokines (Chen and Cao 2010; Johnson and Fleshner 2006). These proteins promote maturation, migration of antigen-presenting cells (APC), and subsequent APC–T cell interaction, thus initiating the adaptive immune response. HSPs can also bind antigenic peptides derived from tumors or viruses and have been applied to vaccine development as adjuvants. According to the "danger signal," theory, immune cells are activated by alarm signals derived from stress or damaged self-proteins (Matzinger 2002). It is accepted that extracellular HSPs fit the criteria for danger signals as they can promote inflammatory cytokine production of APC and initiate antigen-specific immune responses, present antigens to T cells in a "danger" context, and have been linked to the pathogenesis of several autoimmune diseases (Chen and Cao 2010; Millar et al. 2003).

In a previous work of our group, we evaluated the relationship between serum HSP70 immunocontent and oxidant status in sepsis. Patients with severe sepsis were followed up for 28 days after diagnosis or until death. The serum of these septic patients presented augmented HSP70 levels. Analysis of oxidative parameters revealed that septic patients with pronounced oxidative damage in serum had also increased HSP70 levels, while septic patients with control-like serum oxidative parameters had lower HSP70 levels. Furthermore, an analysis of septic patients according to survival outcome indicated that those patients with higher HSP70 serum levels presented increased mortality, leading to the conclusion that the serum HSP70 levels are being modulated according to the patient oxidant status and increased serum HSP70 levels are associated with mortality in sepsis (Gelain et al. 2011).

It is known that the serum of septic patients is able to induce the activation of macrophages and the production of IL-10; also, the phagocytic indices of these macrophages were correlated with the severity and mortality of the disease (Peck et al. 2009). Murine models of lethal sepsis have higher protein carbonyl levels and an imbalance in SOD/CAT (superoxide dismutase/catalase) when compared with the nonlethal group, indicating that oxidative stress is exacerbated in the lethal model (Andrades et al. 2005). Thus, it is likely that several proteins related to an anti-inflammatory response undergo oxidation by reactive species and, consequently, their functions change.

Considering that we had previously demonstrated that sepsis is associated with redox imbalance and oxidative stress, the aim of this work was to investigate a possible relationship between previously oxidized HSP70 and the activation of macrophage cells.

Methods

Preparation of oxidized HSP70

The treatment used to oxidize HSP was briefly modified from Venereau et al. (2012). Purified bovine HSP70 was purchased from Sigma-Aldrich® (H9776). HSP70 was treated with different concentrations (1, 5, 10, 25, 50, and 100 mM) of the oxidizing agent hydrogen peroxide (H_2O_2) for 1 h at 37 °C under agitation and dialyzed before the addition to cells or other analyses to remove the excess of hydrogen peroxide. The final concentration of HSP70 used in all cell treatment experiments was 1 μg/mL.

Polyacrylamide gel electrophoresis

We added 4 μg of protein to 12 μL of H_2O_2 or Milli-Q water (for control), incubated the mixture at 37 °C for 1 h, and then maintained it at −20 °C for 20 min. Samples were mixed with 16 μL of nondenaturing buffer or denaturing buffer and loaded onto 12 % polyacrylamide gel. Electrophoresis followed for approximately 1 h. Gels were stained with Coomassie Blue and digitized.

For the alkylation experiment, 4 μg of HSP70 was previously treated with 10 mM of iodoacetamide for 30 min in the absence of light. After that, samples were lyophilized to

remove the alkylating agent and resuspended in Milli-Q water. Samples were treated with H_2O_2 for 1 h at 37 °C and maintained at −20 °C for 20 min. A nondenaturing buffer was utilized. Electrophoresis followed for approximately 1 h. Gels were stained with Coomassie Blue and digitized.

Cell culture line macrophage RAW 264.7

The exponentially growing macrophage-derived cell line RAW 264.7, obtained from the Rio de Janeiro Cell Bank (BCRJ, Rio de Janeiro, Brazil), was maintained in RPMI 1640 media supplemented with 10 % heat-inactivated fetal bovine serum (FBS), 2 mM of glutamine, 0.28 μg/μL of gentamicin, and 250 μg of amphotericin B, in a humidified atmosphere of 5 % of CO_2 in air at 37 °C. The cell medium was replaced every 2 days, and the cells were subcultured once they reached 90 % confluence. These cells were grown in plastic bottles and scrapped when they reached 70–90 % confluence, counted, and plated. Cells were seeded in 96-well plates for DCFH-DA, nitrite production, sulforhodamine B (SRB), and MTT (3-(4, 5-dimethylthiazol-2-yl)-2, 5-diphenyltetrazolium bromide) assays; in 24-well plates for phagocytosis assay; and in 6-well plates for TNF-α release assay. The concentration of HSP70 used in all cell treatment experiments was 1 μg/mL.

Nitrite assay

The accumulation of NO_2^-, a stable end product of NO formation, in conditioned media was measured as an indicator of NO production. Cells were seeded in a 96 well plate and then treated with oxidized HSP70 (oxHSP70) or nonoxidized HSP70 (HSP70). One hundred microliters of cell-free conditioned medium was transferred and incubated with 100 μL of Griess reagent at 37 °C for 15 min and the absorbance measured in a microplate reader at 540 nm (Li et al. 2002).

SRB assay

Cells were seeded in a 96-well microplate and then treated with oxHSP70 or HSP70. After removal of the medium, cells were fixed with 10 % trichloroacetic acid for 1 h at 4 °C followed by staining for 30 min with 0.4 % (wt/vol) SRB dissolved in 1 %

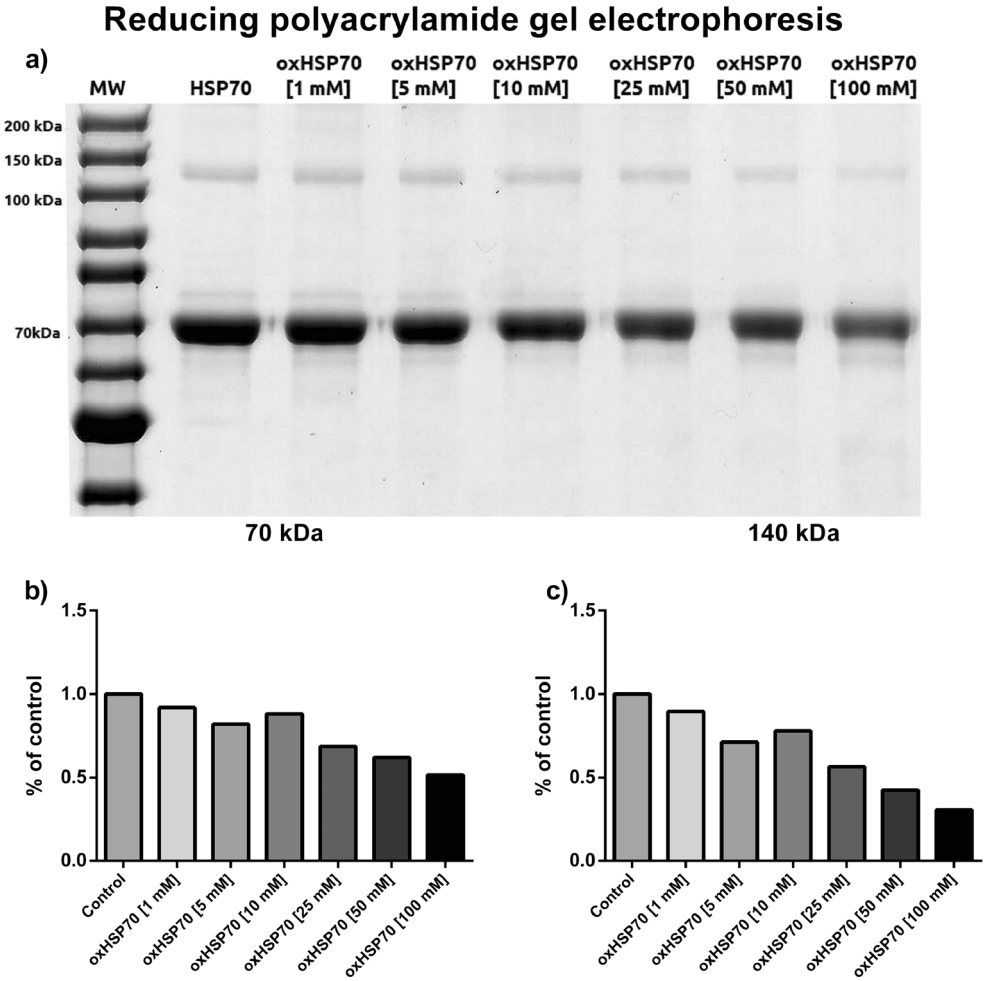

Fig 1 **a** Polyacrylamide gel electrophoresis of HSP70 after 1 h of exposure or not to different concentrations of hydrogen peroxide at 37 °C under agitation. Samples were mixed in reducing buffer containing β-mercaptoethanol. **b** Densitometry of the 70-kDa band. **c** Densitometry of the 140-kDa band. Representative image of three independent experiments. No statistics applied

acetic acid. Unbound dye was removed by four washes with 1 % acetic acid, and protein-bound dye was extracted with 10 mM unbuffered Tris base [tris (hydroxymethyl) aminomethane] for determination of optical density in a computer-interfaced, 96-well microtiter plate reader at 515 nm (Skehan et al. 1990).

MTT assay

Cell viability was measured via MTT assay. RAW 264.7 macrophages were seeded in a 96-well microplate and then treated or not with HSP70 or oxHSP70 for 24 h. The medium was removed, and cells were washed with phosphate-buffered saline (PBS). MTT (0.05 mg/mL) was added for 1 h at 37 °C. Cells were again washed, and DMSO was added for 15 min in the absence of light. Absorbance was read at 560 and 630 nm (Denizot and Lang 1986).

Phagocytic activity

The modulation of the macrophages' phagocytic activity was assessed by the zimosan particles assay. Zimosan (1.25 mg) was incubated under agitation with neutral red dye (200 mg/mL, dissolved in DMSO) for 10 min. This preparation was resuspended in 20 volumes of PBS, centrifuged, and washed. The resulting pellet was resuspended in 2.5 mL of PBS. Fifty microliters of this suspension was mixed with 650 mL of RPMI 1640 medium. Cells seeded in 24-well plates were incubated with 2 mM of PMA (phorbol 12-myristate 13-acetate) or ethanol. After 30 min, the treatments (oxHSP70 or HSP70) were added to the plate for 30 min in an incubator at 37 °C. After that, 50 μL of the preparation of neutral red-stained zimosan was added in each well of the plate. The process of phagocytosis lasted 30 min and then was interrupted by adding cold PBS. The phagocytic

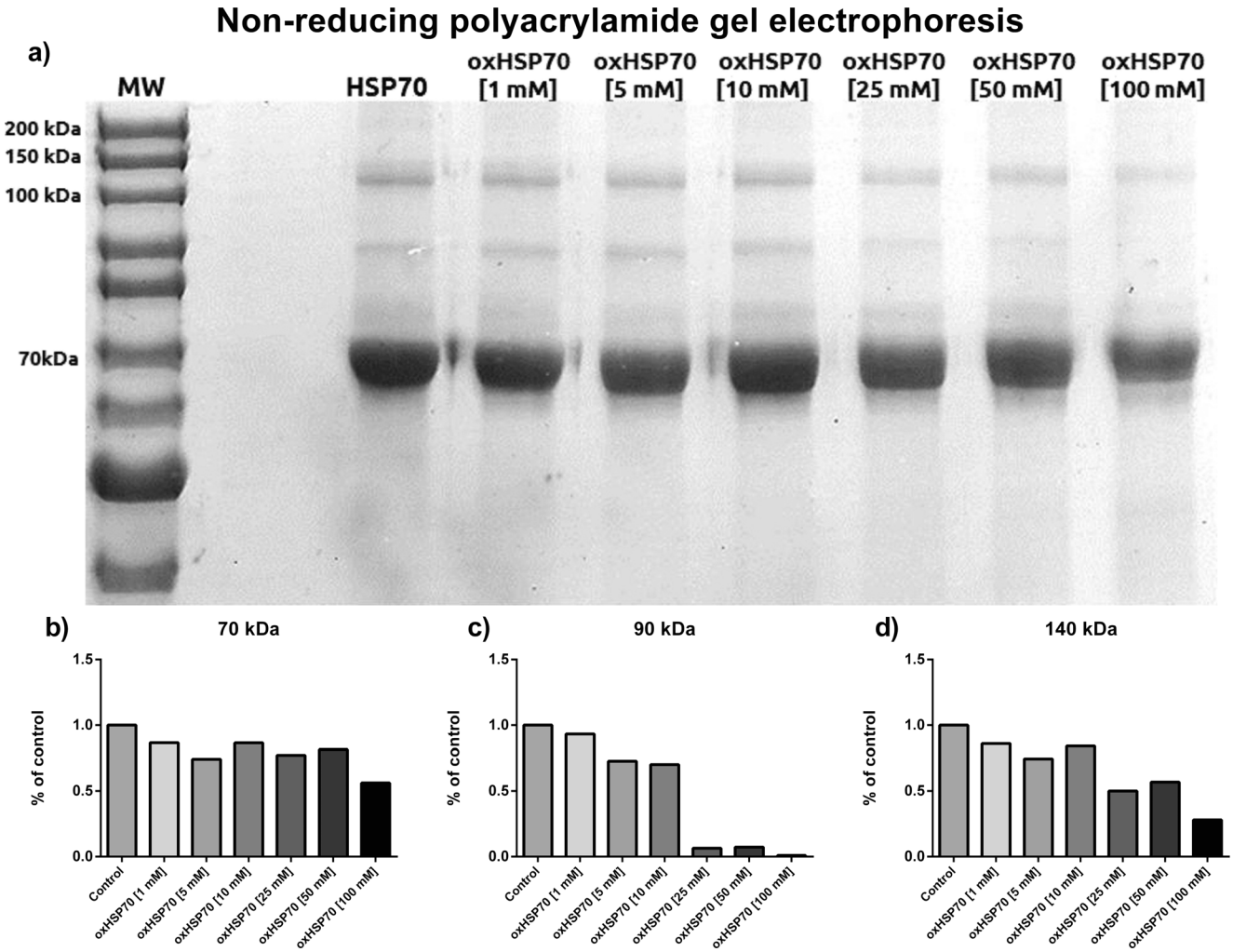

Fig 2 **a** Polyacrylamide gel electrophoresis of HSP70 after 1 h of exposure or not to different concentrations of hydrogen peroxide at 37°C under agitation. Samples were mixed in a nonreducing buffer to preserve oxidative modifications (without β-mercaptoethanol). **b** Densitometry of the 70-kDa band. **c** Densitometry of the 90-kDa band. **d** Densitometry of the 140-kDa band. Representative image of three independent experiments. No statistics applied

macrophages as well as the particles were counted in the digital microscope IX-81 (Olympus) utilizing the program Cell. The phagocytic index was calculated based on the Hishikawa index (Hishikawa et al. 1991). Briefly, in this system, zimosan particles were scored as phagocytized when they were at the same depth of field as the cell and scored as bound when they were seen to be attached to the cell membrane and either at different depth of field compared with the cell or were seen in profile to be outside the cell membrane. The data were presented as a phagocytic index, which was calculated as follows: (number of zimosan particles phagocytized/number of cells scored)×percent phagocytizing cells.

ELISA indirect assay for TNF-α release

The induction of TNF-α release to the incubation medium was quantified by ELISA indirect assay. Cells were seeded in six-well plates and treated for 24 h. After that, 200 μL of the medium was transferred to a 96-well ELISA plate for 36 h for protein adhesion. Following removal of the medium, the plate was washed with TTBS 1× and 100 μ of 1:10,000 antibody anti-TNF-α solution was added for 24 h at 4 °C. After washing, the plate was incubated with a solution containing the secondary antibody (antirabbit 1:10,000) for 3 h at room temperature, washed again with TTBS 1×, and added the revelation solution for 30 min. The reaction was stopped with sulfuric acid, and the absorbance was read at 450 nm in a microplate reader.

Annexin V binding assay

Cells were seeded in six-well plates and then treated or not with HSP70 or oxHSP70 for 24 h. Annexin V binding assay was performed with an Annexin V-FITC Apoptosis Detection Kit from Sigma®. Cells were analyzed in a FACSCalibur flow

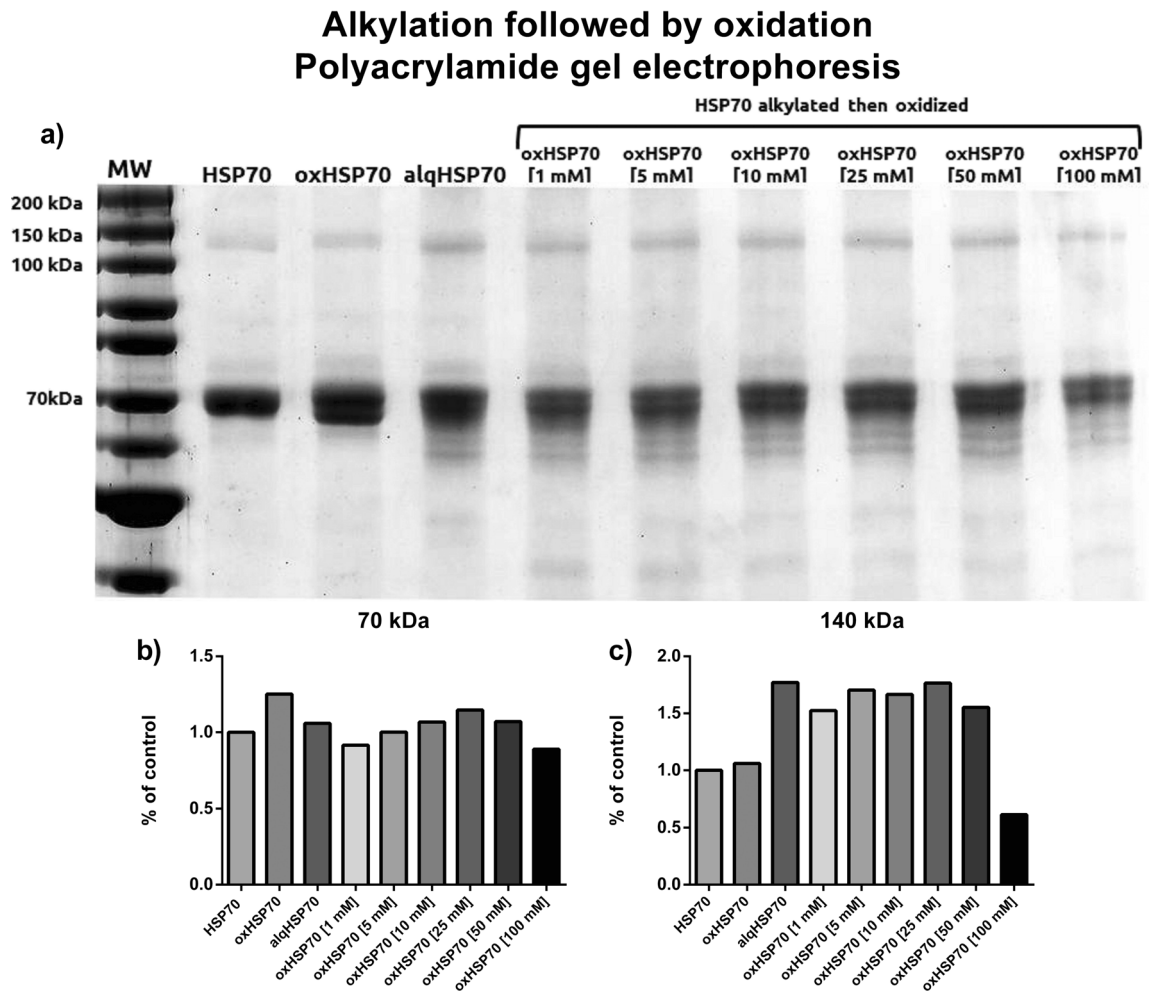

Fig 3 **a** Polyacrylamide gel electrophoresis of HSP70 pretreated or not with iodoacetamide for 1 h then exposed for 1 h to different concentrations of hydrogen peroxide at 37 °C under agitation. Samples were mixed in a nonreducing buffer to preserve alkylating and oxidizing modifications (without β-mercaptoethanol). **b** Densitometry of the 70-kDa band. **c** Densitometry of the 140-kDa band. Representative image of three independent experiments. No statistics applied

cytometer (BD PharMingen). Viable (annexin−/PI−), apoptotic (annexin+/PI−), necrotic nonviable (annexin−/PI+), or late apoptotic/necrotic (annexin+/PI+) cells were characterized as described in Zanotto-Filho et al. (2012).

Results

In order to elucidate the role of oxidation in the possible structural modifications HSP70 may undergo, we treated purified HSP70 with different concentrations of hydrogen peroxide and submitted it to polyacrylamide gel electrophoresis. In the presence of a reducing agent, the protein showed as a major band of 70 kDa, as expected. However, we observed a decrease in the intensity of this band as the concentration of hydrogen peroxide increased. The electrophoretic analysis also showed a 140-kDa band that probably was the dimerized form of HSP70. This band showed the same behavior as the main 70-kDa band, presenting a decrease in its intensity as the hydrogen peroxide concentration increased (Fig. 1).

In an oxidizing environment, proteins with cysteine residues tend to form inter- and intramolecular disulfide bonds, which are reversed by a reducing agent. To eliminate this interfering condition, we utilized a sample buffer without β-mercaptoethanol (Fig. 2). Here, the predominant band was the 70-kDa one, which faded in intensity as the H_2O_2 concentration increased. The 140-kDa band presented the same pattern. In addition, there was a 90-kDa band that was observed in

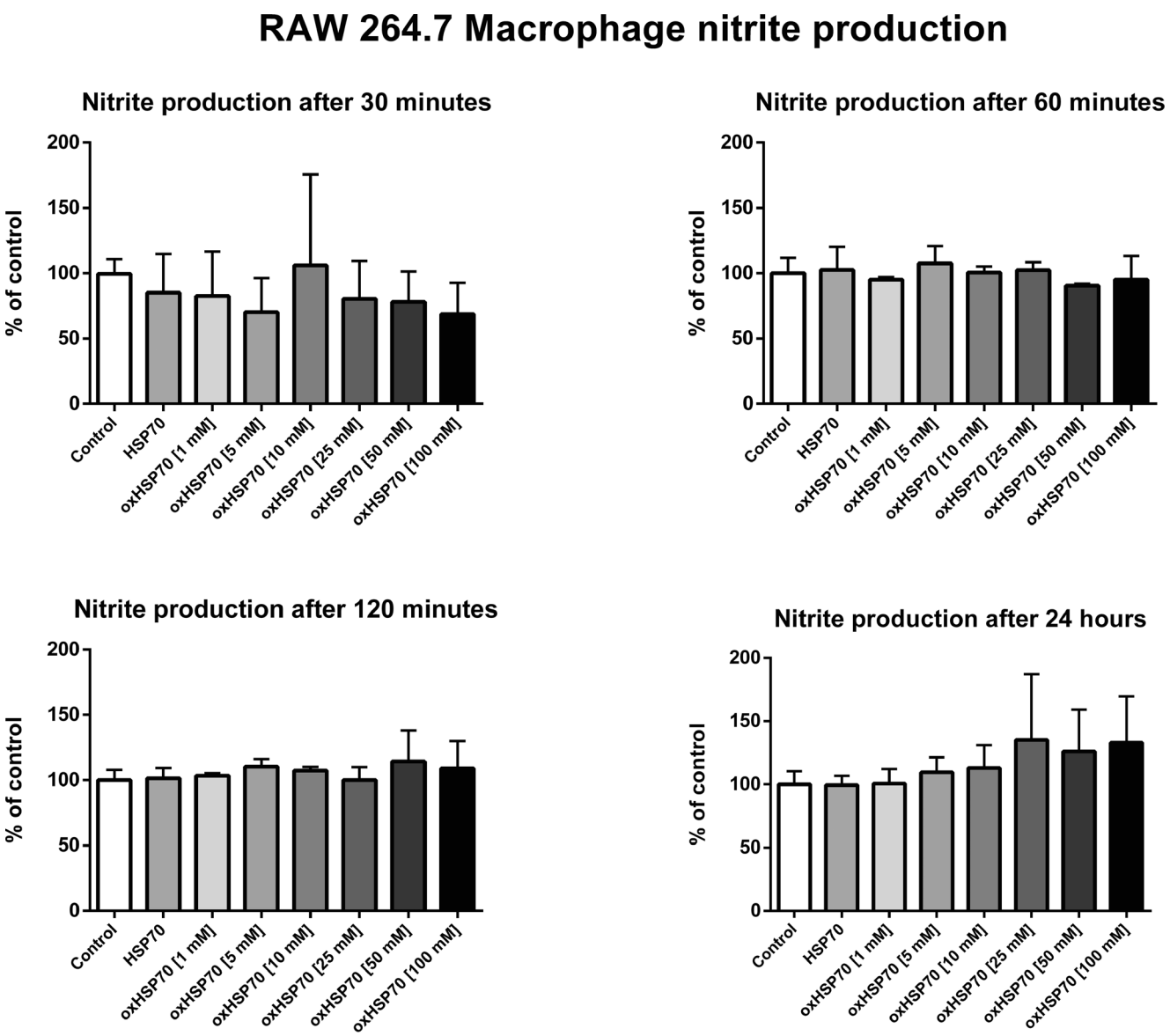

Fig 4 Nitrite production by RAW 264.7 macrophages after 30, 60, and 120 min and 24 h of exposition or not to HSP70 (nonoxidized) and to oxHSP70 (oxidized HSP70 by different concentrations of H_2O_2 for 1 h at 37 °C). Experiments were triplicated, and data are present as mean (SD). One-way ANOVA was performed followed by Tukey's post hoc test. No significant differences between treatments were observed. $P<0.05$

these conditions which also presented the pattern of decreased intensity as the H_2O_2 concentration increased. Although all the bands decreased, the decrease was not as smooth as that in the reducing gel.

If the nonreducing gel has a different pattern than the reducing one, could it be due to the disulfide bonds or the interactions caused by the prooxidizing environment? Moreover, are these interactions important to the correct folding of the protein? When pretreated with an alkylating agent and then treated or not with hydrogen peroxide, the major 70-kDa band was split into two minor bands (Fig. 3). In addition, bands in the range of 60 kDa were visualized, suggesting that the protein was not completely and correctly assembled. This could also be due to partial degradation of alkylated HSP70. This electrophoretic profile differs from the previous two profiles. The 70-kDa band did not decrease in intensity with increasing concentrations of hydrogen peroxide. The 140-kDa bands decreased with intensity only at the highest concentration used. These same treatments were used to investigate the cellular response that oxHSP70 could trigger in macrophages. RAW 264.7 cells were incubated with oxHSP70 for 30, 60, and 120 min and 24 h, after which the nitrite production and cell viability were evaluated. We observed no significant differences in nitrite production on any periods of incubation (Fig. 4).

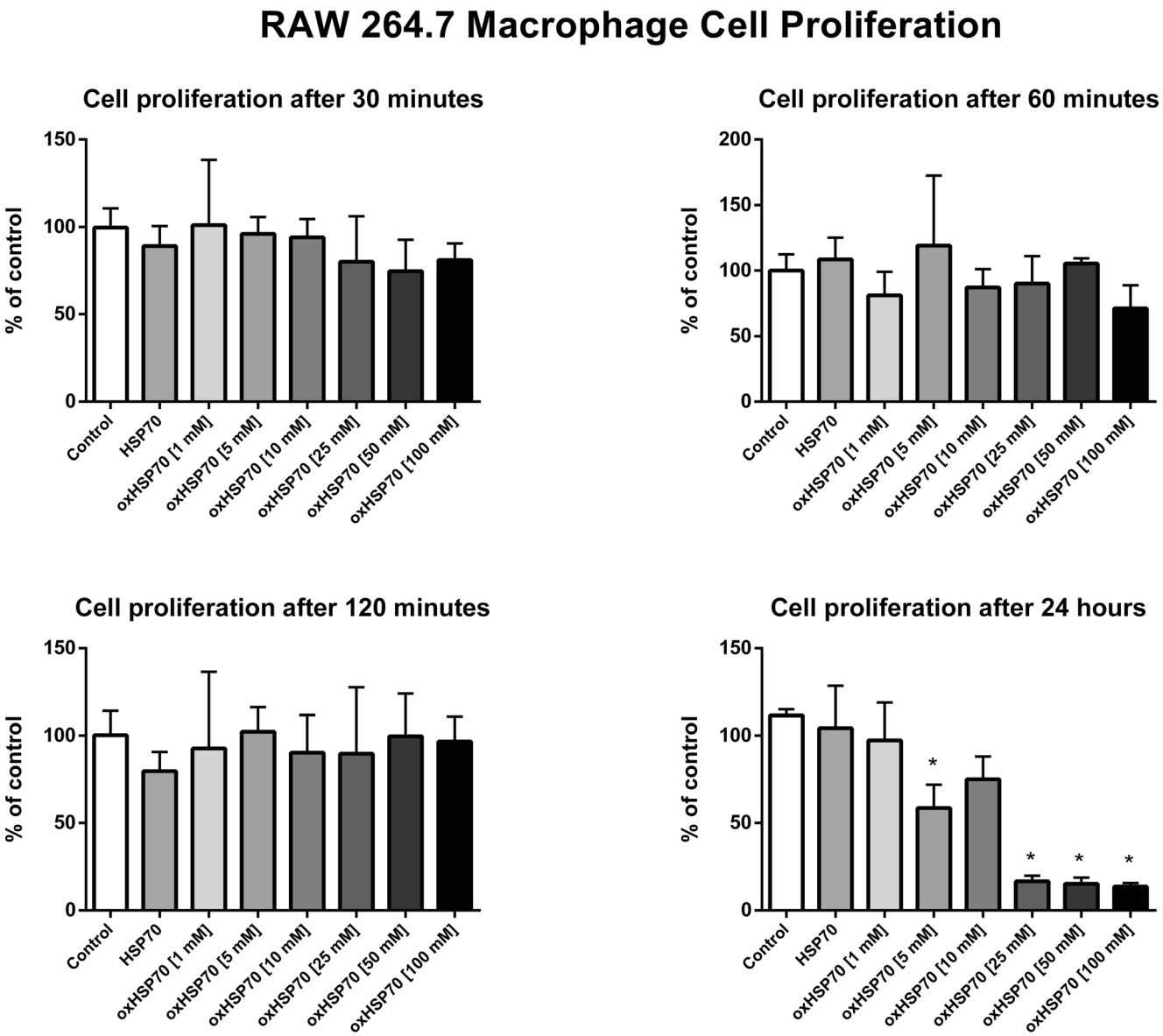

Fig 5 Measurement of RAW 264.7 macrophages cell proliferation after 30, 60, and 120 min and 24 h of exposition or not to HSP70 (nonoxidized) and to oxHSP70 (oxidized HSP70 by different concentrations of H_2O_2 for 1 h at 37 °C). Experiments were triplicated, and data are presented as mean (SD). One-way ANOVA was performed followed by Tukey's post hoc test. HSP70 oxidized by 5, 25, 50, and 100 mM of H_2O_2 differed significantly from control (nontreated) and from HSP70 nonoxidized. $P<0,05$

To assess cell survival, we used the SRB staining assay as a parameter of cell number, and no significant differences were observed at 30, 60, and 120 min of exposure. However, after 24 h of exposure, we observed that the HSP70 oxidized with 5, 25, 50, and 100 mM of hydrogen peroxide induced a decrease in SRB staining compared to the control ($P<0.05$), indicating a decrease in the number of cells (Fig. 5).

To further explore the effect of oxHSP70 on cell numbers, we decided to evaluate the effect of oxHSP70 on a parameter of cell viability. For this purpose, we performed an MTT reduction assay to evaluate cell viability after treatment with either HSP70 or oxHSP70 for the same period. MTT reduction in cells treated with HSP70 was not different from that in the control (not treated cells), while cells treated with oxHSP70 (10, 25, 50, and 100 mM of H_2O_2) had decreased MTT reduction compared to HSP70-treated cells and control ($P<0.05$) (Fig. 6), suggesting oxHSP70 affected cell viability.

After 24 h of treatment with oxHSP70, the proliferation and viability of the cells decreased, but the nature of this loss was still necessary to clarify. We decided to evaluate the effect of oxHSP70 on cell viability by performing an annexin V binding assay. Cells treated with HSP70 oxidized with 1, 5, 10, 25, and 50 mM of H_2O_2 showed no significant changes relative to both the control and HSP70 groups, contrasting with the increase in necrotic populations induced by HSP70 oxidized by 100 mM H_2O_2 (Fig. 7).

We next evaluated the effect of oxHSP70 on the modulation of phagocytosis. RAW 264.7 cells were treated for 30 min with oxHSP70 or HSP70, and then, the phagocytic activity was assessed by the zimosan-based assay. As expected, we observed that HSP70 induced an increase in the score of the Hishikawa index (that is, the higher the index, the higher the activation of the phagocytic activity) when compared to the control; oxHSP70 was not able to induce the same effect as normal HSP70, indicating that oxidation of HSP70 altered its effect on phagocytosis ($P<0.05$) (Fig. 8).

Another classical parameter of macrophage activation, the secretion of the cytokine TNF-α, was assessed. RAW 264.7 macrophages were treated with HSP70 or oxHSP70 for 24 h, and the levels of TNF-α were evaluated by indirect ELISA. As expected, HSP70 induced a significant increase in TNF-α release by RAW 264.7 cells, while oxHSP70 failed to induce this effect ($P<0.05$) (Fig. 9). This result also indicated that oxidation of HSP70 induced a loss of the extracellular signaling function of this protein.

Discussion

Many years have passed since the discovery of HSP70; nowadays, research has shown that its functions and roles are much wider than its chaperone activity. Recently, these proteins have been identified in the serum after diverse forms of stress (heavy exercise, inflammatory process, septic shock, and trauma) (Kindas-Mugge et al. 1993; Trautinger et al. 1996a; Trautinger et al. 1996b). First, it was thought that its presence was caused by the necrotic disruption of the cell membrane and consequently extravasation of cytosolic proteins. After that, it was shown that HSP70 could be actively

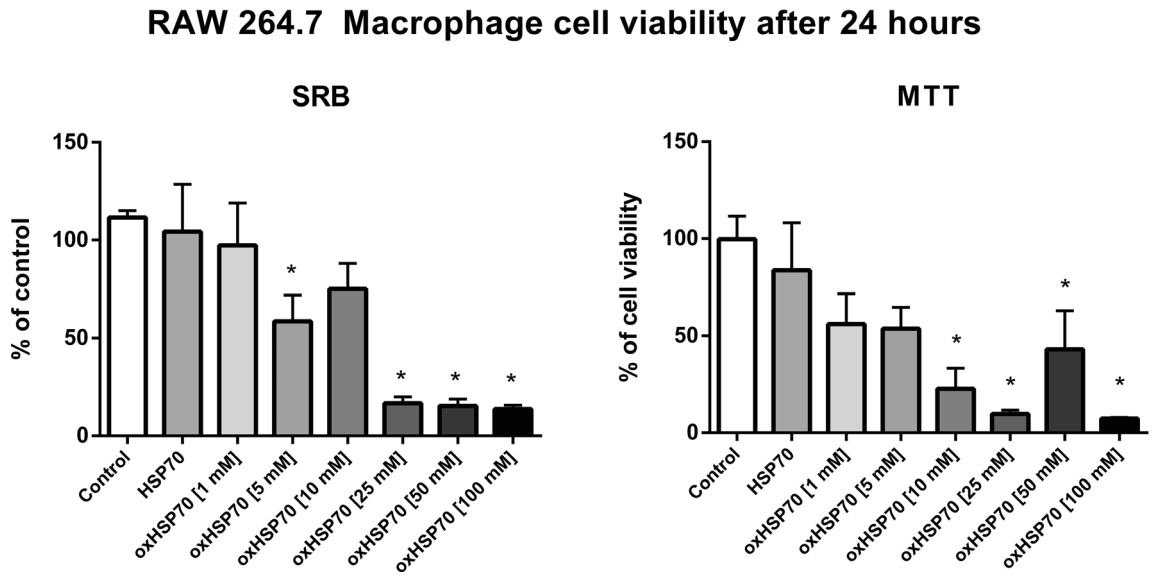

Fig 6 Measurement of RAW 264.7 macrophages cell viability after 24 h of exposition or not to HSP70 (nonoxidized) and to oxHSP70 (oxidized HSP70 by different concentrations of H_2O_2 for 1 h at 37 °C). Experiments were triplicated, and data are presented as mean (SD). 24 h SRB placed by side for comparison. One-way ANOVA was performed followed by Tukey's post hoc test. All oxHSP70 treatments showed lower cell viability when compared to control, but only HSP70 oxidized by 10, 25, 50, and 100 mM of H_2O_2 differed significantly from control (nontreated) and from HSP70 nonoxidized. $P<0.05$

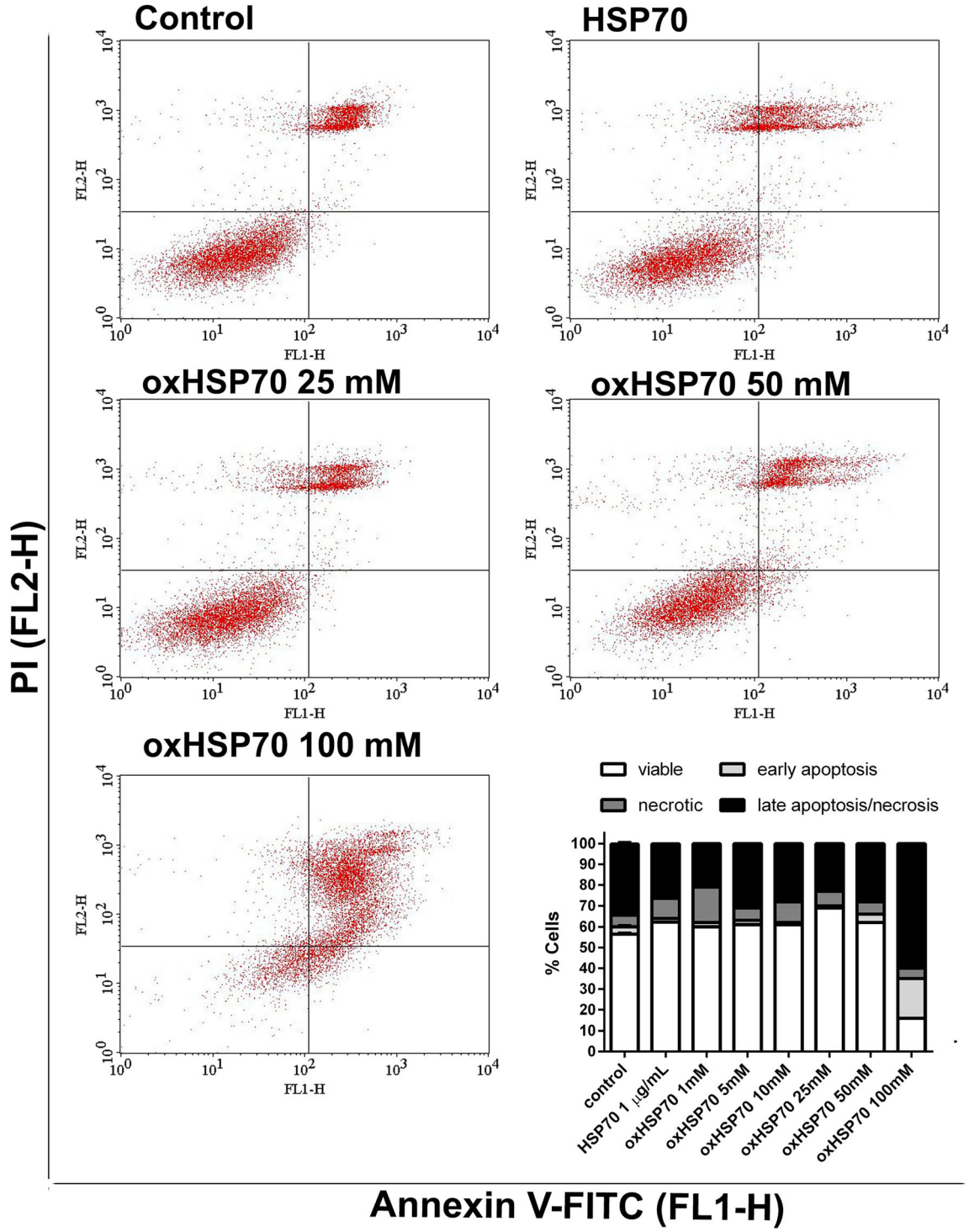

Fig 7 FACS annexin V binding assay. Graphical representation of the annexin V binding assay results. Viable (annexin−/PI−), apoptotic (annexin+/PI−), necrotic nonviable (annexin−/PI+), or late apoptotic/necrotic (annexin+/PI+) cells were characterized

secreted from the intracellular environment to the extracellular space (Vega et al. 2008; Hightower and Guidon 1989), leading to the belief that they could have a deeper signaling role during pathogenic processes.

In a recent study by our group (Gelain et al. 2011), we have shown the correlation between the clinical outcome of septic patients and the presence of HSP70 in their serum. More than that, the patients that died had more oxidative stress levels in their serum and also had increased HSP70 serum levels. Herein, we submitted purified HSP70 to oxidation and evaluated structural changes in the protein and the effects of oxHSP70 on cell viability and immunomodulatory properties.

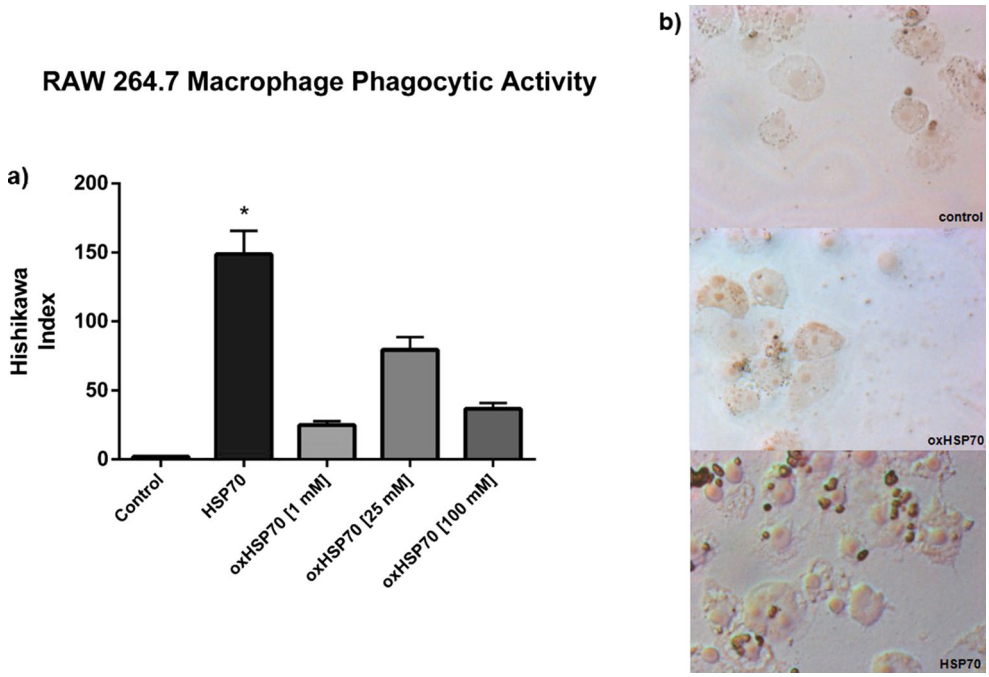

Fig 8 **a** Modulation of phagocytic activity of RAW 264.7 macrophages exposed or not to HSP70 (nonoxidized) and to oxHSP70 (oxidized HSP70 by different concentrations of H_2O_2 for 1 h at 37 °C). Experiments were triplicated, and data are presented as mean (SD). Two-way ANOVA was performed. HSP70 nonoxidized differed significantly from control (nontreated) and from oxHSP70, showing a higher phagocytic index. $P<0.05$. **b** Representative images of the treatment's effect on macrophage phagocytosis

When submitted to an oxidative agent (hydrogen peroxide), HSP70 showed some alterations in its electrophoretic profile when exposed to a reducing sample buffer. The major protein band of 70 kDa and the 140-kDa band (the probable dimer form of the protein) decreased in intensity as the gradient levels of oxidation increased, suggesting that the oxidative environment either damaged the protein or oxidized specific residues, changing the protein's conformation (Fig. 1). In nonreducing conditions, electrophoresis of both normal and oxidized HSP70 evidenced a 90-kDa band, which was not apparent in the gel under reducing conditions. Although we do not know what process caused the appearance of this 90-kDa band in both electrophoretic separations, it is very likely that this process is a redox-related modification, such as disulfide bond formation, since this band was decreased in HSP70 submitted to higher levels of H_2O_2. Thus, we suggest that this 90-kDa band visualized in the gel under reducing conditions is an intermediate, redox-modified form of HSP70 (Fig. 2).

As formation of intramolecular or intermolecular disulfide bonds is one of the most notable modifications of proteins containing cysteine residues, we blocked the possible sites for disulfide formation by pretreating HSP70 with an alkylating agent, iodoacetamide (IAA); so, when the protein was incubated with hydrogen peroxide, any possible disulfide bonds could not be formed. Here, we can observe that the intensity of the bands was different when comparing both reducing and nonreducing conditions. The 70- and 90-kDa bands did not decrease in the same manner. Their intensities were more constant with the increase in the oxidant levels, leading to the possibility of a cysteine oxidation role; also, the electrophoretic profile formed by running HSP70 in this condition showed a splitting of the 70-kDa band, suggesting that this major band was actually formed by bands of very close molecular weight (Fig. 3).

Overall, our results are similar to the findings of Callahan et al. (2002), where HSP70 showed a differential acquisition of antigenic peptides under oxidative condition and a gain of secondary structures (Callahan et al. 2002); Cumming et al.

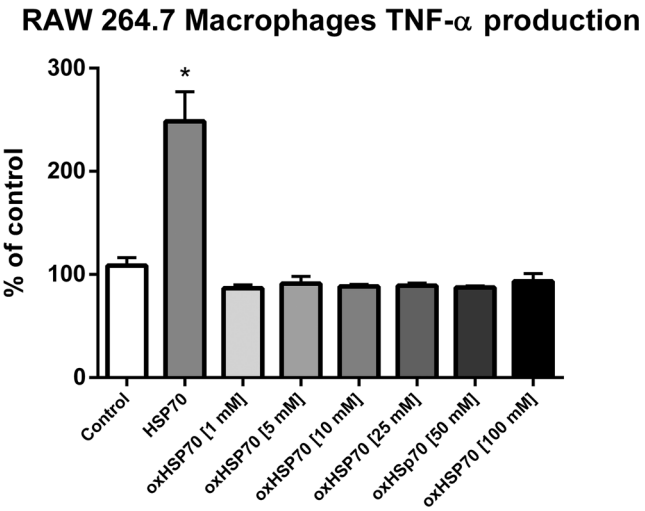

Fig 9 Modulation of RAW 264.7 macrophages TNF-α production after exposition or not to HSP70 (nonoxidized) and to oxHSP70 (oxidized HSP70 by different concentrations of H_2O_2 for 1 h at 37 °C). Experiments were triplicated, and data are presented as mean (SD). One-way ANOVA was performed followed by Tukey's post hoc test. HSP70 nonoxidized differed significantly from control (nontreated) and from oxHSP70, showing a higher TNF-α production. $P<0.05$

2004 also demonstrated that during oxidative stress HSP70 can form mixed disulfide bonds, resulting in the dimer with 140 kDa or even a higher molecular weight oligomer (Cumming et al. 2004).

If extracellular HSP70 plays a role in inflammatory processes, and these are commonly associated with oxidative unbalance and stress, what are the effects of a possible oxidation of oxHSP70 on macrophages? To answer this question, we treated RAW 264.7 cells by 30, 60, 120, and 24 h with HSP70 pretreated or not with hydrogen peroxide. We did not observe any significant differences between the production of nitrite by cells treated with oxHSP70 or HSP70, and cell proliferation quantified through the SRB assay did not change during these short treatment times. However, after 24 h of exposure, we observed an interesting effect. Preoxidized HSP70 diminished the proliferation and viability of the cells as compared to nontreated cells and cells treated with nonoxidized HSP70. Analyses made by flow cytometry showed that cells treated with oxHSP70 oxidized with 1, 5, 10, 25, and 50 mM of H_2O_2 presented an annexin V binding profile similar to both control and HSP70 groups; the majority of the cells were viable, suggesting that oxHSP70 exerted a cytostatic effect. Cells treated with oxHSP70 oxidized with 100 mM showed a large necrotic population, suggesting a cytotoxic effect (Fig. 7).

Also interesting was the observation that the phagocytic activity of the macrophages was diminished in cells treated with preoxidized HSP70 as compared to the cells treated with nonoxidized HSP70, suggesting that oxHSP70 did not activate macrophages with the same efficacy as the nonoxidized HSP70 (Fig. 8).

HSP70 has the ability to induce macrophage activation; one of the parameters observed when this event occurs is the production of inflammatory cytokines, such as IL-8, IL-10, and TNF-α. We treated RAW 264.7 macrophages with HSP70 or oxHSP70 for 24 h and analyzed the content of TNF-α in the incubation medium. The groups treated with oxHSP70 had similar TNF-α levels to the control group; besides, TNF-α release by cells treated with normal HSP70 was increased compared to both oxHSP70-treated and control cells, suggesting that oxHSP70 failed to activate macrophages in a classical way. It is known that TNF-α plays an important role in the proliferation, apoptosis, and differentiation of macrophages. Long-term survival of macrophages is dependent on autocrine signaling by TNF-α (Lombardo et al. 2007). Because TNF-α mediates many of the pathological effects of LPS-TLR4 in conditions such as septic shock, it is suggested that prolonged macrophage survival mediated by TNF-α plays an important role in sepsis (Conte et al. 2006). This can be related to our findings, which showed that after 24 h of treatment with oxHSP70, RAW 264.7 macrophages produced lower levels of TNF-α (Fig. 6) and had lower cell viability (Fig. 10).

In a general way, HSP70 can be released to the extracellular space as a "danger signal" to the system, as it can be recognized by TLR and triggers a proinflammatory signaling

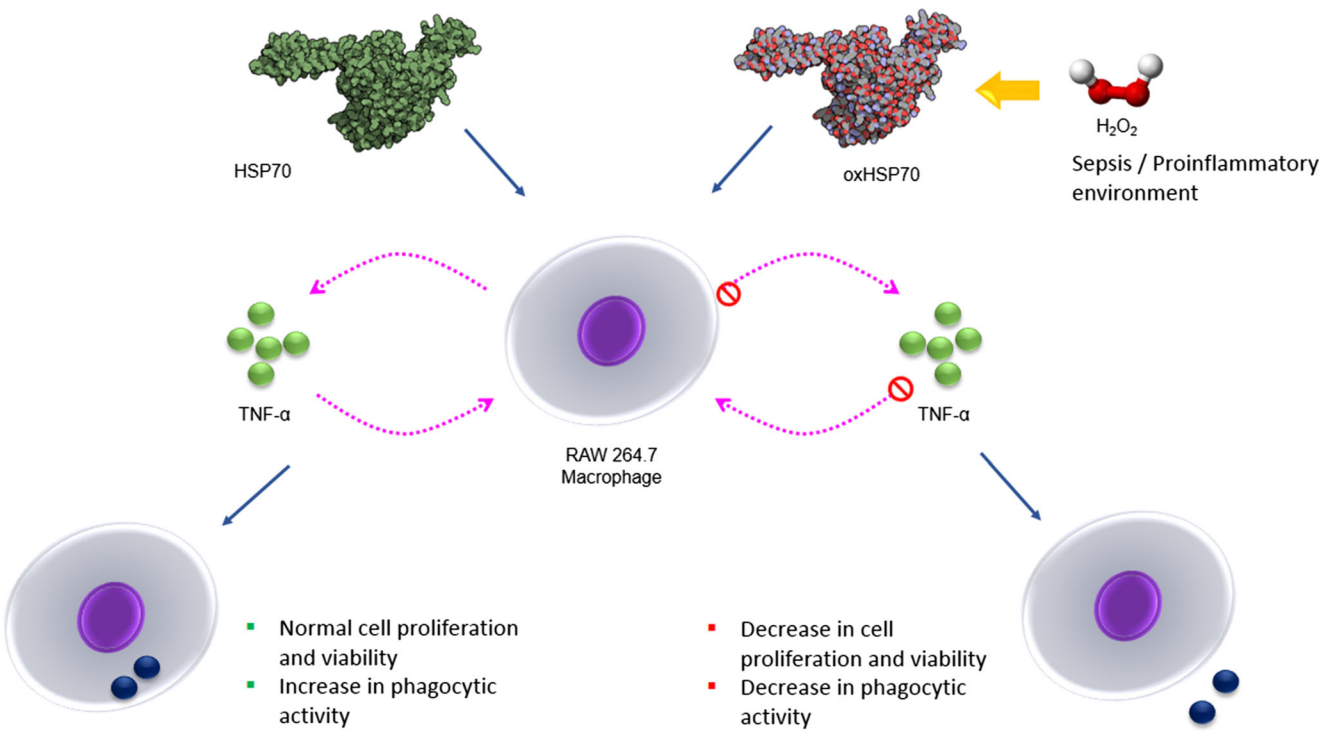

Fig 10 Graphical abstract summarizing the effects of extracellular oxHSP70 on RAW 264.7 macrophage cells on a proinflammatory environment and comparing them to the effects of HSP70

pathway. Proteins characterized as danger signals are known as DAMPS (damage-associated molecular-pattern). In this context, we can infer that the oxidation and subsequent modification and/or impairment of HSP70 can be related to a lack of this "danger signal" when necessary. Recently, it was shown that HMGB1 works as a DAMP and has different redox forms that are responsible for promoting cell recruitment or proinflammatory cytokine release in a similar fashion as the oxidized HSP70 (Venereau et al. 2012). Luong et al. (2012) showed that the stimulation of TLR4 by HSP70 requires structural integrity of the protein; treating HSP70 with proteinase K-agarose digestion lowers the stimulatory capacity of the protein, and this result corroborates the observation that HSP70 acts as a DAMP and with our data (Luong et al. 2012). Moreover, oxHSP70 could be exerting its effects by activating receptors other than TLR, such as the receptor for advanced end-glycation products (RAGE), a key pattern recognition receptor capable of binding a diverse repertoire of soluble and cell-associated molecules involved in the host response to tissue injury, infection, and inflammation. In a recent study (Ruan et al. 2010), it was shown that HSP70 is a possible novel ligand for RAGE. Ligation of RAGE induces the activation of multiple signaling pathways. These pathways may vary depending on the ligand along with the cell and tissue microenvironment, thus mediating diverse cellular responses, possibly the one triggered by oxHSP70.

Nevertheless, it is important to note that the immune effects of HSP may vary depending on several factors including the specific HSP family (HSP60, HSP70, HSP90), the cellular source of the HSP (normal, cancerous, viral-infected, bacterial), cellular location (intracellular, cell surface, serum), and the physiological circumstances modulating HSP expression (oxidative stress, bacterial infection, viral infection, physical stress). Thus, the specific physiological context of these proteins greatly affects their function, preventing any global statements about the in vivo, immunological functions of HSP70 (Johnson and Fleshner 2006).

Taking into account the results presented in this paper and in our previous findings, we suggest that in a prooxidant situation, common to proinflammatory pathologic processes, HSP70 may undergo structural changes that could lead to functional impairment. As we observed before in septic patients, when there is an increase in serum oxidative damage, there is an increase in pathological aggressiveness, even resulting in death (Gelain et al. 2011). In the present paper, we showed that oxidized HSP70 induced a decrease in phagocytic activity, a decrease in TNF-α production, and a decrease in RAW 264.7 macrophage numbers after 24 h of treatment. Cytostatic and cytotoxic effects varied with the oxidative gradient to which the protein was exposed. We believe that this may be correlated with the worst outcome observed in our previous work.

Acknowledgments We are grateful to the National Council for Scientific and Technological Development of the Federal Republic of Brazil (CNPq Universal 472225/2011-1), CAPES (PROCAD 066/2007), FAPERGS (PqG 1008860, PqG 1008857, ARD11/1893-7, PRONEX 1000274), PROPESQ-UFRGS, and IBN-Net #01.06.0842-00. We also would like to express our gratitude to Professor Celia R. Carlini, from LAPROTOX, Department of Biophysics and Center of Biotechnology, Institute of Biosciences, Federal University of Rio Grande do Sul.

References

Andrades M, Ritter C, Moreira JCF, Dal-Pizzol F (2005) Oxidative parameters differences during non-lethal and lethal sepsis development. J Surg Res 125(1):68–72. doi:10.1016/j.jss.2004.11.008

Asea A (2007) Hsp72 release: mechanisms and methodologies. Methods 43(3):194–198. doi:10.1016/j.ymeth.2007.06.002

Asea A, Kraeft SK, Kurt-Jones EA, Stevenson MA, Chen LB, Finberg RW, Koo GC, Calderwood SK (2000) HSP70 stimulates cytokine production through a CD14-dependant pathway, demonstrating its dual role as a chaperone and cytokine. Nat Med 6(4):435–442. doi:10.1038/74697

Asea A, Rehli M, Kabingu E, Boch JA, Bare O, Auron PE, Stevenson MA, Calderwood SK (2002) Novel signal transduction pathway utilized by extracellular HSP70: role of toll-like receptor (TLR) 2 and TLR4. J Biol Chem 277(17):15028–15034. doi:10.1074/jbc.M200497200

Barreto A, Gonzalez JM, Kabingu E, Asea A, Fiorentino S (2003) Stress-induced release of HSC70 from human tumors. Cell Immunol 222(2):97–104

Callahan MK, Chaillot D, Jacquin C, Clark PR, Ménoret A (2002) Differential acquisition of antigenic peptides by Hsp70 and Hsc70 under oxidative conditions. J Biol Chem 277(37):33604–33609. doi:10.1074/jbc.M202890200

Chen T, Cao X (2010) Stress for maintaining memory: HSP70 as a mobile messenger for innate and adaptive immunity. Eur J Immunol 40(6):1541–1544. doi:10.1002/eji.201040616

Conte D, Holcik M, Lefebvre CA, Lacasse E, Picketts DJ, Wright KE, Korneluk RG (2006) Inhibitor of apoptosis protein cIAP2 is essential for lipopolysaccharide-induced macrophage survival. Mol Cell Biol 26(2):699–708. doi:10.1128/MCB.26.2.699-708.2006

Cumming RC, Andon NL, Haynes PA, Park M, Fischer WH, Schubert D (2004) Protein disulfide bond formation in the cytoplasm during oxidative stress *, 279(21):21749–21758. doi:10.1074/jbc.M312267200

Denizot F, Lang R (1986) Rapid colorimetric assay for cell growth and survival. Modifications to the tetrazolium dye procedure giving improved sensitivity and reliability. J Immunol Methods 89(2):271–7. Retrieved from http://www.ncbi.nlm.nih.gov/pubmed/3486233

Febbraio MA, Steensberg A, Walsh R, Koukoulas I, van Hall G, Saltin B, Pedersen BK (2002) Reduced glycogen availability is associated with an elevation in HSP72 in contracting human skeletal muscle. J Physiol 538(Pt 3):911–917. Retrieved from http://www.ncbi.nlm.nih.gov/pubmed/11826174

Fehrenbach E, Niess AM, Voelker K, Northoff H, Mooren FC (2005) Exercise intensity and duration affect blood soluble HSP72. Int J Sports Med 26(7):552–557. doi:10.1055/s-2004-830334

Gelain DP, de Bittencourt Pasquali MA, Comin MC, Grunwald MS, Ritter C, Tomasi CD, Alves SC, Quevedo J, Dal-Pizzol F, Moreira JC (2011) Serum heat shock protein 70 levels, oxidant status, and mortality in sepsis. Shock 35(5):466–470. doi:10.1097/SHK.0b013e31820fe704

Hightower LE, Guidon PT (1989) Selective release from cultured mammalian cells of heat shock (stress) proteins that resemble glia-axon transfer proteins. J Cell Physiol 138(2):257–266

Hishikawa T, Cheung JY, Yelamarty RV, Knutson DW (1991) Calcium transients during Fc receptor-mediated and nonspecific phagocytosis by murine peritoneal macrophages. J Cell Biol 115(1):59–66. Retrieved from http://www.ncbi.nlm.nih.gov/pubmed/1918139

Jaattela M (1999) Heat shock proteins as cellular lifeguards. Ann Med 31(4):261–271

Johnson JD, Fleshner M (2006) Releasing signals, secretory pathways, and immune function of endogenous extracellular heat shock protein 72, 79(March):425–434. doi:10.1189/jlb.0905523.Journal

Kindas-Mugge I, Steiner G, Smolen JS (1993) Similar frequency of autoantibodies against 70-kD class heat-shock proteins in healthy subjects and systemic lupus erythematosus patients. Clin Exp Immunol 92(1):46–50. Retrieved from http://www.ncbi.nlm.nih.gov/pubmed/8467563

Lancaster GI, Moller K, Nielsen B, Secher NH, Febbraio MA, Nybo L (2004) Exercise induces the release of heat shock protein 72 from the human brain in vivo. Cell Stress Chaperones 9(3):276–280. Retrieved from http://www.ncbi.nlm.nih.gov/pubmed/15544165

Li Y.-H, Yan Z.-Q, Brauner A, Tullus K (2002) Activation of macrophage nuclear factor-kappa B and induction of inducible nitric oxide synthase by LPS. Respir Res 3:23. Retrieved from http://www.pubmedcentral.nih.gov/articlerender.fcgi?artid=150509&tool=pmcentrez&rendertype=abstract

Lindquist S, Craig EA (1988) The heat-shock proteins. Annu Rev Genet 22:631–677. doi:10.1146/annurev.ge.22.120188.003215

Lombardo E, Alvarez-Barrientos A, Maroto B, Bosca L, Knaus UG (2007) TLR4-mediated survival of macrophages is MyD88 dependent and requires TNF-alpha autocrine signalling. J Immunol 178(6):3731–3739. Retrieved from http://www.ncbi.nlm.nih.gov/pubmed/17339471

Luong M, Zhang Y, Chamberlain T, Zhou T, Wright JF, Dower K, Hall JP (2012) Stimulation of TLR4 by recombinant HSP70 requires structural integrity of the HSP70 protein itself. J Inflamm (Lond Engl) 9:11. doi:10.1186/1476-9255-9-11

Matzinger P (2002) The danger model: a renewed sense of self. Science 296(5566):301–305. doi:10.1126/science.1071059

Millar DG, Garza KM, Odermatt B, Elford AR, Ono N, Li Z, Ohashi PS (2003) Hsp70 promotes antigen-presenting cell function and converts T-cell tolerance to autoimmunity in vivo. Nat Med 9(12):1469–1476. doi:10.1038/nm962

Ortega E, Giraldo E, Hinchado MD, Martinez M, Ibanez S, Cidoncha A, Collazos ME, Garcia JJ (2006) Role of Hsp72 and norepinephrine in the moderate exercise-induced stimulation of neutrophils' microbicide capacity. Eur J Appl Physiol 98(3):250–255. doi:10.1007/s00421-006-0269-7

Ortega E, Hinchado MD, Martin-Cordero L, Asea A (2009) The effect of stress-inducible extracellular Hsp72 on human neutrophil chemotaxis: a role during acute intense exercise. Stress 12(3):240–249. doi:10.1080/10253890802309853

Peck G, Andrades M, Lorenzi R, da Costa M, Petronilho F, Moreira JCF, … Ritter C (2009). Serum-induced macrophage activation is related to the severity of septic shock. Inflammation research : official journal of the European Histamine Research Society… [et al.] 58(2):89–93. doi:10.1007/s00011-009-8088-z

Pittet JF, Lee H, Morabito D, Howard MB, Welch WJ, Mackersie RC (2002) Serum levels of Hsp 72 measured early after trauma correlate with survival. J Trauma 52(4):611–617, discussion 617

Pockley AG, Georgiades A, Thulin T, de Faire U, Frostegard J (2003) Serum heat shock protein 70 levels predict the development of atherosclerosis in subjects with established hypertension. Hypertension 42(3):235–238. doi:10.1161/01.HYP.0000086522.13672.23

Ribeiro SP, Villar J, Downey GP, Edelson JD, Slutsky AS (1994) Sodium arsenite induces heat shock protein-72 kilodalton expression in the lungs and protects rats against sepsis. Crit Care Med 22(6):922–929. Retrieved from http://www.ncbi.nlm.nih.gov/pubmed/7794296

Ritossa F (1962). A new puffing pattern induced by temperature shock and DNP in drosophila. Cell Mol Life Sci 18(12).

Ruan BH, Li X, Winkler AR, Cunningham KM, Kuai J, Greco RM, Nocka KH, Fitz LJ, Wright JF, Pittman DD, Tan XY, Paulsen JE, Lin LL, Winkler DG (2010) Complement C3a, CpG oligos, and DNA/C3a complex stimulate IFN-alpha production in a receptor for advanced glycation end product-dependent manner. J Immunol 185(7):4213–4222. doi:10.4049/jimmunol.1000863

Ryan AJ, Flanagan SW, Moseley PL, Gisolfi CV (1992) Acute heat stress protects rats against endotoxin shock. J Appl Physiol 73(4):1517–1522

Skehan P, Storeng R, Scudiero D, Monks A, McMahon J, Vistica D, Warren JT, Bokesch H, Kenney S, Boyd MR (1990) New Colorimetric Cytotoxicity Assay for Anticancer-Drug Screening. JNCI J Natl Cancer Inst 82(13):1107–1112. doi:10.1093/jnci/82.13.1107

Srivastava P (2002) Interaction of heat shock proteins with peptides and antigen presenting cells: chaperoning of the innate and adaptive immune responses. Annu Rev Immunol 20:395–425. doi:10.1146/annurev.immunol.20.100301.064801

Trautinger F, Kindas-Mugge I, Knobler RM, Honigsmann H (1996) Stress proteins in the cellular response to ultraviolet radiation. J Photochem Photobiol B 35(3):141–148. Retrieved from http://www.ncbi.nlm.nih.gov/pubmed/8933720

Trautinger F, Knobler RM, Honigsmann H, Mayr W, Kindas-Mugge I (1996) Increased expression of the 72-kDa heat shock protein and reduced sunburn cell formation in human skin after local hyperthermia. J Invest Dermatol 107(3):442–443. Retrieved from http://www.ncbi.nlm.nih.gov/pubmed/8751984

Vega VL, Rodriguez-Silva M, Frey T, Gehrmann M, Diaz JC, Steinem C, Multhoff G, Arispe N, De Maio, A (2008) Hsp70 translocates into the plasma membrane after stress and is released into the extracellular environment in a membrane-associated form that activates macrophages. J Immunol 180(6):4299–4307. Retrieved from http://www.ncbi.nlm.nih.gov/pubmed/18322243

Venereau E, Casalgrandi M, Schiraldi M, Antoine DJ, Cattaneo A, De Marchis F, Liu J, Antonelli A, Preti A, Raeli L, Shams SS, Yang H, Varani L, Andersson U, Tracey KJ, Bachi A, Uguccioni M, Bianchi ME (2012) Mutually exclusive redox forms of HMGB1 promote cell recruitment or proinflammatory cytokine release. J Exp Med 209(9):1519–1528. doi:10.1084/jem.20120189

Villar J, Ribeiro SP, Mullen JB, Kuliszewski M, Post M, Slutsky AS (1994) Induction of the heat shock response reduces mortality rate and organ damage in a sepsis-induced acute lung injury model. Crit Care Med 22(6):914–921

Walsh RC, Koukoulas I, Garnham A, Moseley PL, Hargreaves M, Febbraio MA (2001) Exercise increases serum Hsp72 in humans. Cell Stress Chaperones 6(4):386–393. Retrieved from http://www.ncbi.nlm.nih.gov/pubmed/11795476

Wong HR, Menendez IY, Ryan MA, Denenberg AG, Wispe JR (1998) Increased expression of heat shock protein-70 protects A549 cells against hyperoxia. Am J Physiol 275(4 Pt 1):L836–L841

Wong HR, Ryan M, Menendez IY, Denenberg A, Wispe JR (1997) Heat shock protein induction protects human respiratory epithelium against nitric oxide-mediated cytotoxicity. Shock 8(3):213–218

Zanotto-Filho A, Braganhol E, Battastini AM, Moreira JC (2012) Proteasome inhibitor MG132 induces selective apoptosis in glioblastoma cells through inhibition of PI3K/Akt and NFkappaB pathways, mitochondrial dysfunction, and activation of p38-JNK1/2 signaling. Investig New Drugs 30:2252–2262

Capítulo 2

Artigo publicado na revista Cell Stress & Chaperones

“Putative model for heat shock protein 70 complexation with receptor of advanced glycation end products through fluorescence proximity assays and normal mode analyses”

Cell Stress and Chaperones
DOI 10.1007/s12192-016-0746-9

ORIGINAL PAPER

Putative model for heat shock protein 70 complexation with receptor of advanced glycation end products through fluorescence proximity assays and normal mode analyses

Marcelo Sartori Grunwald[1] · **Rodrigo Ligabue-Braun**[2] · **Cristiane Santos Souza**[1] · **Luana Heimfarth**[1] · **Hugo Verli**[2] · **Daniel Pens Gelain**[1] · **José Cláudio Fonseca Moreira**[1]

Received: 21 July 2016 / Revised: 26 October 2016 / Accepted: 2 November 2016

Abstract Extracellular heat shock protein 70 (HSP70) is recognized by receptors on the plasma membrane, such as Toll-like receptor 4 (TLR4), TLR2, CD14, and CD40. This leads to activation of nuclear factor-kappa B (NF-κB), release of pro-inflammatory cytokines, enhancement of the phagocytic activity of innate immune cells, and stimulation of antigen-specific responses. However, the specific characteristics of HSP70 binding are still unknown, and all HSP70 receptors have not yet been described. Putative models for HSP70 complexation to the receptor for advanced glycation endproducts (RAGEs), considering both ADP- and ATP-bound states of HSP70, were obtained through molecular docking and interaction energy calculations. This interaction was detected and visualized by a proximity fluorescence-based assay in A549 cells and further analyzed by normal mode analyses of the docking complexes. The interacting energy of the complexes showed that the most favored docking situation occurs between HSP70 ATP-bound and RAGE in its monomeric state. The fluorescence proximity assay presented a higher number of detected spots in the HSP70 ATP treatment, corroborating with the computational result. Normal-mode analyses showed no conformational deformability in the interacting interface of the complexes. Results were compared with previous findings in which oxidized HSP70 was shown to be responsible for the differential modulation of macrophage activation, which could result from a signaling pathway triggered by RAGE binding. Our data provide important insights into the characteristics of HSP70 binding and receptor interactions, as well as putative models with conserved residues on the interface area, which could be useful for future site-directed mutagenesis studies.

Keywords Heat shock protein 70 · Receptor of advanced glycation end products · Signal transduction pathways · Molecular docking · Complexation

Introduction

Within the past decade, extracellular heat shock protein 70 (HSP70) was shown to bind with high affinity to the plasma membrane of antigen-presenting cells (APCs), eliciting a rapid intracellular Ca^{+2} flux and activating the transcription factor nuclear factor-kappa B (NF-κB). These events are followed by substantial release of various pro-inflammatory cytokines, including tumor necrosis factor (TNF)-α, interleukin (IL)-1β, IL-6, and IL-12, from APCs through Toll-like receptor (TLR) 2-, TLR4-, and CD-14-dependent processes (Asea et al. 2000a). HSP70 can activate various cells of the immune system, including natural-killer (NK) cells (Gross et al. 2003), APCs (Asea et al. 2002), macrophages, peripheral monocytes (Asea et al. 2000a, b), and B lymphocytes (Arnold-Schild et al. 1999). In addition, this interaction and the resulting signal transduction cascade are also mediated by the scavenger receptor CD36 (Delneste et al. 2002) and the costimulatory molecule CD40 (Becker 2002). The CD40/HSP70 interaction appears to be critical to B-

Electronic supplementary material The online version of this article (doi:10.1007/s12192-016-0746-9) contains supplementary material, which is available to authorized users.

✉ Marcelo Sartori Grunwald
marcelo.sartori@yahoo.com.br

[1] Department of Biochemistry, Institute of Basic Health Sciences, Federal University of Rio Grande do Sul, Porto Alegre, Rio Grande do Sul, Brazil

[2] Center of Biotechnology, Federal University of Rio Grande do Sul, Porto Alegre, Rio Grande do Sul, Brazil

Published online: 17 November 2016

lymphocytes, where this interaction promotes the phosphorylation of p38 and subsequent release of TNF-α and interferon (IFN)-γ (Asea 2003). It is also known that these chaperones are targeted by anti-inflammatory regulatory T-cells (Tregs). After an inflammatory event, the enhanced levels of HSP70 enable the immune system to target Tregs to specifically act on the inflammation sites. This phenomenon has been observed in experimental models with both microbial and endogenous heat shock proteins (van Eden 2015). However, the specific characteristics of surface-bound HSP70 receptors are not known, and all potential receptors have not yet been identified. Despite this lack of clear data regarding HSP70 receptors, we do know that this interaction is important because it results in the chaperokine-induced transduction of signals important for the survival of the host against pathogen infection.

HSP70 is composed by two distinct domains: the N-terminal nucleotide binding domain (NBD), which has ATPase activity, and the C-terminal protein substrate binding domain (SBD), which has two subdomains: a peptide-binding pocket and a helical lid. When the chaperone is in its ATP-bound state, the helical lid is open, allowing the substrate to enter the substrate-binding pocket. The ATP is then hydrolyzed to ADP, and the helical lid closes tightly upon the substrate. To release the substrate, the ADP molecule must be substituted with ATP, which results in subsequent opening of the helical lid. When a new peptide substrate is presented, the ATP is again hydrolyzed, continuing the chaperone binding-release cycle (Sousa 2012). This cycle is partially illustrated by the side by side depiction of the PDB files of 2KHO and 4B9Q (Fig. 1).

In multiple studies, researchers have attempted to assign the biological functions of HSP70 to either the NBD or the SBD. Becker and coworkers showed that HSP70 from different sources binds to different sites on CD40 through different regions of the protein; that is, human recombinant HSP70 binds through the NBD while DnaK (the homolog HSP70 from *Escherichia coli*) binds through the SBD. Moreover, they showed that this interaction depends on the ADP/ATP cycle (Becker 2002). In another work, hepatocytes treated with the truncated 3′ peptide (SBD) were found to have higher activation parameters when compared with cells treated with the 5′ peptide (NDB) (Galloway et al. 2008). These differences can be attributed to the different receptors involved; furthermore, the biological effects observed in these studies have always been found to be stronger when the cells are treated with the full-length protein rather than only the NBD or the SBD. However, there are no structural data at the atomic level describing the complexation of HSP70 with its target receptors.

A recent study showed that HSP70 could act as a ligand for the receptor of advanced glycation endproducts (RAGEs) (Ruan et al. 2010). RAGE is a multiligand, immunoglobulin-type transmembrane protein that functions as a pattern-recognition receptor (PRR) for the innate immune system. RAGE was initially described based on its affinity for advanced glycation endproducts (AGEs) and was later found to bind a vast array of non-glycated endogenous peptides, both soluble and membrane bound, involved in the host response against tissue damage, infections, and inflammatory processes; these other ligands include HGMB1, S100/calgranulin family members, lipopolysaccharide (LPS), and others (Bucciarelli et al. 2002). Increased expression and activation of RAGE affect a variety of pathological conditions, including diabetes and inflammation. Binding of RAGE induces the activation of multiple signaling pathways that may vary depending on the ligand, cell, and tissue microenvironment and thus mediates diverse cellular responses; activation of NF-κB and mitogen-activated protein kinase (MAPK) is among the key pathways activated by RAGE. These intracellular pathways can lead to production of inflammatory cytokines, activation of proteases, and oxidative stress (Schmidt et al. 2000).

In this study, we developed a putative model of the interaction between HSP70 and RAGE through a series of molecular docking simulations, their interaction energy and conformational changes of the complexes by normal mode analyses. Since few studies have considered the ADP/ATP cycle in this context, we performed docking simulations between RAGE and HSP70 in the ADP/APO or ATP state. Moreover, we confirmed our results using a fluorescence proximity assay on a cell line culture.

Experimental procedures

Chemicals Purified recombinant human HSP70 (SRP5190) was purchased from Sigma-Aldrich. Antibodies against RAGE were bought from AbCam (Cambridge, UK). Antibodies against HSP70 were purchased from Sigma (St. Louis, MO, USA).

Cell culture The human non-small cell lung cancer (NSCLC) cell line A549 was grown in RPMI-1640 containing 10% fetal bovine serum (FBS) and maintained at 37 °C in an atmosphere containing 5% CO_2. The media was supplemented with 1% penicillin/streptomycin. Cells were trypsinized after reaching 70–90% confluence, counted, and plated.

Protein proximity ligand assay The detection and visualization of the interaction between HSP70 and RAGE were carried out using a Duolink In Situ kit from Sigma-Aldrich. This assay facilitated the detection, visualization, and quantification of protein interactions in cell samples prepared for microscopy based on the proximity of fluorescent probes to the target primary antibodies. Cells were seeded in 12-well plates with a cover slip on the bottom of each well and then treated with 10 μg HSP70 or 10 μg HSP70 pretreated with 10 μg

ATP. After 30 min, the cells were fixed with 4% paraformaldehyde for 30 min. Blocking solution was then added, and cells were incubated for 30 min at 37 °C. Samples were incubated overnight in a humidified chamber with the primary antibodies (anti-RAGE at a 1:2000 dilution; and anti-HSP70 at a 1:2500 dilution). PLA probes were added, and the samples were incubated in a humidified chamber for 60 min at 37 °C. Next, a ligation-ligase solution was added, and the samples were incubated for 30 min at 37 °C. Finally, an amplification-polymerase solution was added, and the samples were incubated for 100 min at 37 °C.

Preparation for imaging Cover slips were mounted by inversion on a regular microscope slide using a minimal volume of Duolink In Situ Mounting Media with DAPI. Slides were analyzed on a confocal microscope using a ×40 objective. DAPI stained the cell nuclei in blue, whereas the fluorophore from the Detection Reagent kit stained the interaction spots in red, with an excitation of 495 nm and an emission of 624 nm. Images were obtained with ZEN Lite digital imaging software from Carl Zeiss Microscopy GmbH.

Morphometric and intensity of fluorescence analysis Measurements of intensity of fluorescence and morphometric analysis of cytoplasm and nucleus were obtained using the ImageJ software (NIH, Bethesda, MD), and the intensity of fluorescence/cytoplasm/nucleus ratio of the cells was used as quantification of RAGE-HSP70 interaction.

Molecular docking, structural analyses, and interaction energy calculation The protein structures under PDB IDs 2KHO (Bertelsen et al. 2009) and 4B9Q (Kityk et al. 2012) were employed as ligands in the molecular docking calculations, corresponding to HSP70 in the ADP/APO and ATP states, respectively. The protein structures under PDB IDs 3CJJ (Koch et al. 2010) and 4LP5 (Yatime and Andersen 2013) were employed as the receptors, corresponding to the V and C1 domains of RAGE (the ligand-binding domain) and to the V, C1, and C2 domains of RAGE, respectively. Additionally, the oligomeric form of RAGE was also retrieved from PDB ID 4LP5. The PQR files used to calculate the electrostatic potential surface of HSP70 were generated by the webserver PDB2PQR (Dolinsky et al. 2004) using the PDB 4B9Q, with the surface potentials being calculated by APBS (Baker et al. 2001), colored and visualized using UCSF Chimera (Pettersen et al. 2004). In order to increase the diversity of docking solutions, calculations were performed on four different macromolecular docking programs: PatchDock (Schneidman-Duhovny et al. 2005), Hex (Macindoe et al. 2010), GRAMM-X (Tovchigrechko and Vakser 2006), and PIPER via ClusPro 2.0 (Comeau et al. 2004; Kozakov et al. 2006). All docking calculations were performed without restrictions; that is, HSP70 protein was free to search the entire RAGE surface for its preferential binding site. Docking results were clustered by their own docking scores and then submitted to an interaction energy calculation by FoldX (Schymkowitz et al. 2005). In this step, we applied the commands *Optimize* to carry out a quick optimization of the structure, moving all side chains slightly to eliminate small Van der Waals' clashes, and *RepairPDB*, which identifies residues with poor torsion angles, Van der Waals' clashes, or inappropriate total energy and repairs them. The results of each

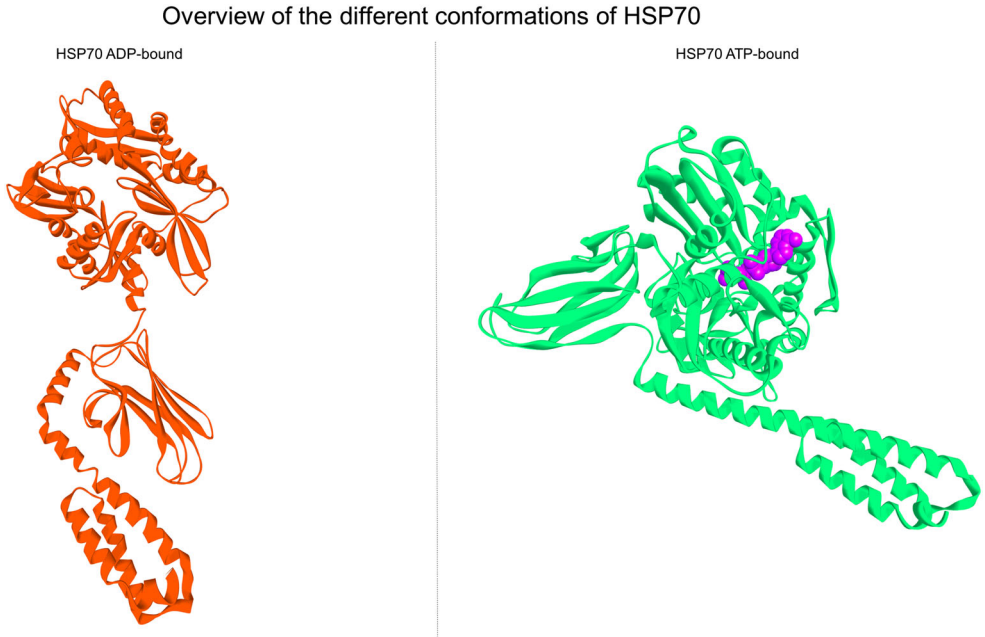

Fig. 1 Overview of the different conformations of HSP70. *Left panel* shows the depiction of PDB file 2KHO, which represents the HSP70 APO state or ADP-bound; *right panel* shows the depiction of the pdb file 4B9Q, which represents the HSP70 ATP state. When HSP70 is bound to an ATP molecule, the SBD lid opens, the NBD becomes more contracted and the overall conformation more compact. Upon ATP hydrolysis to ADP, the SBD lid closes, capturing the substrate. This leads to the relaxation of NBD and extension of the overall conformation

method were used to refine all the docking solutions, allowing us to choose one docking program and one docking structure for each situation (i.e., HSP70 ADP bound to RAGE and HSP70 ATP bound to RAGE).

Normal mode analyses The selected docking solutions were subjected to normal mode analyses using different methods for assessing major potential conformational changes in the complex: elNémo (Suhre and Sanejouand 2004), iMODS (Lopez-Blanco et al. 2014), and ProDy via the Normal Mode Wizard plug-in for VMD (Bakan et al. 2011). Default parameters recommended for each program were employed. To observe possible conformational transitions between different bound and apo states, only the protein coordinates were considered in the calculations. For clarity, we analyzed the first normal mode from each situation and choose the results from iMODS to be represented. The images from each mode are depicted in BIOVIA Discovery Studio 3.5 (Biovia 2015), and the proteins were colored according to the average isotropic displacement which represents the contribution of each residue to the deformability of the system, where blue corresponds to less flexible regions and red corresponds to more flexible regions. In addition, the ribbon size was also represented to match less flexible or more flexible regions, representing the deformability of the structure. For each structure, we created a corresponding scatter plot of the deformability of each residue.

Predictions on the thermostability effect of mutations in the HSP70-RAGE docking complex The mutation energy calculation was used to evaluate the effect of single-point mutations on the binding affinity in the HSP70-RAGE docking complex. Mutagenesis was performed using the Pssm command of FoldX, which mutates each selected residue (selected according to the docking results and analyses of the residues present at the interacting interface) to alanine. The stabilities were calculated using the Stability command of FoldX, and $\Delta\Delta G$ values are computed by subtracting the energy of the WT from that of the mutant. Values were interpreted according to Frappier et al. (2015) (Frappier and Najmanovich 2014) as stabilizing mutations ($\Delta\Delta G < -0.5$ kcal/mol), neutral mutations ($\Delta\Delta G$ [−0.5,0.5] kcal/mol), and destabilizing mutations ($\Delta\Delta G > 0.5$ kcal/mol).

Results

In order to obtain structural evidence to support the hypothesis that HSP70 binds to RAGE, we first compared the amino acid sequences and secondary structures of known RAGE ligands, such as S100B, HMGB1, glycated albumin, and MAC1 protein, with that of HSP70 in both the ADP- and ATP-bound states (PDBs 2KHO and 4B9Q, respectively). No substantial similarities were found, consistent with a previous study (Fritz 2011). However, as shown in this previous work (40), RAGE ligands are predominantly negatively charged molecules. We then calculated the electrostatic surface potential of HSP70 in its different conformations and found it to be negative (Fig. S1), similar to the abovementioned RAGE ligands. Therefore, in order to determine the relationship between the electrostatic properties of HSP70 and its three-dimensional geometry, we performed a series of molecular docking experiments to investigate the possible interaction between the two molecules.

Table 1 Interacting surface information of the best docking solutions generated by ClusPro 2.0

Interacting surface information of HSP70 ATP-bound and RAGE								
	Interaction energy (kcal/mol)	Interface area A ($Å^2$)	Interface area B ($Å^2$)	No. of interacating residues A	No. of interacting residues B	Salt bridges	Hydrogen bounds	Non-bounded contacts
Mode1.00	−9.44961	914	874	19	23	4	21	135
Mode1.01	−26.4293	1397	1331	26	34	6	19	198
Mode1.02	−11.6721	1136	1084	19	22	8	16	106
Mode1.03	−23.9613	1953	1902	33	43	7	34	243
Mode1.04	−15.463	1187	1222	26	25	7	25	192
Mode1.05	−15.9767	1572	1462	29	29	8	23	194
Mode1.06	−18.2888	1331	1269	24	27	6	14	138
Mode1.07	−15.8098	1338	1194	25	33	5	20	143
Mode1.08	−7.3837	1201	1057	20	26	4	19	156
Mode1.09	−2.42895	1654	1513	25	32	7	21	160
Mean	−14.686	1368.3	1290.8	24.6	29.4	6.2	21.2	166.5

Chain A represents HSP70 ATP-bound (PDB/4B9Q) and chain B represents RAGE in the monomeric form (PDB/3CJJ)

Table 2 Interacting surface information of the best docking solutions generated by ClusPro 2.0

Interacting surface information of HSP70 ATP-bound and RAGE oligomeric

	Interaction energy (kcal/mol)	Interface area A ($Å^2$)	Interface area B ($Å^2$)	No. of interacating residues A	No. of interacting residues B	Salt bridges	Hydrogen bounds	Non-bounded contacts
Mode1.00	−22.3043	1695	1500	22	34	11	32	207
Mode1.01	−7.36259	1483	1518	30	26	7	22	199
Mode1.02	−13.4254	1304	1271	17	25	5	23	152
Mode1.03	−4.89881	1056	997	17	24	11	22	161
Mode1.04	−11.0521	1328	1115	18	30	6	21	124
Mode1.05	−17.934	1342	1191	22	29	12	26	179
Mode1.06	−7.39764	1203	1145	25	22	8	18	142
Mode1.07	−20.0421	1474	1422	27	30	9	28	199
Mode1.08	−3.08451	1142	1064	20	23	6	15	154
Mode1.09	−14.6118	1326	1230	29	31	11	23	203
Mean	−12.211325	1335.3	1245.3	22.7	27.4	8.6	23	172

Chain A represents RAGE in the oligomeric form (PDB.4LP5) and chain B represents HSP70 ATP-bound (PDB.4B9Q)

Docking experiments were performed considering the PDB IDs 2KHO for HSP70 in the ADP-bound state and 4B9Q for HSP70 in the ATP-bound state; 3CJJ was used for monomeric RAGE, and 4LP5 was used for oligomeric RAGE with four different macromolecular docking programs: GRAMM-X, PatchDock, Hex, and PIPER via ClusPro 2.0. All docking calculations were performed without restrictions. Docking results were clustered by their docking scores, and the best solution was then submitted to an interaction energy calculation by FoldX. While each program has its own specific strategies, which may make comparisons difficult, their different results may also represent different points on the potential energy surface associated with the complex, which is depth normalized through FoldX.

The results of each method are shown in Supplemental Table 1 and were used to refine all the docking solutions, allowing us to choose one docking program and one docking structure for each situation based on the lowest energy model or the most stable theoretical interaction. A similar approach to choose docking solutions was successfully demonstrated in

Table 3 Interacting surface information of the best docking solutions generated by ClusPro 2.0

Interacting surface information of HSP70 ADP-bound and RAGE

	Interaction energy (kcal/mol)	Interface area A ($Å^2$)	Interface area B ($Å^2$)	No. of interacting residues A	No of interacting residues B	Salt bridges	Hydrogen bounds	Non-bounded contracts
Mode1.00	−13.9867	1527	1467	27	31	9	23	154
Mode1.01	−14.9640	1317	1249	24	28	7	27	173
Mode1.02	−13.5191	1175	1124	19	22	2	16	154
Mode1.03	−10.0052	1244	1182	18	25	4	14	125
Mode1.04	−17.3068	1194	1082	19	27	7	23	180
Mode1.05	−8.7484	1029	1115	22	19	6	12	119
Mode1.06	−13.9595	1699	1417	24	34	4	25	179
Mode1.07	−11.0688	989	1009	21	21	4	17	139
Mode1.08	−8.2834	1431	1551	28	28	7	21	235
Mode1.09	−13.1513	1438	1332	24	30	6	16	181
Mean	−12.549	1304.3	1252.8	22.6	26.5	5.6	19.4	163.9

Chain A represents RAGE in the monomeric form (PDB/3CJJ) and chain B represents HSP70 ADP-bound (PDB/2KHO)

Table 4 Interacting surface information of the best docking solutions generated by ClusPro 2.0

Interacting surface information of HSP70 ADP-bound and RAGE oligomeric

	Interaction energy (kcal/mol)	Interface area A ($Å^2$)	Interface area B ($Å^2$)	No. of interacting residues A	No. of interacting residues B	Salt bridges	Hydrogen bounds	Non-bounded Contracts
Mode1.00	−18.4109	1610	1684	33	32	10	29	220
Mode1.01	−24.6075	1369	1372	30	26	11	33	186
Mode1.02	−15.4286	1256	1558	25	21	4	19	127
Mode1.03	−16.3374	1340	1203	25	33	4	23	145
Mode1.04	−16.2707	2212	2198	34	48	8	30	306
Mode1.05	−8.83572	1960	1721	28	44	12	32	254
Mode1.06	−9.42297	1834	1826	34	33	10	19	107
Mode1.07	−7.12172	1673	1610	35	31	4	19	157
Mode1.08	−13.2064	1622	1631	27	32	7	20	178
Mode1.09	−11.1987	1686	1670	36	37	4	23	202
Mean	−14.084061	1656.2	1647.3	30.7	33.5	7.4	24.7	188.2

Chain A represents RAGE in the oligomeric form (PDB/4LP5) and chain B represents HSP70 ADP-bound (PDB/2KHO)

a previous study (Varecha et al. 2012). We choose to analyze the calculations with the repaired PDBs in order to correct possible errors remaining from the docking force field and from the X-ray structure. These errors could result in non-standard angles or distances, i.e., biased conformations arising from the non-physiological conditions under which the structure was determined. Moreover, in some cases, these errors could represent average rotamers representing two or more true rotamers in equilibrium (Schymkowitz et al. 2005).

Based on the resulting interaction energy, we choose the docking solutions of the simulations performed on the ClusPro 2.0 server for further analysis, allowing us to establish

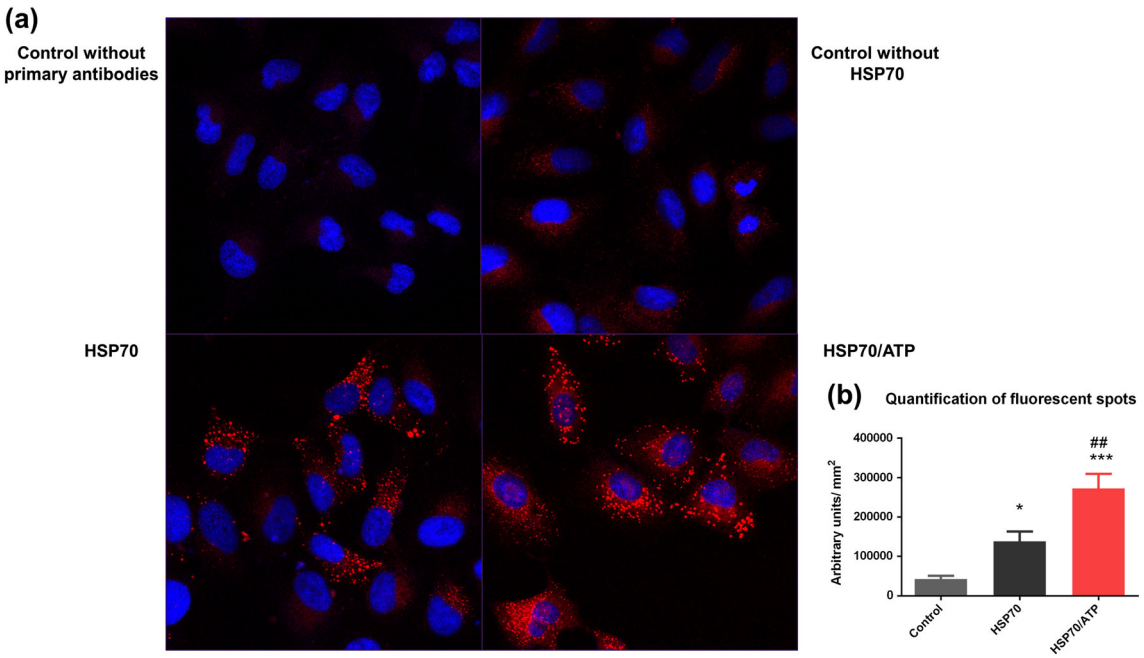

Fig. 2 Fluorescent protein proximity assay. HLA probe chain reacted, producing red fluorescent spots when both target proteins were within interacting range. **a** The *top images* show confocal microscopy analyses of technical control without the addition of primary antibodies and experimental control without the addition of eHSP70. The bottom images show confocal microscopy analyses of A549 cells treated with eHSP70 with or without ATP pretreatment. **b** Fluorescence intensity and morphometric analysis from control and treated cells. The cells were analyzed using the ratio between the intensity of red fluorescence and size of cytoplasm with the ImageJ software. Data are reported as means ± SEM. Statistically significant differences as determined by one-way ANOVA followed by Tukey's test are indicated: $*p < 0.05$; $***p < 0.001$ compared with control group; $\#\#p < 0.01$ compared with HSP70 group

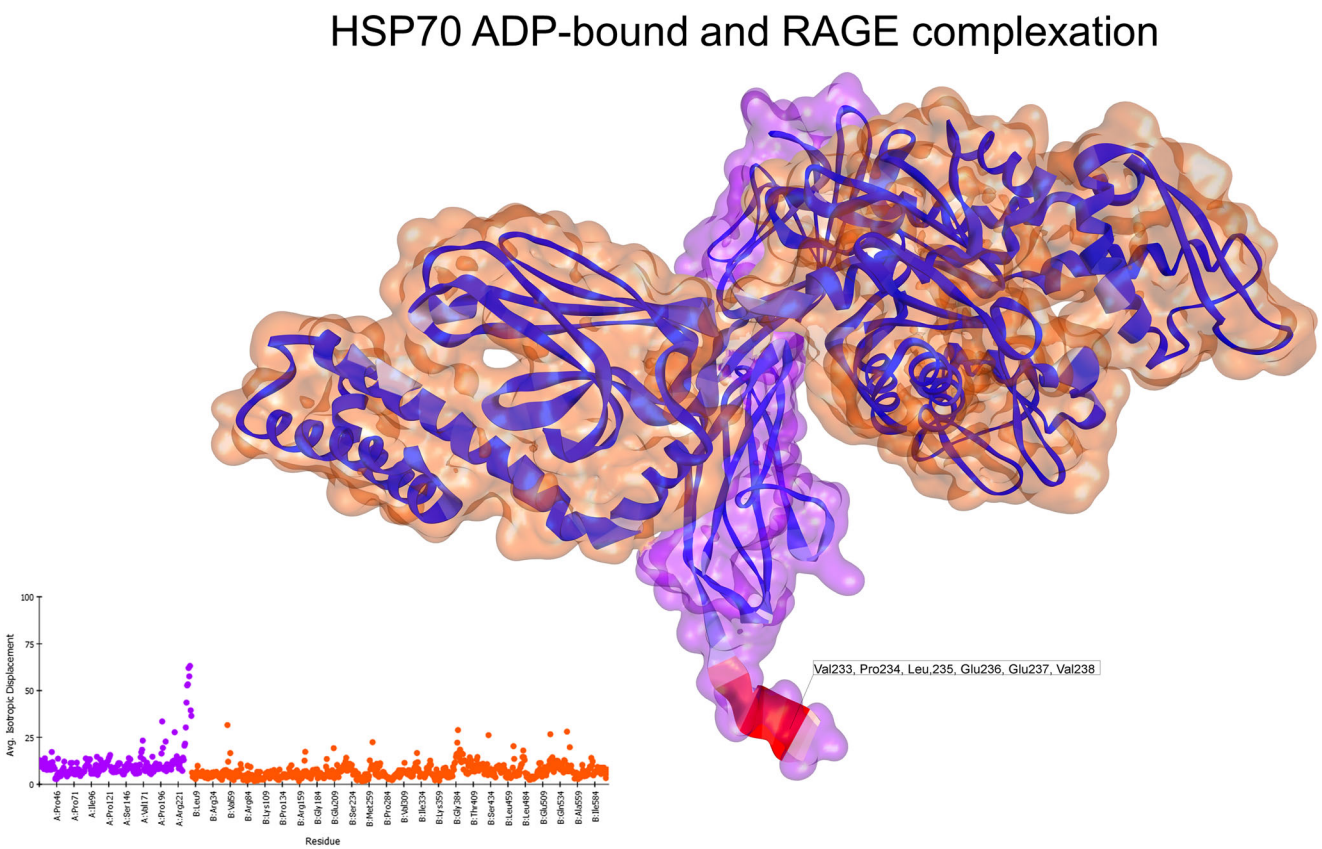

Fig. 3 Normal mode analyses for the complex 3CJJ-2KHO. Structures are shown according to their respective residue deformability. The color scale ranges from *blue* to *red* with increasing flexibility of residues. Every structure includes a corresponding scatter plot for residue deformability. Analysis of the interacting complex between the HSP70 APO state and monomeric RAGE showed that the most flexible regions of the ligand structure were relaxed after the interaction. RAGE surface is colored *purple* and HSP70 surface is colored *orange*. Residues that most contribute to the deformability of the system are indicated

a putative model for HSP70 and RAGE complexation. Tables 1, 2, 3, and 4 show the values for the first ten docking solutions and an in-depth analyses of the interacting interface between HSP70 and RAGE, which contemplates the number of interacting residues, their interface area, and the number of potential hydrogen bonds, non-covalent and non-bonded interactions. This information was later used to identify conserved residues in both HSP70 ADP and ATP-bound, as well as in RAGE and RAGE in its oligomeric form.

In order to confirm that the interaction occurred in vitro, we performed protein interaction assays (Duolink In Situ assays) based on the proximity of the two target proteins using A459 cells, which express high levels of RAGE (Nakano et al. 2006). In this assay, a pair of oligonucleotide-labeled secondary antibodies generates a signal only when the two PLA probes are bound in close proximity to both primary antibodies bound to the sample. Thus, the signal from each detected pair of PLA probes is visualized as a single fluorescent spot. Using confocal microscopy, we found that samples treated with HSP70 exhibited a large number of red fluorescent spots in comparison with the samples that were not incubated with HSP70. When comparing the two experimental groups, the one treated with HSP70 preincubated with ATP showed a higher number of red fluorescent spots in relation to the group treated with only HSP70, as can be seen by both confocal photomicrographs (Fig. 2a) and quantification of the red fluorescent spots (Fig. 2b). These results suggested that the specific conformation of the protein in the extracellular space may be important for the interaction with RAGE. The interaction with RAGE may be more probable and favored in this conformation, whereas in the ADP/APO conformation, the protein may interact with its other receptors with higher affinity, thus creating a possible mechanism that allows a shift in the later cellular signaling cascade.

After detecting and visualizing the interaction by confocal microscopy, we analyzed the best docking solutions (that is, the docking complexes with the lowest interaction energy values) via normal mode analyses in order to observe if the complex underwent any major conformational shifts. Normal mode analysis is a computational technique that allows us to analyze the dynamics of biological macromolecules. This method can provide insights into the large-scale conformational changes occurring in proteins, e.g., upon ligand binding or interaction and complexation, such as the proposed

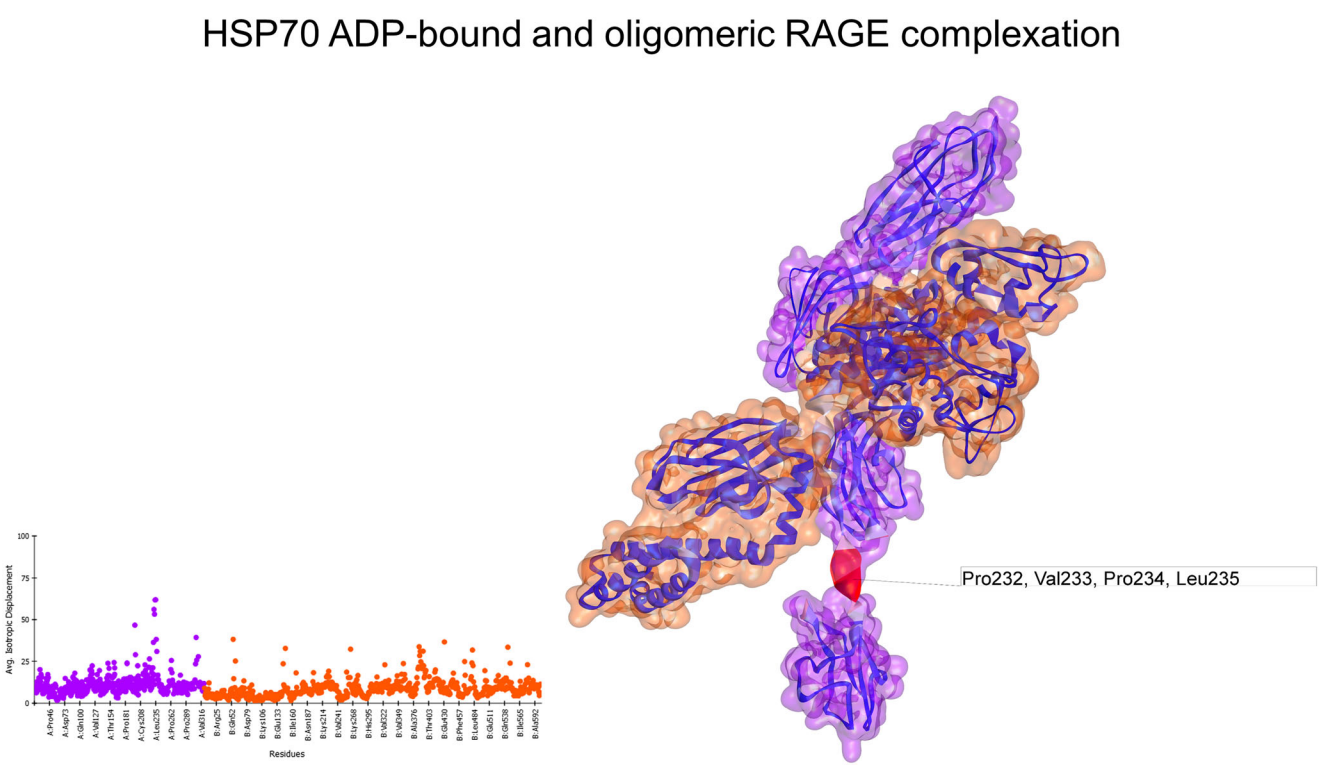

Fig. 4 Normal mode analyses for the complex 4LP5-2KHO. Structures are shown according to their respective residue deformability. The color scale ranges from *blue* to *red* with increasing flexibility of residues. Every structure includes a corresponding scatter plot for residue deformability. Both structures exhibited several spikes of residue deformability. RAGE surface is colored *purple* and HSP70 surface is colored *orange*. Residues that most contribute to the deformability of the system are indicated

interaction between HSP70 and RAGE. The lowest modes are generally thought to dominantly contribute to the global and collective motions of the entire system (Bahar et al. 2010; Mahajan and Sanejouand 2015).

All files involved in the docking simulations were subjected to normal mode analyses prior to complexation, allowing their conformational profiles to be compared under different situations after the interaction. 2KHO, representing the HSP70 ADP-bound, showed a highly flexible region located in the linker between the NBD and the SBD. In addition, the first residues of the helical lid showed high flexibility, consistent with the observation that this region acts as a hinge and is responsible for the opening and closing of the lid over the β-sheet pocket (Fig. S2). The slowest mode also showed that the two domains could rotate in opposite directions, making the protein a not very likely ligand, at least in this conformation. In the model of HSP70 bound to an ATP molecule, the helical lid within the protein was open; however, the overall structure exhibited a more closed, tightened state. Flexible regions were located within the helical lid (Fig. S2).

In its monomeric form (3CJJ), RAGE exhibited only a highly flexible region at the end of the C1 domain. On the other hand, the oligomeric form (4LP5) showed several spikes on the deformability profile of the residues; the most flexible residues were located in the region between the C1 and C2 domains and in the end of the C2 domain (Fig. S3). Normal mode analyses of the docked complex of ADP-bound HSP70 and monomeric RAGE showed that the regions with high flexibility in HSP70 in the ADP-bound state had reduced flexibility after interacting with RAGE. Additionally, the interaction interface showed no major conformational changes or movement (Fig. 3), with an associated interaction energy of −17.80 kcal/mol. In contrast, the complex between HSP70 bound to ADP and oligomeric RAGE exhibited several residues with moderate to high flexibility, as is shown in the depiction and deformability plot (Fig. 4). Nevertheless, the interaction energy (−26.42 kcal/mol) was lower than that of the ATP-bound HSP70 and monomeric RAGE.

The slowest normal mode obtained from the docking between HSP70 in the ATP-bound state (4B9Q) and monomeric RAGE (3CJJ) exhibited an improved deformability plot. Although the helical lid of HSP70 and the C1 domain of RAGE were responsible for some degree of movement, the vast majority of the residues, including those located on the interacting interface, had less flexibility than that observed for the other combinations (Fig. 5). This docking solution had an interacting energy of −22.30 kcal/mol.

The structure 4LP5 had a deformability profile similar to that observed for the interaction with ADP-bound HSP70. Initially, the oligomeric conformation did not appear to be

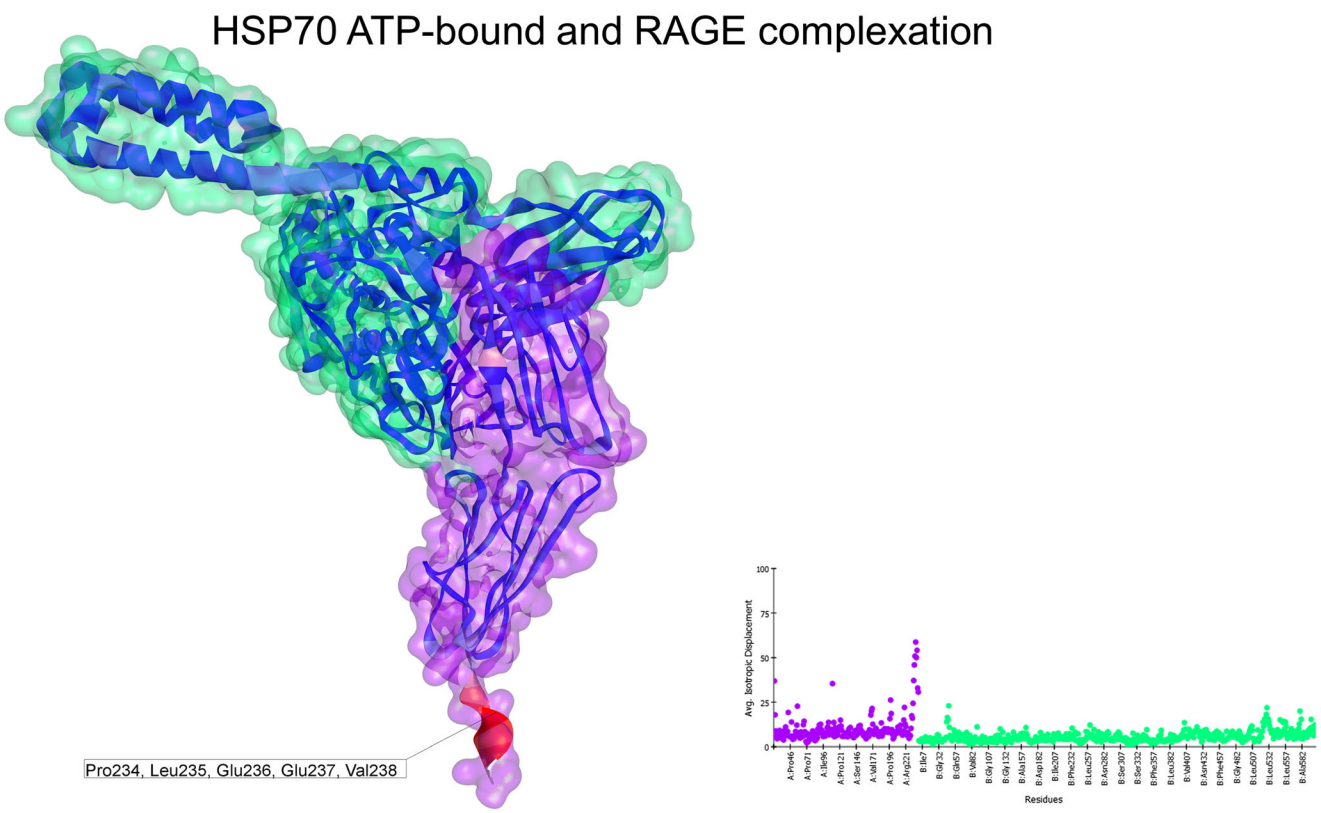

Fig. 5 Normal mode analyses for the complex 3CJJ-4B9Q. Structures are shown according to their respective residue deformability. The color scale ranges from *blue* to *red* with increasing flexibility of residues. Every structure includes a corresponding scatter plot for residue deformability. There was a highly flexible region at the end of the C1 domain of the receptor and a moderately flexible region on the helical lid of HSP70. Overall, this complex exhibited a flattened profile of residue deformability and flexibility compared with the other complexes. Additionally, the interacting region was colored *blue*, indicating the relative stability of this complex. RAGE surface is colored *purple* and HSP70 surface is colored *green*. Residues that most contribute to the deformability of the system are indicated

favorable for any complexation; the structure of HSP70 under these conditions had a higher deformability profile with some spikes in the flexibility of its residues. Moreover, the interaction energy (−26.42 kcal/mol) was lower than that of the monomeric form (Fig. 6).

RAGE residues GLN24, LYS37, ARG216, and ARG218 are present in all docking complexes analyzed, while HSP70 residues GLU206, GLN217, and ASN187 could be important for the interaction of the two proteins and could be targeted for site-directed mutagenesis. A complete list of the interacting residues that form potential hydrogen bonds for every docking situation is presented together with a representation of the structures on supplemental Figs. S4–S7.

The effect of mutations on the thermostability of the HSP70-RAGE docking complex showed that some residues identified to be present on the interacting interface seemed to have an important role on the stability. Mutation of Lys37 and Arg218 of monomeric RAGE resulted on a destabilizing effect when interacting with HSP70 ATP-bound and Arg218 when interacting to HSP70 ADP-bound. Mutation of Arg216 of oligomeric RAGE resulted on a destabilizing effect when the receptor interacts with HSP70 ATP-bound, and mutation of Arg216 and Arg218 resulted on a destabilizing effect when the interaction occurs with HSP70 ADP-bound. HSP70 on its ATP-bound conformation has not been affected by destabilizing mutations on any of the residues, only a mutation on Glu217 resulted on a stabilizing effect when the chaperone interacted with oligomeric RAGE. In contrast, all amino acid mutations resulted on a destabilizing effect on HSP70 in the ADP-bound conformation, with the exception of Asn187 when the chaperone interacted with oligomeric RAGE (Fig. 7).

Discussion

HSP70 was first identified many years ago (Ritossa 1962), and many studies have shown that this protein has a variety of functions in addition to its well-known activity as a chaperone protein. Recently, HSP70 has been shown to be present in serum after induction of different types of stress, such as heavy exercise, inflammation, septic shock, and trauma (Kindas-Mugge et al. 1993; Trautinger et al. 1996a, b). Initially, this extracellular HSP70 was thought to arise from

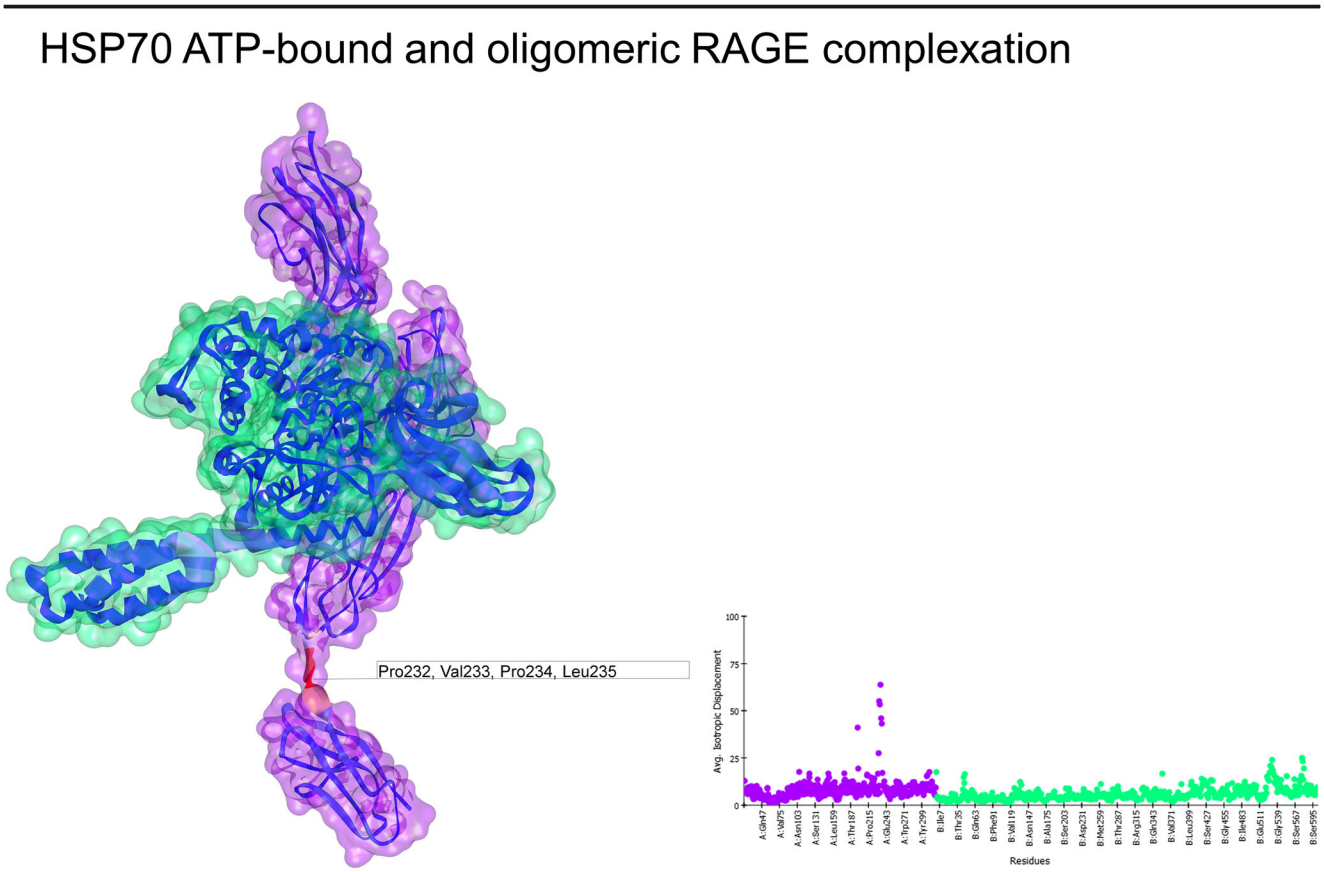

Fig. 6 Normal mode analyses for the complex 4LP5-4B9q. Structures are shown according to their respective residue deformability. The color scale ranges from *blue* to *red* with increasing flexibility of residues. Every structure includes a corresponding scatter plot for residue deformability. RAGE surface is colored *purple* and HSP70 surface is colored *green*. Residues that most contribute to the deformability of the system are indicated

necrotic disruption of cell membranes and extravasation of cytosolic proteins. However, later studies showed that HSP70 could be actively secreted from the intracellular environment to the extracellular space (Vega et al. 2008), suggesting that this protein may have a more prominent role in signal transduction during pathogenic processes.

In a recent study by our laboratory (Gelain et al. 2011), we showed that there is a correlation between clinical outcomes in patients with sepsis and the presence of HSP70 in their serum. Moreover, increased levels of oxidative stress were also associated with increased HSP70 levels in serum in patients who died. Our previous studies (Grunwald et al. 2014) showed that macrophages treated with preoxidized HSP70 exhibited a different pattern of activation compared with that of macrophages treated with HSP70, with lower cell proliferation and viability, lower levels of TNF-α release, and lower phagocytic activity. Similar results, including increased secretion of TNF-α and increased phagocytosis, have been observed in macrophages upon RAGE ligand binding (Fujiya et al. 2014; Ma et al. 2012; Tang et al. 2010), suggesting that RAGE may have unidentified interactions associated with specific signaling pathways.

In this study, we used in silico experiments to confirm the possible interaction between HSP70 and RAGE and to define the mechanism through which such a complexation occurs. The computational simulations provided herein served as guidelines for the additional steps in our experiment design, and the putative models obtained by molecular docking could improve our understanding of this interaction, acting as a baseline for site-directed mutagenesis studies until the exact complex may be obtained through X-ray crystallography. Despite its widespread use, docking has been considered an unreliable technique for the prediction of drug binding (Chen 2015), and macromolecular docking, such as the protein-protein binding predicted here, has improved greatly in the last decade (Musiani and Ciurli 2015; Park et al. 2015).

Theoretically, it is possible for HSP70 in both the ADP/APO and ATP states to complex with RAGE; normal mode analyses showed that the interaction interface did not undergo any major conformational shifts and that the residues in this area did not exhibit elevated flexibility. When these simulations were compared with experiments in actual cells, increased numbers of fluorescent-interacting spots were observed when HSP70 was added in the presence of ATP

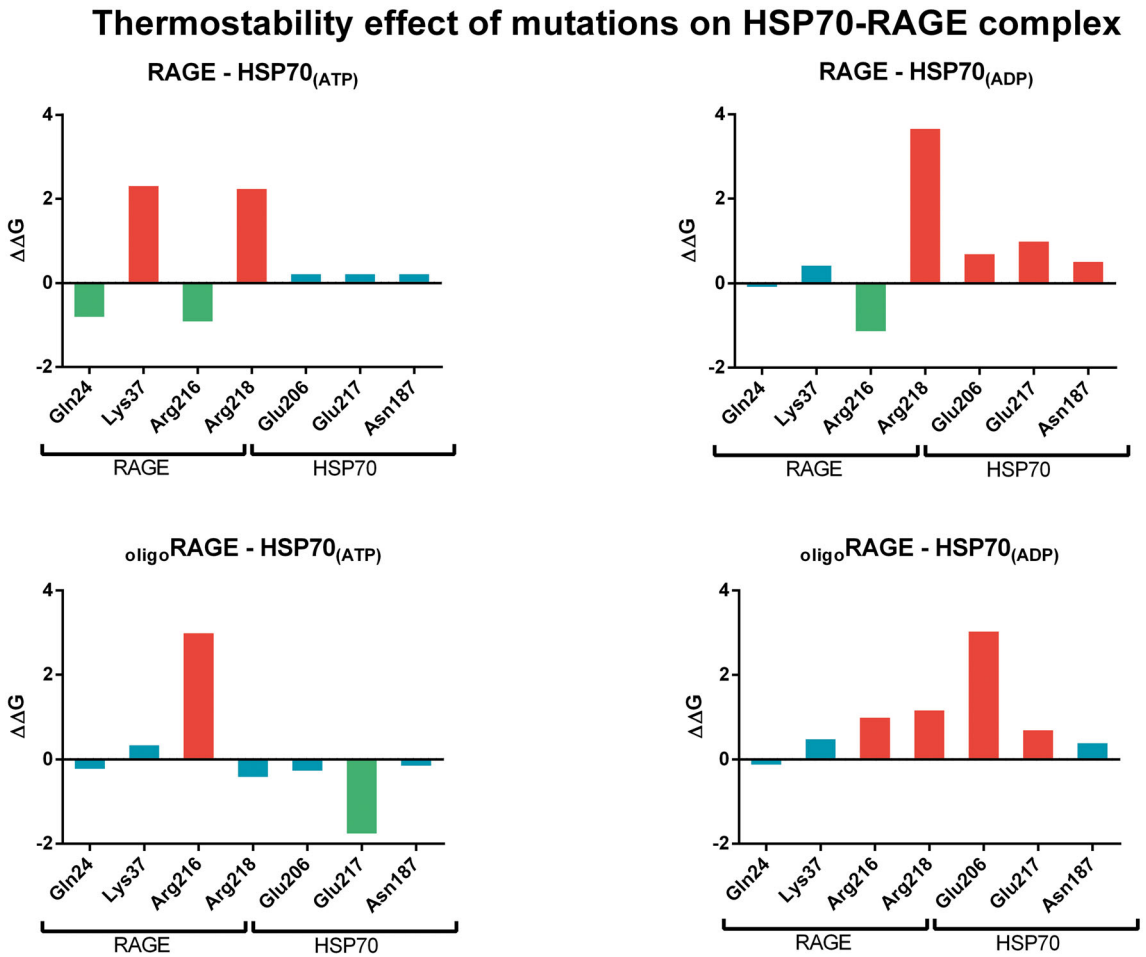

Fig. 7 FoldX energy results and the effect on the thermostability of the HSP70-RAGE docking complex. Stabilizing mutations (ΔΔG < −0.5 kcal/mol) are represented by *green-colored bars*, neutral mutations (ΔΔG [−0.5,0.5] kcal/mol) by *blue bars*, and destabilizing mutations (ΔΔG > 0.5 kcal/mol) are represented by *red-colored bars*

compared with that when HSP70 was added alone. This is consistent with the observed lowest calculated interacting energy for ATP-bound HSP70 and oligomeric RAGE (PDB IDs 4B9Q and 4PL5, respectively). From these observations, we can form hypotheses regarding the conditions under which such an interaction could occur. RAGE has four disulfide bonds when in the monomeric form and ten disulfide bonds in the oligomeric form. In the case of 4LP5, oligomerization occurs between the V domains of the receptor, meaning that the soluble form could interact and complex under the right conditions. This oligomerization can be extended to more than two molecules, increasing the interacting site and creating a larger area capable of interacting with larger proteins, such as HSP70. The abovementioned disulfide bonds could play an important role under pathological conditions involving excessive oxidative stress because these structures could help to stabilize some interactions and particular conformations. Moreover, in all situations, we observed the involvement of different domains of HSP70 when the protein interacted with the receptor.

Our results not only supported the observations made by Ruan and collaborators (12), who showed that there may be an interaction between RAGE and HSP70, but also showed that this interaction occurred within a cell culture model. Thus, our findings demonstrated that the ADP/ATP cycle may be important for mediating the affinity and stability of the interaction and that the different domains of HSP70 may contribute to the strength of the signaling response initiated upon RAGE binding.

This new interaction could have important implications in future studies of the pathological conditions associated with high levels of RAGE expression and the presence of HSP70 in the extracellular medium and serum in response to some form of injury or stress.

Acknowledgements This work was supported by Conselho Nacional de Desenvolvimento Científico e Tecnológico (CNPq), Fundação de Amparo à Pesquisa do Estado do Rio Grande do Sul (FAPERGS), CAPES, and Propesq-UFRGS. The authors thank the Electron Microscopy Center of the Federal University of Rio Grande do Sul for

their assistance with the microscopy analyses. The authors also thank Mr. Henrique Biehl for his technical assistance.

Compliance with ethical standards

Conflict of interest The authors declare that they have no conflicts of interest.

Author contribution JCFM and HV conceived and coordinated the study. DPG helped conceive the idea. MSG designed, performed, and analyzed all the experiments, as well as wrote the manuscript and prepared all the figures. RLB provided technical assistance for normal mode analyses and contributed with the writing of the manuscript. CSS and LH provided technical assistance and contributed to the preparation of Fig. 2. All authors reviewed the results and approved the final version of the manuscript.

References

Arnold-Schild D, Hanau D, Spehner D, Schmid C, Rammensee HG, de la Salle H, Schild H (1999) Cutting edge: receptor-mediated endocytosis of heat shock proteins by professional antigen-presenting cells. J Immunol 162(7):3757–3760

Asea A (2003) Chaperokine-induced signal transduction pathways. Exerc Immunol Rev 9:25–33

Asea A, Kabingu E, Stevenson MA, Calderwood SK (2000a) HSP70 peptidem bearing and peptide-negative preparations act as chaperokines. Cell Stress Chaperones 5(5):425–431

Asea A, Kraeft SK, Kurt-Jones EA, Stevenson MA, Chen LB, Finberg RW, Koo GC, Calderwood SK (2000b) HSP70 stimulates cytokine production through a CD14-dependant pathway, demonstrating its dual role as a chaperone and cytokine. Nat Med 6:435–442. doi:10.1038/74697

Asea A, Rehli M, Kabingu E, Boch JA, Bare O, Auron PE, Stevenson MA, Calderwood SK (2002) Novel signal transduction pathway utilized by extracellular HSP70: role of toll-like receptor (TLR) 2 and TLR4. J Biol Chem 277(17):15028–15034. doi:10.1074/jbc.M200497200

Bahar I, Lezon TR, Bakan A, Shrivastava IH (2010) Normal mode analysis of biomolecular structures: functional mechanisms of membrane proteins. Chem Rev 110(3):1463–1497. doi:10.1021/cr900095e

Bakan A, Meireles LM, Bahar I (2011) ProDy: protein dynamics inferred from theory and experiments. Bioinformatics 27(11):1575–1577. doi:10.1093/bioinformatics/btr168

Baker NA, Sept D, Joseph S, Holst MJ, McCammon JA (2001) Electrostatics of nanosystems: application to microtubules and the ribosome. Proc Natl Acad Sci U S A 98(18):10037–10041. doi:10.1073/pnas.181342398

Becker T (2002) CD40, an extracellular receptor for binding and uptake of Hsp70-peptide complexes. J Cell Biol 158(7):1277–1285. doi:10.1083/jcb.200208083

Bertelsen EB, Chang L, Gestwicki JE, Zuiderweg ER (2009) Solution conformation of wild-type *E. coli* Hsp70 (DnaK) chaperone complexed with ADP and substrate. Proc Natl Acad Sci U S A 106(21):8471–8476. doi:10.1073/pnas.0903503106

Biovia, D. S. (2015). Discovery studio modeling environment (version 4.5). San Diego

Bucciarelli LG, Wendt T, Rong L, Lalla E, Hofmann MA, Goova MT, Taguchi A, Yan SF, Yan SD, Stern DM, Schmidt AM (2002) RAGE is a multiligand receptor of the immunoglobulin superfamily: implications for homeostasis and chronic disease. Cell Mol Life Sci 59(7):1117–1128

Chen YC (2015) Beware of docking! Trends Pharmacol Sci 36(2):78–95. doi:10.1016/j.tips.2014.12.001

Comeau SR, Gatchell DW, Vajda S, Camacho CJ (2004) ClusPro: a fully automated algorithm for protein-protein docking. Nucleic Acids Res 32(Web Server issue):W96–W99. doi:10.1093/nar/gkh354

Delneste Y, Magistrelli G, Gauchat J, Haeuw J, Aubry J, Nakamura K, Kawakami-Honda N, Goetsch L, Sawamura T, Bonnefoy J, Jeannin P (2002) Involvement of LOX-1 in dendritic cell-mediated antigen cross-presentation. Immunity 17(3):353–362

Dolinsky TJ, Nielsen JE, McCammon JA, Baker NA (2004) PDB2PQR: an automated pipeline for the setup of Poisson-Boltzmann electrostatics calculations. Nucleic Acids Res 32(Web Server issue):W665–W667. doi:10.1093/nar/gkh381

Frappier V, Najmanovich RJ (2014) A coarse-grained elastic network atom contact model and its use in the simulation of protein dynamics and the prediction of the effect of mutations. PLoS Comput Biol 10(4):e1003569. doi:10.1371/journal.pcbi.1003569

Frappier V, Chartier M, Najmanovich RJ (2015) ENCoM server: exploring protein conformational space and the effect of mutations on protein function and stability. Nucleic Acids Res 43(W1):W395–W400. doi:10.1093/nar/gkv343

Fritz G (2011) RAGE: a single receptor fits multiple ligands. Trends Biochem Sci 36(12):625–632. doi:10.1016/j.tibs.2011.08.008

Fujiya A, Nagasaki H, Seino Y, Okawa T, Kato J, Fukami A, Himeno T, Uenishi E, Tsunekawa S, Kamiya H, Nakamura J, Oiso Y, Hamada Y (2014) The role of S100B in the interaction between adipocytes and macrophages. Obesity (Silver Spring) 22(2):371–379. doi:10.1002/oby.20532

Galloway E, Shin T, Huber N, Eismann T, Kuboki S, Schuster R, Blanchard J, Wong HR, Lentsch AB (2008) Activation of hepatocytes by extracellular heat shock protein 72. Am J Physiol Cell Physiol 295(2):C514–C520. doi:10.1152/ajpcell.00032.2008

Gelain DP, de Bittencourt Pasquali MA, Comin MC, Grunwald MS, Ritter C, Tomasi CD, Alves SC, Quevedo J, Dal-Pizzol F, Moreira JC (2011) Serum heat shock protein 70 levels, oxidant status, and mortality in sepsis. Shock 35(5):466–470. doi:10.1097/SHK.0b013e31820fe704

Gross C, Schmidt-Wolf IG, Nagaraj S, Gastpar R, Ellwart J, Kunz-Schughart LA, Multhoff G (2003) Heat shock protein 70-reactivity is associated with increased cell surface density of CD94/CD56 on primary natural killer cells. Cell Stress Chaperones 8(4):348–360

Grunwald MS, Pires AS, Zanotto-Filho A, Gasparotto J, Gelain DP, Demartini DR, Schöler CM, de Bittencourt PI Jr, Moreira JC (2014) The oxidation of HSP70 is associated with functional impairment and lack of stimulatory capacity. Cell Stress Chaperones 19(6):913–925. doi:10.1007/s12192-014-0516-5

Kindas-Mugge I, Hammerle AH, Frohlich I, Oismuller C, Micksche M, Trautinger F (1993) Granulocytes of critically ill patients spontaneously express the 72 kD heat shock protein. Circ Shock 39(4):247–252

Kityk R, Kopp J, Sinning I, Mayer MP (2012) Structure and dynamics of the ATP-bound open conformation of Hsp70 chaperones. Mol Cell 48(6):863–874. doi:10.1016/j.molcel.2012.09.023

Koch M, Chitayat S, Dattilo BM, Schiefner A, Diez J, Chazin WJ, Fritz G (2010) Structural basis for ligand recognition and activation of RAGE. Structure 18(10):1342–1352. doi:10.1016/j.str.2010.05.017

Kozakov D, Brenke R, Comeau SR, Vajda S (2006) PIPER: an FFT-based protein docking program with pairwise potentials. Proteins 65(2):392–406. doi:10.1002/prot.21117

Lopez-Blanco JR, Aliaga JI, Quintana-Orti ES, Chacon P (2014) iMODS: internal coordinates normal mode analysis server. Nucleic Acids Res 42(Web Server issue):W271–W276. doi:10.1093/nar/gku339

Ma W, Rai V, Hudson BI, Song F, Schmidt AM, Barile GR (2012) RAGE binds C1q and enhances C1q-mediated phagocytosis. Cell Immunol 274(1–2):72–82. doi:10.1016/j.cellimm.2012.02.001

Macindoe G, Mavridis L, Venkatraman V, Devignes MD, Ritchie DW (2010) HexServer: an FFT-based protein docking server powered by graphics processors. Nucleic Acids Res 38(Web Server issue): W445–W449. doi:10.1093/nar/gkq311

Mahajan S, Sanejouand YH (2015) On the relationship between low-frequency normal modes and the large-scale conformational changes of proteins. Arch Biochem Biophys 567:59–65. doi:10.1016/j.abb.2014.12.020

Musiani F, Ciurli S (2015) Evolution of macromolecular docking techniques: the case study of nickel and iron metabolism in pathogenic bacteria. Molecules 20(8):14265–14292. doi:10.3390/molecules200814265

Nakano N, Fukuhara-Takaki K, Jono T, Nakajou K, Eto N, Horiuchi S, Takeya M, Nagai R (2006) Association of advanced glycation end products with A549 cells, a human pulmonary epithelial cell line, is mediated by a receptor distinct from the scavenger receptor family and RAGE. J Biochem 139(5):821–829. doi:10.1093/jb/mvj092

Park H, Lee H, Seok C (2015) High-resolution protein-protein docking by global optimization: recent advances and future challenges. Curr Opin Struct Biol 35:24–31. doi:10.1016/j.sbi.2015.08.001

Pettersen EF, Goddard TD, Huang CC, Couch GS, Greenblatt DM, Meng EC, Ferrin TE (2004) UCSF chimera—a visualization system for exploratory research and analysis. J Comput Chem 25(13):1605–1612. doi:10.1002/jcc.20084

Ritossa F (1962) A new puffing pattern induced by temperature shock and DNP in drosophila. Experientia 18(12):571–573. doi:10.1007/BF02172188

Ruan BH, Li X, Winkler AR, Cunningham KM, Kuai J, Greco RM, Nocka KH, Fitz LJ, Wright JF, Pittman DD, Tan XY, Paulsen JE, Lin LL, Winkler DG (2010) Complement C3a, CpG oligos, and DNA/C3a complex stimulate IFN-alpha pzcation end product-dependent manner. J Immunol 185(7): 4213–4222. doi:10.4049/jimmunol.1000863

Schmidt AM, Hofmann M, Taguchi A, Yan SD, Stern DM (2000) RAGE: a multiligand receptor contributing to the cellular response in diabetic vasculopathy and inflammation. Semin Thromb Hemost 26(5): 485–493. doi:10.1055/s-2000-13204

Schneidman-Duhovny D, Inbar Y, Nussinov R, Wolfson HJ (2005) PatchDock and SymmDock: servers for rigid and symmetric docking. Nucleic Acids Res 33(Web Server issue):W363–W367. doi:10.1093/nar/gki481

Schymkowitz J, Borg J, Stricher F, Nys R, Rousseau F, Serrano L (2005) The FoldX web server: an online force field. Nucleic Acids Res 33(Web Server issue):W382–W388. doi:10.1093/nar/gki387

Sousa R (2012) A dancer caught midstep: the structure of ATP-bound Hsp70. Mol Cell 48(6):821–823. doi:10.1016/j.molcel.2012.12.008

Suhre K, Sanejouand YH (2004) ElNemo: a normal mode web server for protein movement analysis and the generation of templates for molecular replacement. Nucleic Acids Res 32(Web Server issue): W610–W614. doi:10.1093/nar/gkh368

Tang D, Loze MT, Zeh HJ, Kang R (2010) The redox protein HMGB1 regulates cell death and survival in cancer treatment. Autophagy 6(8):1181–1183. doi:10.4161/auto.6.8.13367

Tovchigrechko A, Vakser IA (2006) GRAMM-X public web server for protein-protein docking. Nucleic Acids Res 34(Web Server issue): W310–W314. doi:10.1093/nar/gkl206

Trautinger F, Kindas-Mugge I, Knobler RM, Honigsmann H (1996a) Stress proteins in the cellular response to ultraviolet radiation. J Photochem Photobiol B 35(3):141–148

Trautinger F, Knobler RM, Honigsmann H, Mayr W, Kindas-Mugge I (1996b) Increased expression of the 72-kDa heat shock protein and reduced sunburn cell formation in human skin after local hyperthermia. J Invest Dermatol 107(3):442–443

van Eden W (2015) Diet and the anti-inflammatory effect of heat shock proteins. Endocr Metab Immune Disord Drug Targets 15(1):31–36

Varecha M, Potesilova M, Matula P, Kozubek M (2012) Endonuclease G interacts with histone H2B and DNA topoisomerase II alpha during apoptosis. Mol Cell Biochem 363(1–2):301–307. doi:10.1007/s11010-011-1182-x

Vega VL, Rodriguez-Silva M, Frey T, Gehrmann M, Diaz JC, Steinem C, Multhoff G, Arispe N, De Maio A (2008) Hsp70 translocates into the plasma membrane after stress and is released into the extracellular environment in a membrane-associated form that activates macrophages. J Immunol 180(6):4299–4307

Yatime L, Andersen GR (2013) Structural insights into the oligomerization mode of the human receptor for advanced glycation end-products. FEBS J 280(24):6556–6568. doi:10.1111/febs.12556

Capítulo 3

“Interação entre o receptor TLR4 e a proteína de choque térmico HSP70”

Metodologia

Docking molecular, análise estrutural e cálculo da energia de interação

As estruturas proteicas identificadas como PDB 5DMI, 5D3I, 2Z64 e 3A79, foram empregadas como os receptores nas simulações de *docking* molecular e, correspondem às proteínas CD40, TLR2, TLR4 e ao complexo TRL2-TLR4, respectivamente. As proteínas identificadas como PDB 2KHO e 4B9Q foram empregadas como ligantes e, correspondem à proteína HSP70 nas suas diferentes conformações, isto é, ligada à ADP e ligada à ATP, respectivamente. As simulações de *docking* molecular foram executadas no servidor PIPER via ClusPro 2.0. Todas as possibilidades de interação foram calculadas sem a imposição de restrições; ou seja, o ligante HSP70 ficou livre para procurar por toda a superfície dos receptores pelo seu sítio de interação preferencial. Os resultados foram agrupados pelo algoritmo do próprio programa de *docking* e então submetidos a um cálculo da energia livre de interação através do software FoldX.

Predições sobre o efeito de mutações na termoestabilidade dos complexos TLR4-HSP70

O cálculo da energia de interação foi utilizado para avaliar o efeito de mutações de resíduos de aminoácidos específicos na afinidade da interação nos complexos TLR4-HSP7 obtidos na etapa anterior. A mutagênese foi executada utilizando o comando Pssm do software FoldX, o qual realiza a troca dos resíduos selecionados por Alanina. As estabilidades dos complexos foram calculadas com o comando Stability, e os valores de ΔΔG foram calculados pela subtração da energia de interação do complexo selvagem (WT – wild type) do complexo mutante. Os valores foram interpretados de acordo com Frappier el al como: mutações de efeito estabilizante (ΔΔG < -0.5 kcal/mol), de efeito neutro (ΔΔG [-0,5,0,5]) e de efeito desestabilizante (ΔΔG > 0,5 kcal/mol).

Todas as análises estruturais e imagens foram realizadas e obtidas utilizando o programa Biovia Discovery Studio 3.5.

Resultados

Complexos HSP70-receptores

Os cálculos de *docking* molecular entre HSP70, representada por suas duas conformações diferentes, ligada à ADP e ligada à ATP, e os diferentes receptores conhecidos por interagirem com a chaperona e responsáveis, em parte, pela sinalização de sua função de chaperoquina. Os melhores complexos gerados pelo programa ClusPro foram submetidos a um cálculo de energia de interação através do programa FoldX. HSP70 ligada à ADP formou complexos com o receptor CD40 (-13.14 kcal/mol), TLR2 (-23.81 kcal/mol), TLR4 (-28.93 kcal/mol) e TLR2-TLR4 (-28.45 kcal/mol). HSP70 ligada à ATP formou complexos com o receptor CD40 (-14.37 kcal/mol), TLR2 (-29.91 kcal/mol), TLR4 (-25.50 kcal/mol) e TLR2-TLR4 (-24.69 kcal/mol). Estes resultados estão apresentados na tabela 1.

Modelo putativo para a interação TLR4-HSP70

Os melhores complexos gerados pelo programa ClusPro 2.0 entre HSP70 ligada à ADP e ligada à ATP e o receptor TLR4 foram analisados mais detalhadamente e suas superfícies de interação foram caracterizadas. Essa informação é encontrada nas tabelas 2 e 3, respectivamente. Os complexos de menor energia de interação foram selecionados e os resíduos presentes na superfície de interação do receptor TLR4 foram comparados com aqueles resíduos que formam interações entre TLR4 e o peptídeo correspondente ao peptídeo MD-2 presente na estrutura PDB 2Z64 (Figura 1). Os resíduos ARG288, AR337, ASP59, ASP53, HIS158, TYR183, ASP264 e PHE62 do receptor TLR4 foram encontrados tanto no complexo cristalizado como no complexo obtido por *docking* TLR4-HSP70 ligada à ADP. Os resíduos ASP59, ASP83 e

LYS263 foram encontrados tanto no complexo cristalizado como no complexo obtido por *docking* TLR4-HSP70 ligada à ATP. Os resíduos do receptor TLR4 ASP59, ASP83, ASN115 e LYS153 foram encontrados na superfície de interação dos dois complexos obtidos por *docking*, mas não no complexo cristalizado. Estes resíduos foram posteriormente submetidos ao processo de mutagênese com a finalidade de avaliar seu efeito na termoestabilidade dos complexos obtidos por *docking*. Apenas mutações nos resíduos ASP59 e ASN115 apresentaram efeito neutro no complexo TLR4-HSP70 ligada à ADP, com valores de ΔΔG de 0,42 e 0,35 kcal/mol, respectivamente; e a mutação do resíduo LYS153 apresentou efeito neutro no complexo TLR4-HSP70 ligada à ATP, com o valor de ΔΔG de 0,39 kcal/mol. Todas as outras mutações apresentaram efeito desestabilizante nos complexos TLR4-HSP70 (Figura 2).

Tabela 1. Resultados das simulações de *docking* molecular entre o receptor TLR4 e a proteína HSP70 nas suas duas diferentes conformações. Os dez melhores resultados obtidos pelo escore interno do programa ClusPro 2.0 foram submetidos a um cálculo de energia de interação externa pelo programa FoldX.

Interaction Energy Analyses (kcal/mol)

HSP70[ADP]

TLR2.TLR4[3A79]		TLR2[5D3I]	
m0	-18.48	m0	-14.01
m1	-18.79	m1	-15.14
m2	-16.66	m2	-22.53
m3	-12.36	m3	-22.53
m4	-11.98	m4	-15.22
m5	-19.3	m5	-14.95
m6	-6.75	***m6***	***-23.81***
m7	-14.45	m7	-21.96
m8	-9.3	m8	-20.86
m9	***-28.45***	m9	-15.93

CD40[5DMI]		TLR4[2Z64]	
m0	-3.15	***m0***	***-28.93***
m1	-2.15	m1	-10.25
m2	-5.38	m2	-7.62
m3	-5.92	m3	-22.50
m4	-11	m4	-28.21
m5	-8.02	m5	-23.88
m6	***-13.14***	m6	-9.66
m7	-6.27	m7	-19.04
m8	-9.53	m8	-24.09
m9	-11.33	m9	-7.92

HSP70[ATP]

TLR2.TLR4[3A79]		TLR2[5D3I]	
m0	-16.28	m0	-10.94
m1	-22.6	m1	-19.23
m2	-17.69	m2	-5.09
m3	***-24.69***	m3	-16.86
m4	-19.36	m4	-27.73
m5	-13.25	m5	-13.18
m6	-24.66	m6	-21.84
m7	-27.18	m7	-14.92
m8	-23.16	***m8***	***-29.91***
m9	-18.87	m9	-16.38

CD40[5DMI]		TLR4[2Z64]	
m0	-3.4	m0	-15.31
m1	-6.5	m1	-21.89
m2	-9.03	m2	-21.27
m3	-2.2	m3	-21.78
m4	-11.92	m4	-10.39
m5	-8.61	***m5***	***-25.50***
m6	-13.39	m6	-15.97
m7	-11.7	m7	-24.73
m8	-5.33	m8	-13.80
m9	***-14.37***	m9	-16.42

Tabela 2. Informações da superfície de interação do complexo TLR4-HSP70 ligada à ADP

Interacting surface information of HSP70 ADP-bound and TLR4

	Interaction energy (kcal/mol)	Interface Area A ($Å^2$)	Interface Area B ($Å^2$)	No. Interacting residues A	No. Interacting residues B	Salt Bridges	Hidrogen Bounds	Non-bounded Contacts
model.00	***-28.93***	1647	1794	36	28	5	22	208
model.01	-10.25	1442	1396	27	25	4	12	166
model.02	-7.62	1385	1524	34	27	2	15	160
model.03	-22.50	1697	1731	37	32	9	33	239
model.04	-28.21	2056	2041	41	31	3	20	169
model.05	-23.88	1732	1822	37	36	13	27	198
model.06	-9.66	1816	1913	40	35	5	22	270
model.07	-19.04	1647	1595	32	33	5	23	158
model.08	-24.09	2091	2134	48	38	6	27	265
model.09	-7.92	1121	1099	19	22	4	14	197
Mean	-18.21	1663.4	1704.9	35.1	30.7	5.6	21.5	203

Table 2. Interacting surface information of the best docking solutions generated by ClusPro 2.0. Chain A represents TLR4 (PDB:2Z64) and chain B represents HSP70 ADP-bound (PDB:2KHO).

Tabela 3. Informações da superfície de interação do complexo TLR4-HSP70 ligada à ATP

Interacting surface information of HSP70 ATP-bound and TLR4

	Interaction energy (kcal/mol)	Interface Area A ($Å^2$)	Interface Area B ($Å^2$)	No. Interacting residues A	No. Interacting residues B	Salt Bridges	Hidrogen Bounds	Non-bounded Contacts
model.00	-15.31	1443	1436	26	27	4	12	106
model.01	-21.89	2136	2168	42	37	6	26	242
model.02	-21.27	1784	1800	38	32	3	20	236
model.03	-21.78	1584	1733	35	24	6	21	189
model.04	-10.39	1726	1834	39	29	8	20	208
model.05	***-25.50***	1542	1529	31	33	6	19	195
model.06	-15.97	1530	1578	30	26	1	14	174
model.07	-24.73	1618	1651	32	26	2	15	161
model.08	-13.80	1241	1226	23	23	3	15	129
model.09	-16.42	1268	1189	22	31	2	11	130
Mean	-18.70	1587.2	1614.4	31.8	28.8	4.1	17.3	177

Table 3. Interacting surface information of the best docking solutions generated by ClusPro 2.0. Chain A represents TLR4 (PDB2Z64:) and chain B represents HSP70 ATP-bound (PDB:4B9Q).

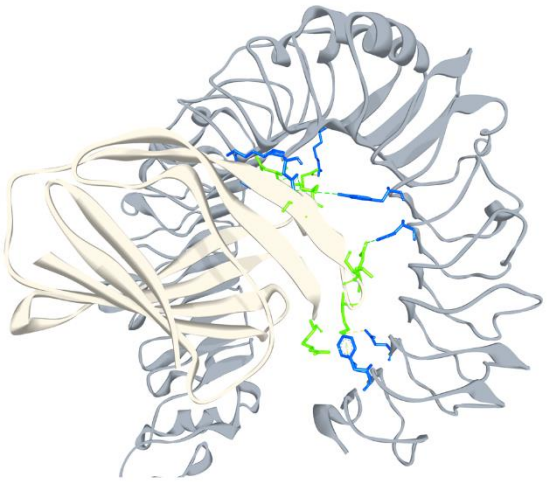

Residues TLR4	Residues Peptide	Interaction	Distance
ARG288:NH1	ASP99:OD2	Hydrogen Bond;Electrostatic	2.87
ARG337:NH1	ASP101:OD1	Hydrogen Bond;Electrostatic	3.07
ASP59:OD2	LYS109:NZ	Hydrogen Bond;Electrostatic	3.26
ASP83:OD2	LYS109:NZ	Hydrogen Bond;Electrostatic	2.85
HIS158:ND1	GLU111:OE1	Hydrogen Bond	2.94
TYR183:OH	SER103:OG	Hydrogen Bond	3.14
LYS263:N	ASP101:O	Hydrogen Bond	2.82
ARG337:NH1	ASP99:O	Hydrogen Bond	2.89
ARG337:NH2	HIS98:O	Hydrogen Bond	2.73
ASP264:OD2	SER103:N	Hydrogen Bond	2.70
ASP264:OD1	SER103:OG	Hydrogen Bond	2.76
ASP264:OD1	THR115:OG1	Hydrogen Bond	2.91
HIS158:CE1	THR112:O	Hydrogen Bond	3.68
ARG288:CD	ASP99:OD2	Hydrogen Bond	3.07
PHE62	ARG68:NH1	Hydrogen Bond	3.50

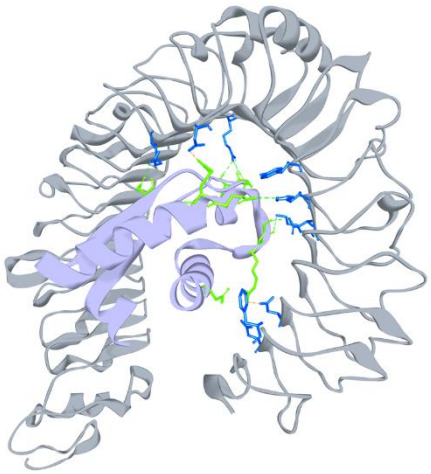

Residues TLR4	Residues HSP70[ADP]	Interaction	Distance
ASP59:OD2	ARG253:NH1	Hydrogen Bond;Electrostatic	2.78
ASP83:OD1	ARG253:NH1	Hydrogen Bond;Electrostatic	2.58
ASP264:OD2	ARG261:NH1	Hydrogen Bond;Electrostatic	2.67
LYS153:NZ	ASN254:OD1	Hydrogen Bond	3.37
ASN155:ND2	ASN254:O	Hydrogen Bond	2.86
ARG288:NH1	ASP289:O	Hydrogen Bond	2.79
ARG288:NH1	THR291:O	Hydrogen Bond	2.73
ARG288:NH2	ALA290:O	Hydrogen Bond	2.66
ARG337:NH1	ASN282:OD1	Hydrogen Bond	2.55
HIS158:NE2	GLN260:NE2	Hydrogen Bond	3.00
PHE62	ASN238:ND2	Hydrogen Bond	3.45

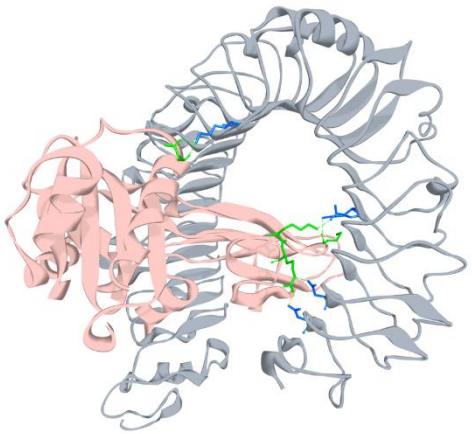

Residues TLR4	Residues HSP70[ATP]	Interaction	Distance
ASP59:OD2	ARG447:NH2	Hydrogen Bond;Electrostatic	2.57
LYS153:NZ	MET404:O	Hydrogen Bond	2.92
LYS263:NZ	GLN325:O	Hydrogen Bond	2.70
LYS263:NZ	GLN325:OE1	Hydrogen Bond	2.91
ASN155:OD1	LYS446:NZ	Hydrogen Bond	2.64
ASP83:OD2	ARG447:NE	Hydrogen Bond	2.88

Figura 1. Complexos obtidos por *docking* entre TLR4 e HSP70. O painel à esquerda mostra os modelos para a interação entre TLR4 e MD-2, TLR4 e HSP70 ligada à ADP e TLR4 e HSP70 ligada à ATP. As estruturas protéicas são representadas como fitas e os aminoácidos que formam interação são representados como paus. A estrutura de TLR4 está colorida de cinza, MD-2 de amarelo suave, HSP70 ligada à ADP de roxo suave e HSP70 ligada à ATP de rosa suave/salmão. Por motivos de clareza, apenas parte da estrutura de HSP70 está representada. Os resíduos de TLR4 estão coloridos de azul, os de HSP70 e do MD-2 de verde. O painel à direita detalha os resíduos e seus átomos que formam interações e a distância é medida em angstroms.

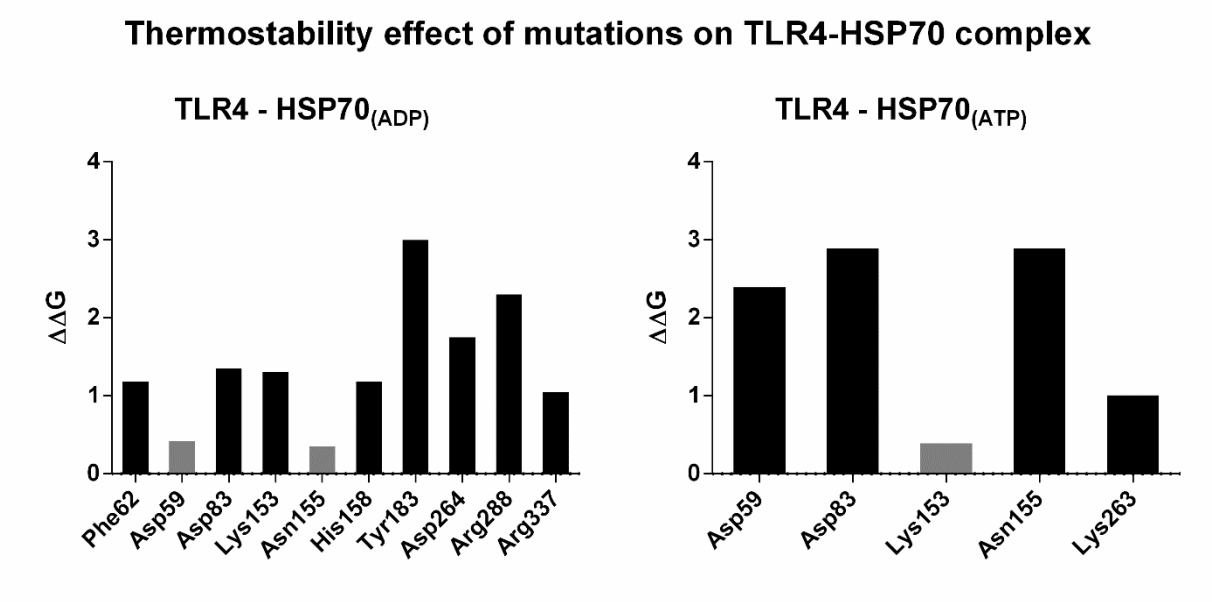

Figura 2. Resultados dos cálculos da energia de interação dos mutantes e de seus efeitos na termoestabilidade dos complexos TLR4-HSP70 obtidos por *docking* molecular. Mutações de efeito neutro (ΔΔG[−0.5,0.5] kcal/mol) estão representadas por barras cinza claro e mutações de efeito desestabilizante (ΔΔG > 0.5 kcal/mol) estão representadas por barras pretas.

Parte 3

4. Discussão

Muitos anos se passaram desde que a HSP70 foi descoberta; os estudos atuais nos mostram que suas funções e seus papéis são muito maiores do que a atividade de chaperona primeiramente descrita. Recentemente, essas proteínas têm sido observadas presentes no soro após diversas formas de estresse (exercício físico intenso, processos inflamatórios, choque séptico e trauma); em um primeiro momento, pensou-se que sua presença era causada pelo rompimento da membrana celular de células em processo de necrose com consequente extravasamento do conteúdo proteico citosólico, incluindo a HSP70. Logo após, foi demonstrado que a HSP70 poderia ser ativamente secretada de um ambiente intracelular para um ambiente extracelular, levando à hipótese de que essa proteína poderia ter um papel muito mais complexo e importante na sinalização celular durante processos patogênicos.

No ano de 2011, na publicação **Serum Heat Shock Protein 70 Levels, Oxidant Status, And Mortality In Sepsis** (**Anexo I**) nosso grupo de pesquisa demonstrou a relação entre a presença da HSP70 no soro de pacientes com sepse, os níveis séricos de estresse oxidativo e o desfecho clínico. Os mecanismos moleculares que estão por trás da sepse são complexos e relacionam-se com diferentes níveis de coordenação metabólica; por isso, faz-se importante estudar e caracterizar as perturbações celulares e moleculares decorrentes da sepse. Fato este, que é evidenciado pelas diferentes conclusões dos estudos bioquímicos realizados acerca deste assunto quando tentam atribuir funções e elucidar mecanismos baseados em aspectos isolados. Temos como exemplo, diversos estudos animais e ensaios clínicos que associam a sepse com o desbalanço redox e estresse oxidativo; enquanto que outros estudos falham ao estabelecer uma correlação entre terapias baseadas em antioxidantes e a melhora na condição séptica (Berger and Chiolero 2007, Andrades, Ritter et al. 2009, Rinaldi, Landucci et al. 2009). Esse fato é também verdadeiro em relação aos estudos sobre as funções HSP70 na sepse. Modelos animais e celulares corroboram com a existência de uma relação entre HSP70 e sepse, porém,

observações clínicas não obtiveram êxito em estabelecer uma correlação direta entre a modulação da HSP70 e um efeito protetor contra o choque séptico (Bruemmer-Smith, Stuber et al. 2001).

Com base no fato de que a sinalização redox exerce uma importante influência na regulação da resposta do sistema imunológico contra a sepse, foi demonstrado que os níveis séricos de HSP70 são modulados de acordo com o status oxidativo do soro, o qual varia de acordo com o paciente. Assim, é possível que a amplitude do estresse oxidativo possa contribuir com a modulação dos níveis séricos de HSP70, através de um aumento na expressão e da liberação da HSP70 para o meio extracelular e também pela liberação por células necróticas. Uma vez no espaço extracelular, a HSP70 funciona como uma das proteínas enquadradas na teoria "danger signal", realizando uma sinalização imunoestimulatória, ativando receptores TLR2 e TLR4, aumentando a liberação de TNF-α e citocinas pró-inflamatórias, espécies reativas de oxigênio e óxido nítrico, principalmente de macrófagos.

De modo geral, é possível concluir que os níveis séricos de HSP70 são modulados de acordo com o estado oxidativo durante a sepse, e, que os níveis elevados de HSP70 no soro estão associados à mortalidade dos pacientes.

Tomando como base as crescentes observações sobre a HSP70 extracelular e os dados mencionados no **anexo I**, nós procuramos no **capítulo 1** estabelecer e elucidar os mecanismos por trás da relação existente entre o estado redox, HSP70 e os efeitos decorrentes. Para isso, nós submetemos a HSP70 purificada a ação um agente oxidante e avaliamos as mudanças estruturais na proteína e os efeitos da oxHP70 na viabilidade celular e nas propriedades imunomodulatórias de macrófagos em cultura celular.

Quando submetida a um agente oxidante (peróxido de hidrogênio), a HSP70 apresentou algumas alterações no perfil eletroforético com tampão de amostra redutor, a banda majoritária

da proteína de 70 kDa e a banda de 140 kDa (peso molecular da provável forma dímérica) diminuíram em intensidade conforme o gradiente do agente oxidativo aumentou, sugerindo que o ambiente oxidativo está danificando a proteína e, possivelmente, alterando em algum nível sua estrutura. Em condições não-redutoras, a eletroforese da HSP70 e da oxHSP70 evidenciou uma banda de aproximadamente 90 kDa, que não é aparente no gel sob condições redutoras. Apesar de não podermos estabelecer exatamente qual o processo responsável pelo surgimento dessa banda, é bastante provável que seja um mecanismo redox dependente, tal como a formação ou redução de ligações dissulfeto, visto que essa banda também diminui em intensidade quando a HSP70 é submetida a concentrações maiores de H_2O_2. Assim, essa banda pode corresponder a uma forma intermediária, redox-modificada da HSP70.

A formação de ligações dissulfeto intramoleculares e intermoleculares sob condições redox é uma das modificações mais marcantes das proteínas que contêm resíduos de cisteína. Para avaliar o papel das ligações dissulfeto e/ou das interações entres os resíduos de cisteína, nós bloqueamos os possíveis sítios de formação de ligações dissulfeto com o pré-tratamento da HSP70 com o agente alquilante iodoacetamida; assim, quando a proteína é incubada com o agente oxidante, as ligações dissulfeto são impedidas de acontecer. O perfil eletroforético resultante nessas condições mostrou uma leve divisão da banda majoritária de 70 kDa, sugerindo que esta banda era formada por bandas de peso molecular muito próximo, e, que este processo pode estar relacionado à correta interação entre os resíduos de cisteína.

De um modo geral, nossos resultados são similares aos encontrados por Callahan et. al., nos quais a HSP70 apresentou uma aquisição diferencial de peptídeos antigênicos sob condições de estresse oxidativo e também ganho de estruturas secundárias (Callahan, Chaillot et al. 2002).

Cumming el. al. também demonstrou que durante condições de estresse oxidativo a HSP70 pode formar ligações dissulfeto mista, resultando em uma forma dimérica de 140 kDa ou até mesmo uma forma oligomérica de peso molecular maior (Cumming, Andon et al. 2004).

É válido mencionar que realizamos diversas tentativas de quantificar e qualificar as modificações estruturais ocasionadas pelo tratamento da HSP70 com um agente oxidativo através de espectrometria de massas, tanto por MALDI-TOFF quanto por Q-TOF. Nossos esforços não foram exitosos, provavelmente devido a um procedimento inadequado no que diz respeito ao preparo das amostras ou a uma inadequada abordagem de avaliação dos resultados obtidos.

Se a HSP70 extracelular está envolvida com processos inflamatórios, e estes são associados com estresse oxidativo e desbalanço redox, nós nos perguntamos quais seriam os efeitos in vitro da oxidação da HSP70 sobre a modulação da ativação de células do sistema imunológico? Para responder essa questão, macrófagos da linhagem RAW 264.7 foram tratados por 30, 60, 120 minutos, e 24 horas com a HSP70 pré-tratada ou não com agente oxidante e avaliamos a produção de nitrito e proliferação e viabilidade celular. Em relação à produção de nitrito, não foram observadas diferenças significativas; porém, a proliferação celular quantificada pela técnica de SRB mostrou que os macrófagos tratados com oxHSP70 apresentam menor proliferação do que os não tratados e do que os tratados com HSP70 após 24 horas de tratamento.

Outro fato interessante também foi observado: a atividade fagocítica dos macrófagos estava diminuída nas células tratadas com oxHSP70 quando comparadas com as não tratadas e com o controle, sugerindo que a oxHSP70 não ativou os macrófagos RAW 264.7 com a mesma eficácia que a HSP70.

Sabe-se que a HSP70 tem a habilidade de induzir a ativação de macrófagos; um dos parâmetros observados quando este evento ocorre é a produção de citocinas inflamatórias, tais como IL8, IL10 e TNF-α. Macrófagos RAW 264.7 foram tratados com HSP70 ou oxHSP70 por 24 horas e o conteúdo de TNF-α no meio de incubação foi analisado. Os grupos tratados com oxHSP70 apresentaram níveis de TNF-α semelhantes aos do grupo controle; além disso, a liberação de TNF-α pelas células tratadas foi maior quando comparada a tanto com os grupos tratados com oxHSP70 quanto com o grupo controle, sugerindo que a oxHSP70 não foi capaz de ativar os macrófagos RAW 264.7 pela via clássica.

Sabe-se que a citocina TNF-α têm um importante papel na proliferação, apoptose e diferenciação de macrófagos. A sobrevivência a longo prazo dos macrófagos é dependente da sinalização autócrina por TNF-α (Lombardo, Alvarez-Barrientos et al. 2007). Devido ao fato de a TNF-α mediar muitos dos efeitos patológicos da interação LPS-TLR4 em condições patológicas, como na sepse por exemplo, é sugerido que a sobrevivência prolongada dos macrófagos mediada por TNF-α têm um importante papel no curso da sepse (Conte, Holcik et al. 2006); assim, esse fato pode ser relacionado com nossos resultados que mostram que após 24 horas de tratamento com oxHSP70 os macrófagos da linhagem RAW 264.7 produziram menores níveis de TNF-α e também tiveram menor viabilidade e proliferação celular.

De um modo geral, a HSP70 pode ser liberada no meio extracelular com um "sinal de perigo" (teoria "danger signal") para o sistema, pois ela pode ser reconhecida pelos receptores TLR2 e TLR4 e desencadear uma rota de sinalização pró-inflamatória. Proteínas caracterizadas como sinais de perigo também são conhecidas como DAMPS (*damage-associated molecular-pattern*). Nesse contexto, nós podemos inferir que a oxidação e subsequente modificação com prejuízo da estrutura proteica da HSP70 pode ser relacionado à perda desse "sinal de perigo" quando ele se faz necessário. Recentemente, foi observado que a proteína HMGB1 (*High*

mobility group box 1 protein) atua como um DAMP e apresenta diferentes formas redox dependentes, as quais são responsáveis por promover o recrutamento celular ou a liberação de citocinas pró-inflamatórias de uma forma bastante similar à da HSP70 (Venereau, Casalgrandi et al. 2012). Luong et. al. demonstrou que o estimulo de TLR4 pela HSP70 requer que a proteína seja apresentada com integridade estrutural; o tratamento da HSP70 com uma proteinase reduziu sua capacidade estimulatória (Luong, Zhang et al. 2012), corroborando com o fato de que a proteína atua como um DAMP e com os nossos resultados.

Além disso, a oxHSP70 poderia exercer seus efeitos pela ativação de outros receptores além dos TLR2, TLR4 e CD40, como o receptor dos produtos finais de glicação avançada (RAGE), um receptor de padrões capaz de ligar a um vasto repertório de proteínas solúveis e também associadas à membrana envolvidas na resposta do hospedeiro à injúria tecidual, infecção e inflamação. Em um estudo recente (Ruan, Li et al. 2010), foi demonstrado através de um ELISA screening que a HSP70 é um dos novos possíveis ligantes de RAGE. A ligação de RAGE induz a ativação de múltiplas rotas de sinalização celular que podem variar de acordo com o agonista, tipo celular e microambiente tecidual, e assim é o mediador de diversas respostas celulares, tais como a observada após o tratamento com oxHSP70 nos macrófagos.

Ainda assim, é importante salientar que os efeitos imunológicos das HSPs podem variar dependendo de diversos fatores, incluindo a família da proteína de choque térmico (HSP60, HSP70, HSP90), a fonte celular de HSP (normal, cancerosa, infecção-viral ou bacteriana), a localização celular (intracelular, extracelular ou associada à membrana) e ainda as circunstâncias fisiológicas modulando a expressão de HSP (estresse oxidativo, infecção bacteriana, infecção viral, estresse físico, etc.). Assim, o contexto fisiológico específico no qual essas proteínas estão inseridas tem um grande impacto na sua função, impedindo qualquer

afirmação global sobre as funções imunológicas in vivo da HSP70 (Johnson and Fleshner 2006).

Levando em consideração os resultados apresentados no **capítulo 1** e as informações presentes no **anexo I**, é sugerido que em uma situação pró-oxidante, comum a todos os processos patológicos, a HSP70 pode sofrer modificações estruturais as quais podem levar à perda da funcionalidade da proteína, como a observada nos pacientes sépticos. No **capítulo 2** foi demonstrado que a HSP70 oxidada induz um decréscimo na viabilidade e na proliferação de macrófagos RAW 264.7 após 24 horas de tratamento e um decréscimo na produção de TNF-α. Assim, acredita-se que essa relação possa estar correlacionada com o desfecho clínico observado anteriormente.

Apesar de os efeitos celulares da HSP70 extracelular serem descritos através da interação com TLR-2, TLR-4 e CD40 em macrófagos, os efeitos exercidos e observados pela oxHSP70 não podem ser explicados, em sua totalidade, através dessa interação, como exposto por Asea et al, 2002, trabalho no qual o autor aponta que a sinalização desencadeada pela interação da HSP70 com um receptor de membrana ainda não está completamente elucidada, e, nem todos os receptores participantes dessa interação estão descritos (Asea, Rehli et al. 2002). Em 2010, Ruan et al, publicou um trabalho no qual é demonstrada a interação por afinidade de ligação entre HSP70 e RAGE, através de um ensaio de screening para novos ligantes através de ELISA. Quando comparadas lado a lado, as rotas de sinalização celular ativadas pela ligação de um agonista ao RAGE e ao TLR são compartilhadas em diversos pontos, sendo bastante difícil a caracterização de qual rota está ativa somente pela identificação de seus componentes downstream.

Considerando as novas informações acerca da interação HSP70 e RAGE, e que no capítulo 1 observamos que os macrófagos tratados com a proteína oxidada exibiram um padrão de

ativação diferente dos macrófagos tratados com a proteína íntegra: menor proliferação e viabilidade celular, menores níveis de liberação de TNF-α e menor atividade fagocítica, sugere-se a hipótese de que este receptor possa apresentar interações ainda não identificadas e caracterizadas, as quais, por sua vez, resultem em vias de sinalização específicas; uma vez que resultados semelhantes, incluindo o aumento na secreção de TNF-α e na atividade fagocítica foram observados em macrófagos diante da interação de ligantes com o receptor RAGE (Tang, Loze et al. 2010, Ma, Rai et al. 2012, Fujiya, Nagasaki et al. 2014). Dessa forma, nós estabelecemos no **capítulo 2** o objetivo de identificar essa interação através de *docking* molecular refinado pela análise de seus modos normais e comprovada pela observação qualitativa e quantitativa de sondas fluorescentes, tentando caracterizá-la, fortalecendo e corroborando com a ideia.

Nesse estudo fizemos uso de experimentos *in silico* com a finalidade de confirmar a possibilidade de interação entre HSP70 e RAGE e definir o mecanismo responsável por esta complexação. As simulações computacionais realizadas serviram como guias para as etapas posteriores do desenho experimental, e os modelos putativos obtidos através de *docking* molecular podem ajudar na compreensão dessa interação, atuando como indicadores em futuros estudos de mutagênese sítio-dirigido até que as estruturas exatas sejam determinadas por algum meio físico, como por exemplo cristalografia de raios-x e ressonância nuclear magnética (NMR). Apesar de sua ampla utilização, técnicas de *docking* são, geralmente, consideradas não confiáveis para a predição da interação de fármacos; enquanto que o chamado *docking* macromolecular, como o aplicado neste trabalho, tem recebidos diversas melhorias na última década (Musiani and Ciurli 2015, Park, Lee et al. 2015).

Em teoria, é possível que a molécula de HSP70 nas suas duas conformações, ligada à ADP e à ATP possa se complexar com o RAGE; a análise de modos normais nos mostra que a interface

de interação não apresenta nenhuma alteração conformacional substanciosa e que os resíduos dessa área não exibem flexibilidade elevada; pelo contrário, as regiões de maior flexibilidade observadas na análise de modos normais das proteínas não complexadas são atenuadas após a interação, sugerindo que ocorra uma estabilização da estrutura do ligante após a complexação com o receptor. Quando essas simulações são comparadas com experimentos realizados em modelos de cultura celular, é possível observar um aumento no número de pontos fluorescentes quando a HSP70 é adicionada na presença de ATP em contraste à quando a proteína é adicionada sem o nucleotídeo. Essa observação é consistente com a energia de interação mais baixa, calculada na interação entre HSP70 ligada à ATP e RAGE na sua forma oligomérica (PDB: 4B9Q e 4LP5, respectivamente). Com base nessas observações, podemos formar hipóteses de acordo com as condições nas quais essa interação pode ocorrer. O receptor RAGE possui 4 ligações dissulfeto quando está na sua forma monomérica, e 10 quando na sua forma oligomérica. No caso da estrutura representada pelo PDB:4LP5, o processo de oligomerização ocorre entre os domínios V do receptor, isso significa que a forma solúvel pode interagir e complexar com a forma presente na membrana sob as condições necessárias. Essa oligomerização pode ser ampliada para mais de duas moléculas, aumentando a porção onde ocorrem ligações, criando uma área maior capaz de interagir com proteínas de elevado peso molecular, como a HSP70. As interações dissulfeto podem também ter um importante papel em situações patológicas que envolvam estresse oxidativo, pois essas estruturas ajudam a estabilizar algumas interações e conformações específicas. Além disso, em todas as situações foi possível observar a participação de diferentes domínios da HSP70 quando a proteína interage com o receptor.

Os resíduos GLU206, GLU217 e ASN187 da proteína HSP70 foram encontrados nas superfícies de interação de todos os complexos; porém, apenas quando a interação ocorre entre RAGE, tanto nas suas formas monomérica e oligomérica, e HSP70 ligada à ADP, é possível

observar mutações com efeito desestabilizante para o complexo. Uma vez que o contrário não é observado com a interação que ocorre com a HSP70 ligada à ATP, pode-se sugerir que a conformação da chaperona desempenha papel importante na interação com o receptor. A conformação ligada à ATP apresenta uma estrutura mais compacta em relação à estrutura quando ligada à ADP, isso poderia, em parte, explicar a preferência de interação, observada tanto nos cálculos de energia de interação dos complexos obtidos por *docking* como no experimento de fluorescência. Ainda assim, temos que considerar que os níveis de ATP no meio extracelular são mais baixos do que no meio intracelular, e que, possivelmente, a proteína HSP70 deveria ser transportada ativamente com uma molécula de ATP para o meio extracelular para que a interação com RAGE ocorra.

Antes de a interação HSP70-RAGE ser considerada, os receptores da família toll-like já eram apontados, com base em diversas evidências experimentais, como os receptores responsáveis pela sinalização celular da qual decorrem os efeitos de citocina da HSP70. No **capítulo 3** tivemos como objetivo comparar as diferentes formas e afinidades de interação da proteína HSP70 com os receptores CD40, TLR2, TLR4 e o complexo TLR2-TLR4 através de uma série de experimentos de *docking* molecular e do cálculo das suas energias de interação.

De modo geral, pode-se notar maiores valores de energia de interação calculada para os complexos formados entre HSP70 e CD40 em comparação com as energias calculadas para os complexos entre HSP70 e os receptores toll-like. Estes valores são ainda menores do que aqueles observados no **capítulo 2**, para a interação com RAGE, reforçando as teorias que apontam o TLR4 como o principal, mas não como sendo o único e exclusivo, receptor de HSP70. Estas conclusões sugerem que possa existir alguma situação ou fator que altere a preferência da HSP70 por um ou outro receptor, modulando não somente a interação, mas os seus efeitos decorrentes.

É importante salientar que a aplicação da técnica de *docking* molecular é utilizada, geralmente, na predição da possibilidade de interação e do modo de interação entre duas macromoléculas, mesmo que esta interação não tenha sido caracterizada a nível estrutural. A interação entre HSP70 e TLR4 não possui estrutura resolvida por cristalografia de raios-x ou obtida por ressonância magnética nuclear, porém, diversos experimentos em diferentes modelos de cultura celular foram responsáveis pela aceitação dessa interação. Assim, fica excluído de nosso objetivo "provar" essa ocorrência, apenas caracterizamos e utilizamos as informações de modo comparativo. A estrutura representativa de TLR4 utilizada nesta etapa apresenta o peptídeo MD-2 co-cristalizado. Este peptídeo é capaz de se associar à região extracelular de TLR4, formando um complexo TLR4-MD-2 responsável pela interação com LPS (lipopolissacarídeo), sendo essencial para o seu reconhecimento. Quando analisamos a superfície de interação entre TLR4 e MD-2, encontramos além do modo de interação similar, na mesma região, resíduos de TRL4 que também estão presentes nas interações dos complexos TLR4-HSP70; sendo que a interação do receptor com HSP70 ligada à ADP apresenta um número maior de aminoácidos compartilhados entre as duas situações. Quando submetidos à experimentos de mutagênese, os resíduos Phe62, Asp83, Lys153, His158, Tyr183, Asp264, Arg288 e Arg337 tem efeito desestabilizante na termoestabilidade do complexo TLR4-HSP ligada à ADP, sugerindo que esta seja a conformação favorecida ou com maior probabilidade de interação com o receptor. Além disso, a energia de interação calculada é de -28.93 kcal/mol para a interação com HSP70 ligada à ADP contra -25.50 kcal/mol para a interação com HSP70 ligada à ATP.

Considerando que o peptídeo MD-2 atua como um componente essencial na apresentação e reconhecimento de ligantes de TLR4, sejam eles agonistas ou antagonistas, como por exemplo LPS e Eritran, é possível que a proteína HSP70 também tenha atuação semelhante. Como parte de sua função de chaperona, a proteína poderia fazer o intermédio entre ligante e receptor, assim como o faz uma proteína do complexo MHC. Ademais, essa função também poderia explicar a

interação com o receptor RAGE, assim teríamos uma situação hipotética na qual a HSP70 apresenta ligantes ao receptor, não sendo por si própria responsável pelos efeitos celulares observados.

Independentemente da sua forma exata de atuação, os resultados aqui apresentados nos levam a formação de situações distintas, nas quais as diferentes conformações da HSP70 interagiriam fisicamente ou com RAGE ou com TLR4, sob condições fisiológicas ou patológicas, e que a ação de um agente oxidante, seja por consequência de um agravamento de estresse oxidativo, é capaz de modificar a estrutura da proteína reduzindo e até cessando os efeitos celulares observados. Assim, em condições fisiológicas ou quando for necessário que as células do sistema imunológico sejam ativadas, é possível que ocorra a translocação ativa da HSP70 para o meio extracelular; a proteína na conformação ligada à uma molécula de ADP apresenta sua tampa de alfa hélice fechada sobre algum substrato peptídico, o qual pode ser apresentado ao receptor TLR4, com consequente sinalização e observação de parâmetros de ativação celular. Em contrapartida, em condições patológicas, a proteína HSP70 na sua conformação ligada à ATP, pode estar presente no meio extracelular devido ao rompimento de células necróticas, alterando sua preferência de ligação, interagindo dessa forma com o receptor RAGE. Essa interação por sua vez, pode ser responsável pelo agravamento do processo patológico e pelo estabelecimento de uma situação de estresse oxidativo, que por sua vez, através da ação de agentes oxidantes, pode agir sobre e alterar a estrutura da chaperona, oxidando resíduos específicos, tornando-a inativa, incapaz de exercer os efeitos modulatórios sobre as células do sistema imunológico. Dessa forma, no momento em que for necessário cessar os estímulos e instaurar a fase de resolução de um processo patológico (ou inflamatório), a HSP70, por se encontrar oxidada, é incapaz de tal ação. A **figura 4** mostra um resumo gráfico dos resultados e sua discussão.

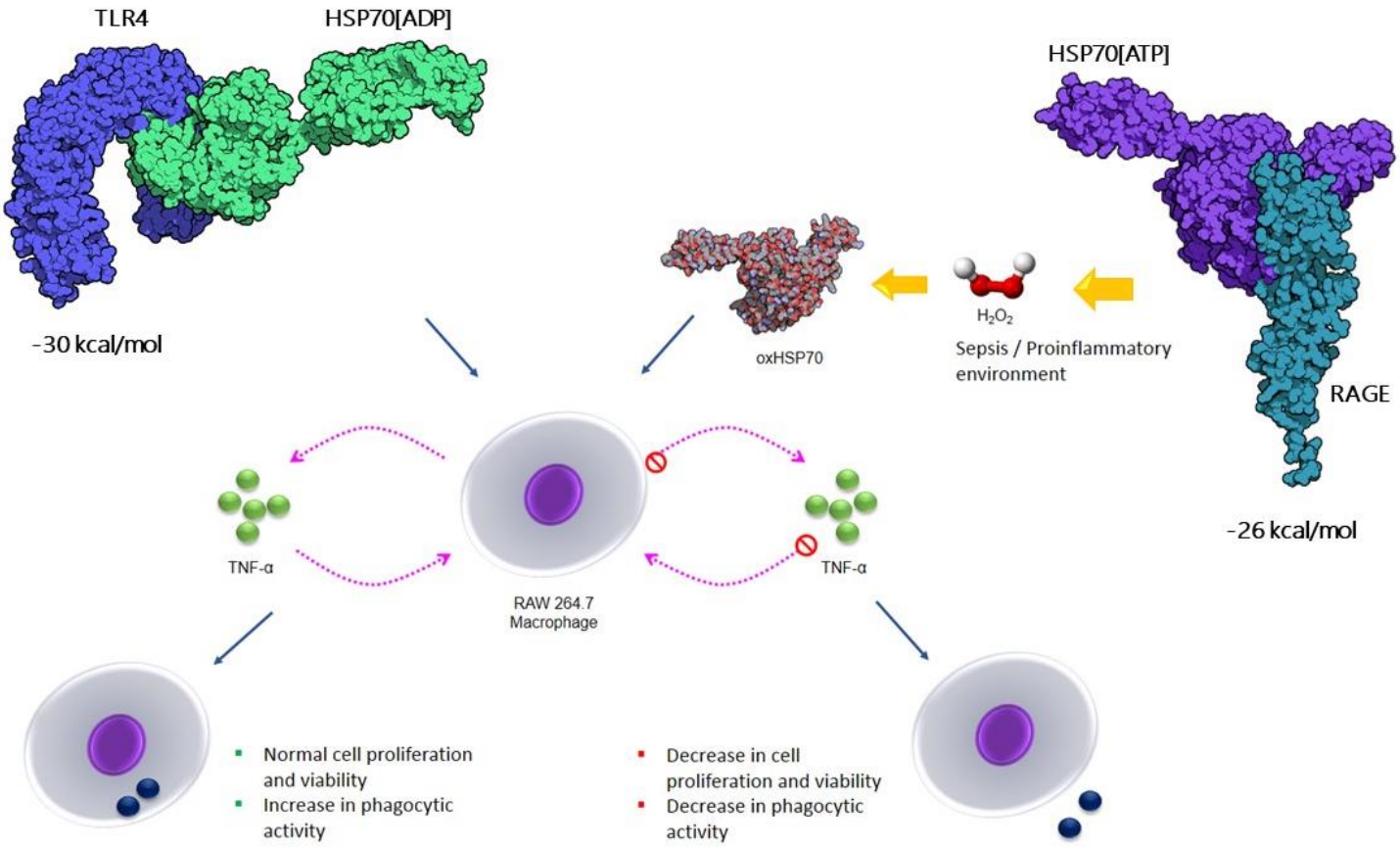

Figura 4. Resumo gráfico das diferentes interações da HSP70 de acordo com sua conformação e estado REDOX

5. Conclusões

Os resultados dispostos nessa dissertação foram publicados em revistas científicas internacionais (capítulo 1 e 2) ou encontram-se em processo de escrita para futura submissão (capítulos 3).

Podemos sumarizar o corpo de resultados encontrados em:

i). Caracterizamos algumas das possíveis modificações estruturais decorrentes da oxidação da HSP70 em ambiente extracelular;

ii). Observamos diferentes efeitos modulatórios da HSP70 extracelular oxidada sobre a ativação de macrófagos RAW 264.7;

iii). Visualizamos e quantificamos a interação da proteína HSP70 em sua conformação ligada à ADP e à ATP com o receptor dos produtos finais de glicação avançada – RAGE;

iv). Com a utilização de ferramentas de *docking* molecular e análise de modos normais, foi possível caracterizarmos um modelo putativo para a interação HSP70 e RAGE;

vi). Através de *docking* molecular e uma série de experimentos de mutações sítio dirigidas *in silico*, caracterizamos a interação de HSP70 em sua conformação ligada à ADP e à ATP com o receptor TLR4.

6. Perspectivas

(i). Caracterizar a cinética de interação entre a proteína HSP70 e o receptor RAGE através de ressonância plasmônica de superfície**;**

(ii). Caracterizar a cinética de interação entre a proteína HSP70 e o receptor TLR4 através de ressonância plasmônica de superfície**;**

(iii). Comparar os dados de cinética de interação e definir em quais conformações a proteína HSP70 apresenta maior constante de associação e afinidade de ligação;

(iv). Caracterizar extensivamente os complexos obtidos por docking molecular HSP70-RAGE e HSP70-TLR4 através de simulações de dinâmica molecular ou de análise de modos normais;

(v). Caracterizar as formas REDOX da HSP70 através de espectrometria de massas e marcação de isótopos radioativos;

(vi). Obter as estruturas das formas REDOX da HSP70 e dos complexos HSP70-RAGE e HSP70-TLR4 por cristalografia de raios-x.

7. Referências

Andrades, M., C. Ritter, J. C. Moreira and F. Dal-Pizzol (2005). "Oxidative parameters differences during non-lethal and lethal sepsis development." J Surg Res **125**(1): 68-72.

Andrades, M. E., C. Ritter and F. Dal-Pizzol (2009). "The role of free radicals in sepsis development." Front Biosci (Elite Ed) **1**: 277-287.

Arnold-Schild, D., D. Hanau, D. Spehner, C. Schmid, H. G. Rammensee, H. de la Salle and H. Schild (1999). "Cutting edge: receptor-mediated endocytosis of heat shock proteins by professional antigen-presenting cells." J Immunol **162**(7): 3757-3760.

Asea, A. (2003). "Chaperokine-induced signal transduction pathways." Exerc Immunol Rev **9**: 25-33.

Asea, A. (2008). "Hsp70: a chaperokine." Novartis Found Symp **291**: 173-179; discussion 179-183, 221-174.

Asea, A., E. Kabingu, M. A. Stevenson and S. K. Calderwood (2000). "HSP70 peptidembearing and peptide-negative preparations act as chaperokines." Cell Stress Chaperones **5**(5): 425-431.

Asea, A., S. K. Kraeft, E. A. Kurt-Jones, M. A. Stevenson, L. B. Chen, R. W. Finberg, G. C. Koo and S. K. Calderwood (2000). "HSP70 stimulates cytokine production through a CD14-dependant pathway, demonstrating its dual role as a chaperone and cytokine." Nature medicine **6**: 435-442.

Asea, A., M. Rehli, E. Kabingu, J. A. Boch, O. Bare, P. E. Auron, M. A. Stevenson and S. K. Calderwood (2002). "Novel signal transduction pathway utilized by extracellular HSP70: role of toll-like receptor (TLR) 2 and TLR4." J Biol Chem **277**(17): 15028-15034.

Becker, T. (2002). "CD40, an extracellular receptor for binding and uptake of Hsp70-peptide complexes." The Journal of Cell Biology **158**(7): 1277-1285.

Berger, M. M. and R. L. Chiolero (2007). "Antioxidant supplementation in sepsis and systemic inflammatory response syndrome." Crit Care Med **35**(9 Suppl): S584-590.

Bruemmer-Smith, S., F. Stuber and S. Schroeder (2001). "Protective functions of intracellular heat-shock protein (HSP) 70-expression in patients with severe sepsis." Intensive Care Med **27**(12): 1835-1841.

Bucciarelli, L. G., T. Wendt, L. Rong, E. Lalla, M. A. Hofmann, M. T. Goova, A. Taguchi, S. F. Yan, S. D. Yan, D. M. Stern and A. M. Schmidt (2002). "RAGE is a multiligand receptor of the immunoglobulin superfamily: implications for homeostasis and chronic disease." Cell Mol Life Sci **59**(7): 1117-1128.

Callahan, M. K., D. Chaillot, C. Jacquin, P. R. Clark and A. Menoret (2002). "Differential acquisition of antigenic peptides by Hsp70 and Hsc70 under oxidative conditions." J Biol Chem **277**(37): 33604-33609.

Campisi, J., T. H. Leem and M. Fleshner (2003). "Stress-induced extracellular Hsp72 is a functionally significant danger signal to the immune system." Cell Stress Chaperones **8**(3): 272-286.

Chen, T. and X. Cao (2010). "Stress for maintaining memory: HSP70 as a mobile messenger for innate and adaptive immunity." Eur J Immunol **40**(6): 1541-1544.

Conte, D., M. Holcik, C. A. Lefebvre, E. Lacasse, D. J. Picketts, K. E. Wright and R. G. Korneluk (2006). "Inhibitor of apoptosis protein cIAP2 is essential for lipopolysaccharide-induced macrophage survival." Mol Cell Biol **26**(2): 699-708.

Cumming, R. C., N. L. Andon, P. A. Haynes, M. Park, W. H. Fischer and D. Schubert (2004). "Protein disulfide bond formation in the cytoplasm during oxidative stress." J Biol Chem **279**(21): 21749-21758.

Delneste, Y., G. Magistrelli, J. Gauchat, J. Haeuw, J. Aubry, K. Nakamura, N. Kawakami-Honda, L. Goetsch, T. Sawamura, J. Bonnefoy and P. Jeannin (2002). "Involvement of LOX-1 in dendritic cell-mediated antigen cross-presentation." Immunity **17**(3): 353-362.

Febbraio, M. A., P. Ott, H. B. Nielsen, A. Steensberg, C. Keller, P. Krustrup, N. H. Secher and B. K. Pedersen (2002). "Exercise induces hepatosplanchnic release of heat shock protein 72 in humans." J Physiol **544**(Pt 3): 957-962.

Febbraio, M. A., A. Steensberg, R. Walsh, I. Koukoulas, G. van Hall, B. Saltin and B. K. Pedersen (2002). "Reduced glycogen availability is associated with an elevation in HSP72 in contracting human skeletal muscle." J Physiol **538**(Pt 3): 911-917.

Fehrenbach, E., A. M. Niess, K. Voelker, H. Northoff and F. C. Mooren (2005). "Exercise intensity and duration affect blood soluble HSP72." Int J Sports Med **26**(7): 552-557.

Fujiya, A., H. Nagasaki, Y. Seino, T. Okawa, J. Kato, A. Fukami, T. Himeno, E. Uenishi, S. Tsunekawa, H. Kamiya, J. Nakamura, Y. Oiso and Y. Hamada (2014). "The role of S100B in the interaction between adipocytes and macrophages." Obesity (Silver Spring) **22**(2): 371-379.

Galloway, E., T. Shin, N. Huber, T. Eismann, S. Kuboki, R. Schuster, J. Blanchard, H. R. Wong and A. B. Lentsch (2008). "Activation of hepatocytes by extracellular heat shock protein 72." Am J Physiol Cell Physiol **295**(2): C514-520.

Gelain, D. P., M. A. de Bittencourt Pasquali, M. C. C, M. S. Grunwald, C. Ritter, C. D. Tomasi, S. C. Alves, J. Quevedo, F. Dal-Pizzol and J. C. Moreira (2011). "Serum heat shock protein 70 levels, oxidant status, and mortality in sepsis." Shock **35**(5): 466-470.

Gross, C., E. Holler, S. Stangl, A. Dickinson, A. G. Pockley, A. A. Asea, N. Mallappa and G. Multhoff (2008). "An Hsp70 peptide initiates NK cell killing of leukemic blasts after stem cell transplantation." Leuk Res **32**(4): 527-534.

Gross, C., I. G. Schmidt-Wolf, S. Nagaraj, R. Gastpar, J. Ellwart, L. A. Kunz-Schughart and G. Multhoff (2003). "Heat shock protein 70-reactivity is associated with increased cell surface density of CD94/CD56 on primary natural killer cells." Cell Stress Chaperones **8**(4): 348-360.

He, H., C. Chen, Y. Xie, A. Asea and S. K. Calderwood (2000). "HSP70 and heat shock factor 1 cooperate to repress Ras-induced transcriptional activation of the c-fos gene." Cell Stress Chaperones **5**(5): 406-411.

Johnson, J. D. and M. Fleshner (2006). "Releasing signals, secretory pathways, and immune function of endogenous extracellular heat shock protein 72." J Leukoc Biol **79**(3): 425-434.

Kindas-Mugge, I., A. H. Hammerle, I. Frohlich, C. Oismuller, M. Micksche and F. Trautinger (1993). "Granulocytes of critically ill patients spontaneously express the 72 kD heat shock protein." Circ Shock **39**(4): 247-252.

Kindas-Mugge, I., W. R. Pohl, E. Zavadova, H. D. Kohn, S. Fitzal, F. Kummer and M. Micksche (1996). "Alveolar macrophages of patients with adult respiratory distress syndrome express high levels of heat shock protein 72 mRNA." Shock **5**(3): 184-189.

Lancaster, G. I., K. Moller, B. Nielsen, N. H. Secher, M. A. Febbraio and L. Nybo (2004). "Exercise induces the release of heat shock protein 72 from the human brain in vivo." Cell Stress Chaperones **9**(3): 276-280.

Lombardo, E., A. Alvarez-Barrientos, B. Maroto, L. Bosca and U. G. Knaus (2007). "TLR4-mediated survival of macrophages is MyD88 dependent and requires TNF-alpha autocrine signalling." J Immunol **178**(6): 3731-3739.

Luong, M., Y. Zhang, T. Chamberlain, T. Zhou, J. F. Wright, K. Dower and J. P. Hall (2012). "Stimulation of TLR4 by recombinant HSP70 requires structural integrity of the HSP70 protein itself." J Inflamm (Lond) **9**: 11.

Ma, W., V. Rai, B. I. Hudson, F. Song, A. M. Schmidt and G. R. Barile (2012). "RAGE binds C1q and enhances C1q-mediated phagocytosis." Cell Immunol **274**(1-2): 72-82.

Matzinger, P. (2002). "The danger model: a renewed sense of self." Science **296**(5566): 301-305.

Millar, D. G., K. M. Garza, B. Odermatt, A. R. Elford, N. Ono, Z. Li and P. S. Ohashi (2003). "Hsp70 promotes antigen-presenting cell function and converts T-cell tolerance to autoimmunity in vivo." Nat Med **9**(12): 1469-1476.

Musiani, F. and S. Ciurli (2015). "Evolution of Macromolecular *docking* Techniques: The Case Study of Nickel and Iron Metabolism in Pathogenic Bacteria." Molecules **20**(8): 14265-14292.

Ortega, E., E. Giraldo, M. D. Hinchado, M. Martinez, S. Ibanez, A. Cidoncha, M. E. Collazos and J. J. Garcia (2006). "Role of Hsp72 and norepinephrine in the moderate exercise-induced stimulation of neutrophils' microbicide capacity." Eur J Appl Physiol **98**(3): 250-255.

Ortega, E., M. D. Hinchado, L. Martin-Cordero and A. Asea (2009). "The effect of stress-inducible extracellular Hsp72 on human neutrophil chemotaxis: a role during acute intense exercise." Stress **12**(3): 240-249.

Park, H., H. Lee and C. Seok (2015). "High-resolution protein-protein *docking* by global optimization: recent advances and future challenges." Curr Opin Struct Biol **35**: 24-31.

Peck, G., M. Andrades, R. Lorenzi, M. da Costa, F. Petronilho, J. C. Moreira, F. Dal-Pizzol and C. Ritter (2009). "Serum-induced macrophage activation is related to the severity of septic shock." Inflamm Res **58**(2): 89-93.

Ribeiro, S. P., J. Villar, G. P. Downey, J. D. Edelson and A. S. Slutsky (1994). "Sodium arsenite induces heat shock protein-72 kilodalton expression in the lungs and protects rats against sepsis." Crit Care Med **22**(6): 922-929.

Rinaldi, S., F. Landucci and A. R. De Gaudio (2009). "Antioxidant therapy in critically septic patients." Curr Drug Targets **10**(9): 872-880.

Ritossa, F. (1962). "A new puffing pattern induced by temperature shock and DNP in drosophila." Experientia **18**(12): 571 - 573.

Ruan, B. H., X. Li, A. R. Winkler, K. M. Cunningham, J. Kuai, R. M. Greco, K. H. Nocka, L. J. Fitz, J. F. Wright, D. D. Pittman, X. Y. Tan, J. E. Paulsen, L. L. Lin and D. G. Winkler (2010). "Complement C3a, CpG oligos, and DNA/C3a complex stimulate IFN-alpha production in a receptor for advanced glycation end product-dependent manner." J Immunol **185**(7): 4213-4222.

Ryan, A. J., S. W. Flanagan, P. L. Moseley and C. V. Gisolfi (1992). "Acute heat stress protects rats against endotoxin shock." J Appl Physiol (1985) **73**(4): 1517-1522.

Schmidt, A. M., M. Hofmann, A. Taguchi, S. D. Yan and D. M. Stern (2000). "RAGE: a multiligand receptor contributing to the cellular response in diabetic vasculopathy and inflammation." Semin Thromb Hemost **26**(5): 485-493.

Sherman, M. and G. Multhoff (2007). "Heat shock proteins in cancer." Ann N Y Acad Sci **1113**: 192-201.
Sousa, R. (2012). "A dancer caught midstep: the structure of ATP-bound Hsp70." Mol Cell **48**(6): 821-823.

Srivastava, P. (2002). "Interaction of heat shock proteins with peptides and antigen presenting cells: chaperoning of the innate and adaptive immune responses." Annu Rev Immunol **20**: 395-425.

Tang, D., M. T. Loze, H. J. Zeh and R. Kang (2010). "The redox protein HMGB1 regulates cell death and survival in cancer treatment." Autophagy **6**(8): 1181-1183.

Tsan, M. F. and B. Gao (2009). "Heat shock proteins and immune system." J Leukoc Biol **85**(6): 905-910.

Vega, V. L., M. Rodriguez-Silva, T. Frey, M. Gehrmann, J. C. Diaz, C. Steinem, G. Multhoff, N. Arispe and A. De Maio (2008). "Hsp70 translocates into the plasma membrane after stress and is released into the extracellular environment in a membrane-associated form that activates macrophages." J Immunol **180**(6): 4299-4307.

Venereau, E., M. Casalgrandi, M. Schiraldi, D. J. Antoine, A. Cattaneo, F. De Marchis, J. Liu, A. Antonelli, A. Preti, L. Raeli, S. S. Shams, H. Yang, L. Varani, U. Andersson, K. J. Tracey, A. Bachi, M. Uguccioni and M. E. Bianchi (2012). "Mutually exclusive redox forms of HMGB1 promote cell recruitment or proinflammatory cytokine release." J Exp Med **209**(9): 1519-1528.

Villar, J., J. D. Edelson, M. Post, J. B. Mullen and A. S. Slutsky (1993). "Induction of heat stress proteins is associated with decreased mortality in an animal model of acute lung injury." Am Rev Respir Dis **147**(1): 177-181.

Walsh, R. C., I. Koukoulas, A. Garnham, P. L. Moseley, M. Hargreaves and M. A. Febbraio (2001). "Exercise increases serum Hsp72 in humans." Cell Stress Chaperones **6**(4): 386-393.

Wong, H. R., I. Y. Menendez, M. A. Ryan, A. G. Denenberg and J. R. Wispe (1998). "Increased expression of heat shock protein-70 protects A549 cells against hyperoxia." Am J Physiol **275**(4 Pt 1): L836-841.

Wong, H. R., M. Ryan, I. Y. Menendez, A. Denenberg and J. R. Wispe (1997). "Heat shock protein induction protects human respiratory epithelium against nitric oxide-mediated cytotoxicity." Shock **8**(3): 213-218.

Yang, Y. L. and M. T. Lin (1999). "Heat shock protein expression protects against cerebral ischemia and monoamine overload in rat heatstroke." Am J Physiol **276**(6 Pt 2): H1961-1967.

8. Anexo I

SHOCK, Vol. 35, No. 5, pp. 466–470, 2011

SERUM HEAT SHOCK PROTEIN 70 LEVELS, OXIDANT STATUS, AND MORTALITY IN SEPSIS

Daniel Pens Gelain,* Matheus Augusto de Bittencourt Pasquali,* Clarissa M. Comim,† Marcelo Sartori Grunwald,* Cristiane Ritter,† Cristiane Damiani Tomasi,† Sarah Cascaes Alves,† Joao Quevedo,† Felipe Dal-Pizzol,† and José Cláudio Fonseca Moreira*

**Centro de Estudos em Estresse Oxidativo, Departamento de Bioquímica, Instituto de Ciências Básicas da Saúde, Universidade Federal do Rio Grande do Sul, Porto Alegre, Rio Grande do Sul; and †Laboratory of Experimental Physiopathology and National Institute of Translational Science and Technology in Medicine, Posgraduation Program in Programa de Pós-Graduação em Ciências da Saúde, Unidade Acadêmica de Ciências da Saúde, Universidade do Extremo Sul Catarinense, Criciúma, Santa Catarina, Brazil*

Received 15 Dec 2010; first review completed 3 Jan 2011; accepted in final form 5 Jan 2011

ABSTRACT—Animal studies as well as prospective randomized clinical trials associated sepsis with redox imbalance and oxidative stress, but other studies failed to establish a correlation between antioxidant-based therapies and improvement of sepsis condition. This is also true for studies on the role of the chaperone heat shock protein 70 (HSP70), which is increased in serum during sepsis. Heat shock protein 70 is affected at several levels by oxidative stress, but this relationship has never been studied in sepsis. Here, we evaluated the relationship between serum HSP70 immunocontent and oxidant status in sepsis. Patients with severe sepsis were followed up for 28 days after diagnosis, or until death. Up to a maximum of 12 h after sepsis diagnosis, serum was collected for determination of HSP70 immunocontent by Western blot and evaluation of oxidative parameters (TRAP [total radical-trapping antioxidant parameter], TBARSs [thiobarbituric acid–reactive substances], and carbonyl levels). Serum of sepsis patients presented enhanced HSP70 levels. Analysis of oxidative parameters revealed that septic patients with pronounced oxidative damage in serum had also increased HSP70 serum levels. Sepsis patients in whom serum oxidative stress markers were not different from control presented normal serum HSP70. Analysis of septic patients according to survival outcome also indicated that patients with increased HSP70 serum levels presented increased mortality. We concluded that serum HSP70 levels are modulated according to the patient oxidant status, and increased serum HSP70 is associated to mortality in sepsis.

KEYWORDS—Sepsis, oxidative stress, HSP70, serum

INTRODUCTION

Sepsis is an inflammation-induced syndrome resulting from a complex interaction between host and infectious agents. Sepsis is considered severe when associated with acute organ dysfunction, which accounts for the main cause underlying sepsis-induced death. Severe sepsis has become a leading cause of mortality in critical illness and a major public health burden throughout the world (1). The rate of severe sepsis ranges between 6% and 14% among critical-care admissions, with a hospital mortality rate between 27% and 59% (2).

Heat shock proteins (HSPs) are upregulated in cells subjected to stressful stimuli, including inflammation and oxidative stress (3). Upregulation of intracellular HSP results in protective effects against hypoxia, excess oxygen radicals, endotoxin, infections, and fever (4). This cytoprotective effect is attributed to their ability to stabilize protein structures through chaperone-like reversible interactions (5). Heat shock protein 70, a 70-kd member of the HSP superfamily, has been recently observed to exert extracellular effects in cells of the immune system (6–8). In humans, serum HSP70 is associated to stress conditions as inflammation, bacterial or viral infections, and oncological diseases (9). However, very little is known on the role and function of extracellular HSP70.

Sepsis has been associated with redox imbalance and oxidative stress (10). Animal studies as well as prospective randomized clinical trials have been providing increasing evidence in support of antioxidant therapies in sepsis (11, 12). Some studies, however, failed to establish a correlation between antioxidant-based therapies and improvement of sepsis condition (13). Previous works attempted to establish a correlation with either HSP70 or oxidative stress with sepsis, but there are no works studying the relationship between both parameters in sepsis. Here, we studied the relation between oxidative stress and modulation of HSP70 in the serum of septic patients and aimed to establish an association with clinical outcome.

METHODS

Subjects and serum samples

This study was approved by the local ethics committee. Fifteen patients admitted to a general intensive care unit with severe sepsis according to the Consensus Conference of the American College of Chest Physicians and Society of Critical Care Medicine (1992), 18 years or older, without chronic hepatic or renal insufficiency, without cancer or immunodeficiency, were included in the study. These patients were followed up for 28 days after sepsis diagnosis or until death. Up to a maximum of 12 h after sepsis diagnosis, blood was drawn into dry tubes, and the serum was stored at −80°C until the

Address reprint requests to Daniel Pens Gelain, PhD, Rua Ramiro Barcelos, 2600-anexo, CEP 90035-003, Porto Alegre, RS, Brazil. E-mail: dgelain@yahoo.com.br.

D.P.G., M.A.B.P., and C.C. contributed equally to this work.

This research was supported by grants from the following Brazilian funding agencies/programs: Rede de Estudos em Sepse PROCAD/CAPES #066/2007, Conselho Nacional de Desenvolvimento Científico e Tecnológico (J.C.F.M., J.Q., and F.D.-P.), UNESC (J.Q. and F.D.-P.), UFRGS (J.C.F.M.), and IBN-Net #01.06.0842-00 (all authors). J.C.F.M., J.Q., and F.D.-P. are CNPq research fellows. C.M.C. is holder of a CNPq studentship.

DOI: 10.1097/SHK.0b013e31820fe704

determination of HSP70 and oxidative parameters. All patients' data and analyses were obtained under informed consent before their inclusion in the study. The group of sepsis had eight patients with severe sepsis and seven with septic shock. The origin of infection was pneumonia in eight patients, intra-abdominal infection in five patients, pyelonephritis in one patient, and catheter-related infection in one patient. The control group consisted of 24 normal, healthy subjects (15 males, 9 females; aged 45 ± 18 years) in whom blood was collected for routine checkups.

Heat shock protein 70

Heat shock protein 70 serum detection was performed by Western blot analysis using a mouse monoclonal anti-HSP70 (Sigma, St Louis, Mo) at 1:1,000 dilution range and anti–mouse immunoglobulin G peroxidase-linked secondary antibody (1:5,000 dilution range) suitable for enhanced chemiluminescence detection (ECL Plus kit, Rockford, Ill). Densitometric analysis of the films was performed with ImageQuant software. Blots were developed to be linear in the range used for densitometry.

Oxidative stress parameters

Nonenzymatic antioxidant potential of serum samples was determined by the total radical-trapping antioxidant parameter (TRAP) assay (14). Serum lipoperoxidation levels were estimated by quantifying levels of thiobarbituric acid–reactive substances (TBARSs) (15), whereas the oxidative damage to serum proteins was assessed by the determination of carbonyl group levels in samples through reaction with dinitrophenylhydrazine (16).

Statistical analysis

The results are expressed as means ± SE; differences among multiple groups were compared by one-way ANOVA followed by Tukey post hoc test. Statistical significance was assigned to $P < 0.05$.

RESULTS

The group of sepsis had eight patients with severe sepsis and seven with septic shock. The origin of infection was pneumonia in eight patients, intra-abdominal infection in five patients, pyelonephritis in one patient, and catheter-related infection in one patient. In Table 1, we show age, Acute Physiology andM Chronic Health Evaluation II (APACHE II), Sequential Organ Failure Assessment (SOFA) D1, and SOFA D3 scores of survivor and nonsurvivor patients. These patients presented altered values for oxidative parameters in serum. As depicted in Table 2, TRAP assay indicated an increase in nonenzymatic antioxidant reactivity in serum, whereas TBARSs and carbonyl assays showed increased lipoperoxidation and protein oxidative damage in septic serum. To better understand this apparent divergence between TRAP and TBARSs/carbonyl results, we analyzed the results from each patient individually. Total radical-trapping antioxidant parameter results indicated the existence of two subgroups of septic patients according to the oxidant status in serum; eight patients had antioxidant TRAP values in relation to control subjects, with a mean significantly below control (15.71%), whereas seven patients presented pro-oxidant TRAP values, with a mean significantly greater than control (138.11%). Thiobarbituric acid–reactive substance and carbonyl levels were also decreased in patients with antioxidant TRAP values, whereas the group of patients with pro-oxidant status of TRAP presented significant increases in both parameters, which reinforced the indication that sepsis patients may present two distinct profiles of oxidant status. Figure 1 shows the dual distribution of TRAP values of serum from septic patients in relation to control; individual values greater than control

TABLE 1. **APACHE II, SOFA D1, and SOFA D3 scores of sepsis patients**

	Patients	
	Nonsurvivors	Survivors
Age, y	57.4 (14.6)	58.4 (17.9)
APACHE II	15.2 (8.4)*	11.2 (7.1)
SOFA D1	3.2 (1.3)	1.9 (1.1)*
SOFA D3	2.6 (2.4)	(1.4)*

Values are presented as mean (SD).
*Significant differences (one-way ANOVA followed by Newman-Keuls post hoc, $P < 0.05$).

TABLE 2. **Serum oxidative parameters of sepsis patients**

	TRAP, % control	TBARSs, nmol/mg protein	Carbonyl, nmol/mg protein
Control (n = 24)	100 ± 1.92	0.145 ± 0.003	1.35 ± 0.28
Sepsis (n = 15)	72.86 ± 16.81*	0.394 ± 0.050†	3.14 ± 0.38‡
Antioxidant (n = 8)	15.71 ± 3.11§	0.233 ± 0.053‡	2.02 ± 0.28
Pro-oxidant (n = 7)	138.11 ± 8.34‡	0.588 ± 0.041‖	4.43 ± 0.32‡
Survivors (n = 8)	48.12 ± 21.01*	0.340 ± 0.020†	2.40 ± 1.66
Nonsurvivors (n = 7)	106.14 ± 23.65	0.280 ± 0.011‡	3.40 ± 2.20‡

Serum samples from 24 healthy subjects (control) and 15 sepsis patients were used to measure the nonenzymatic antioxidant potential by TRAP analysis, lipoperoxidation by TBARS quantification, and protein damage by carbonyl quantification. The values depicted for TRAP represent the chemiluminescence induced by the free radical generator AAPH in the samples (converted to % of control) and were normalized by the protein content of the sample. Thiobarbituric acid–reactive substances and carbonyl serum levels were quantified in the same samples. Antioxidant, pro-oxidant, survivors, and nonsurvivors groups refer to different subsets of the group of sepsis patients. Control group consisted of 24 normal, healthy subjects (15 males, 9 females, aged 45 ± 18 years).
Values represent mean ± SEM.
*Lower than control.
†Higher than ‡group.
‡Higher than control.
§Lower than *group.
‖Higher than †group (one-way ANOVA followed by Newman-Keuls post hoc, $P < 0.05$).

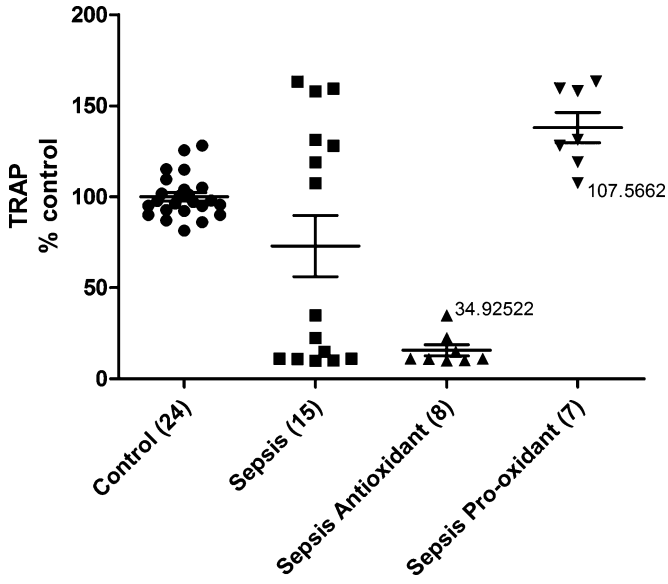

FIG. 1. **Total radical-trapping antioxidant parameter values of serum samples from septic patients**. Distribution of individual TRAP values of control and sepsis patients shown in Table 2 with the subgroups of antioxidant and pro-oxidant sepsis patients with respective cutoff values. Control group consisted of 24 normal, healthy subjects (15 males, 9 females, aged 45 ± 18 years).

TABLE 3. **APACHE II, SOFA D1, SOFA D3 scores, and type and origin of sepsis at the pro-oxidant and antioxidant groups of patients**

	Patients	
	Pro-oxidant	Antioxidant
Age, mean (SD), y	57.2 (13.9)	57.9 (20.1)
APACHE II, mean (SD)	13.8 (9.2)	12.1 (8.7)
SOFA D1, mean (SD)	3.1 (2.0)	2.2 (1.5)
SOFA D3, mean (SD)	2.6 (2.3)	1.9 (1.4)
Severe sepsis, no. patients	3	5
Septic shock, no. patients	4	3
Pneumonia, no. patients	5	3
Intra-abdominal infection, no. patients	2	3
Pyelonephritis, no. patients	0	1
Catheter-related infection, no. patients	1	0

Values represent mean (SD) for APACHE II, SOFA D1, and SOFA D3 scores, and number of patients for type of sepsis and origin of infection. No significant differences were detected among groups.

(100%) were grouped as pro-oxidant sepsis, whereas values less than control were grouped as antioxidant sepsis. We plotted in Table 3 APACHE II, SOFA D1, and SOFA D3 scores for pro-oxidant and antioxidant groups of sepsis patients, along with origin of infection.

We next analyzed the serum immunocontent of HSP70 of septic patients, and we observed significant increased values for serum HSP70 immunocontent compared with control (Fig. 2A). Considering the well-known relationship between oxidative stress and induction of HSP70 expression, we plotted the values for serum HSP70 immunocontent of septic patients according to their TRAP-based antioxidant or pro-oxidant serum status. Interestingly, we observed a very distinct pattern for serum HSP70 immunocontent between antioxidant and pro-oxidant patients. The subgroup of septic antioxidant patients presented serum HSP70 levels not different from those of control subjects, whereas the subgroup of septic pro-oxidant patients had 30-fold increased serum HSP70 compared with control. Altogether, these data indicate a relationship among serum oxidant status and modulation of extracellular HSP70 in sepsis patients.

Oxidative stress parameters and HSP70 levels in serum were also analyzed according to the survival outcome of septic patients, to identify a possible relationship between sepsis severity and oxidant-dependent modulation of extracellular HSP70. Compared with control, sepsis survivors had a small decrease in TRAP values, whereas nonsurvivors presented a small although significant increase (Table 2). Thiobarbituric acid–reactive substance levels were increased in both survivors and nonsurvivors, whereas carbonyl levels were increased only in nonsurvivor patients. Serum HSP70 immunocontent was also significantly increased in nonsurvivor patients (Fig. 2B). Altogether, these results suggest that serum HSP70 levels in sepsis patients are related to serum oxidant status and that oxidative stress and increased HSP70 in serum may be also related to sepsis severity and outcome.

DISCUSSION

The molecular mechanisms underlying sepsis are complex and relate different levels of metabolic and signal coordination; for such reason, comprehensive studies relating different aspects of sepsis-induced perturbations at cellular and molecular levels are more urged than ever. This is evidenced by the differential outcomes of biochemical studies focusing on isolated aspects of sepsis molecular mechanisms. For instance, many animal studies as well as prospective randomized clinical trials associated sepsis with redox imbalance and oxidative stress, but other studies failed to establish a correlation between antioxidant-based therapies and improvement of sepsis condition (11, 17, 18). This is also true for studies on the role of HSP70 in sepsis. Animal and cellular models corroborated the existence of a relationship between HSP70 and sepsis, but clinical observations failed to establish a direct correlation between HSP70 modulation and protection against septic shock (19).

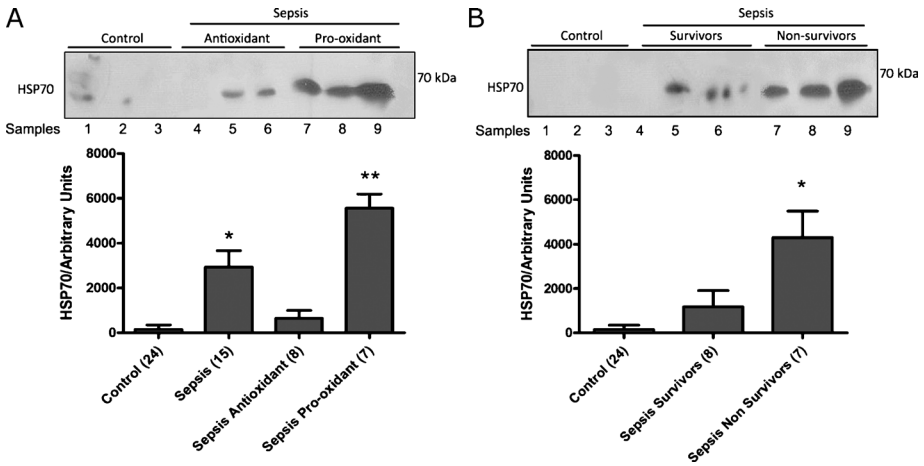

FIG. 2. **Representative immunoblots of HSP70 immunocontent of serum samples from sepsis patients**. A, Heat shock protein70 gel immunoblot showing three representative samples of control subjects and six of sepsis patients (three from antioxidant patients and three from pro-oxidant patients). Bars represent mean ± SEM of all patients; samples contained equal amounts of protein. B, Representative gel showing HSP70 immunoblots of control patients (three samples), sepsis survivors (three samples), and sepsis nonsurvivors (three samples). The graph shows replotted HSP70 mean ± SEM according to survival outcome. *Different from control, $P < 0.05$; **different from control ($P < 0.001$) and from *group ($P < 0.05$) according to one-way ANOVA followed by Newman-Keuls post hoc, $P < 0.05$.

There is a more or less generalized effort to establish a correlation among increased HSP70 expression and protection against septic shock in the literature, probably because of the usual cytoprotective effects of this protein. So far, most works focused on modulation of intracellular HSP70 in blood cells (19–22), but the outcomes are controversial. Results of different works suggest that an attenuation of cytokine liberation caused by inducible HSP70 expression could have beneficial effects in cases of systemic inflammation (19). On the other hand, cellular levels of HSP70 were shown to be markedly decreased in critically ill patients of sepsis (21). A potential role for extracellular HSP70 in sepsis and other conditions has been addressed only recently, and results are still scarce. In children with septic shock, a significant increase in serum HSP70 levels was reported (23), and similar observations were made earlier with patients from severe trauma (24, 25). Administration of exogenous HSP70 was observed to protect rats from endotoxic shock and modify the response of myeloid cells to lipopolysaccharide (26), but a role for extracellular HSP70 in clinical sepsis has not been established yet.

Our group has been studying the role of oxidative stress in sepsis, and we believe that redox signaling exerts an important influence in the regulation of sepsis response. Our data confirmed that sepsis patients have increased serum levels of HSP70. But, most interestingly, we also observed here that serum HSP70 is modulated according to the serum oxidant status, which vary among different patients. Based on the analysis of serum oxidative stress parameters (TRAP, lipid peroxidation, and protein carbonyl levels), septic patients may be classified into two opposite phenotypes, one presenting a general antioxidant profile and the other being pro-oxidant. This is an important observation as many biochemical parameters with clinical relevance may be subjected to oxidant-dependent regulatory processes, which could lead one to data misinterpretation when analyzing sepsis patients as a homogenous group. To our knowledge, the correlation between HSP70 levels and sepsis has never been studied based on oxidative parameters.

Heat shock protein 70 levels in different organs, cells, and fluids may undergo several types of regulation, which may include active release to extracellular medium in response to different mechanisms (27). In sepsis, it is possible that increased HSP70 levels are a result of cytokine action stimulating gene expression in blood cells and that the extent of oxidative stress may contribute to serum HSP70 levels modulation by causing HSP70 active secretion or lytic release by necrotic cell death. This might also explain the different observations reported by studies correlating HSP70 expression in different tissues or cells and sepsis outcome. Sepsis affects many physiological processes and the function of different organs to an extent that varies according to the origin of sepsis, severity, and history of each patient. Because oxidative stress and HSP70 expression, activation, and release are also affected and modulated at several degrees by infection, inflammation, water deprivation, and oxygen supply, it is not surprising that HSP70 release is regulated according to the oxidant status during sepsis.

Diverse mechanisms may account for the modulation of extracellular levels of HSP70. Physiologically, necrotic cell lysis from injury or infection is known to release HSPs into the extracellular compartment where they activate antigen-presenting cell–mediated defense (28). Active release of HSP70 to the extracellular environment was also observed in different cells, via exosomal export originated from trans-Golgi and endoplasmic reticulum–derived vesicles (29). Once at the extracellular space, HSP70 is believed to act as an immunostimulatory signal, as it was reported to activate Toll-like receptors 2 and 4 (7). Besides, a plethora of immune responses was reported to follow HSP70 immunostimulation, such as increased release of TNF-α, IL-1β, IL-6, IL-12, granulocyte-macrophage colony-stimulating factor, nitric oxide, macrophage inflammatory protein 1, monocyte chemotactic protein 1, and RANTES (6). Most of these data were acquired with the inducible isoform of HSP70 (i.e., HSP72), and it is believed that this is the predominant isoform in active release to the extracellular space (29). Here, we used a pan-HSP70 antibody that detects both the constitutive (HSP73) and the inducible isoforms, which contribute to the total pool of extracellular HSP70.

The patient's oxidant status may influence both HSP70 modulation during sepsis and its activity toward immune system regulation, which could account for many of the differences in the outcome of such patients. This could also explain why different works present different correlations between serum or plasma HSP70 levels and sepsis outcome. It is possible that variations in individual antioxidant defense systems (enzymes plus nonenzymatic antioxidants at cellular and systemic levels) may account to the differences in serum HSP70 levels and that combination of oxidative stress and extracellular HSP70 action is responsible for various deleterious effects observed in the course of sepsis. However, oxidative stress may not be the sole factor influencing HSP70 expression, activity, and release. Differences in sepsis outcome possibly related to HSP70 function and oxidative stress may also reflect differences in such other factors.

In conclusion, we report that serum HSP70 levels are modulated according to the oxidant status during sepsis, and increased serum HSP70 seems to be also associated to mortality. Although serum oxidative stress was observed to be correlated to HSP70 modulation, markers of oxidant damage in serum (i.e., TRAP, TBARSs, and carbonyl levels) showed variable degrees of association to sepsis outcome.

REFERENCES

1. Sands KE, Bates DW, Lanken PN, Graman PS, Hibberd PL, Kahn KL, Parsonnet J, Panzer R, Orav EJ, Snydman DR, et al.: Epidemiology of sepsis syndrome in 8 academic medical centers. *JAMA* 278:234–240, 1997.
2. Brun-Buisson C: The epidemiology of the systemic inflammatory response. *Intensive Care Med* 26(Suppl 1):S64–S74, 2000.
3. Ziegler TR, Ogden LG, Singleton KD, Luo M, Fernandez-Estivariz C, Griffith DP, Galloway JR, Wischmeyer PE: Parenteral glutamine increases serum heat shock protein 70 in critically ill patients. *Intensive Care Med* 31:1079–1086, 2005.
4. Tang D, Kang R, Xiao W, Wang H, Calderwood SK, Xiao X: The anti-inflammatory effects of heat shock protein 72 involve inhibition of high-mobility-group box 1 release and proinflammatory function in macrophages. *J Immunol* 179:1236–1244, 2007.
5. Ribeiro SP, Villar J, Downey GP, Edelson JD, Slutsky AS: Sodium arsenite induces heat shock protein-72 kilodalton expression in the lungs and protects rats against sepsis. *Crit Care Med* 22:922–929, 1994.

6. Asea A: Mechanisms of HSP72 release. *J Biosci* 32:579–584, 2007.
7. Asea A, Kraeft SK, Kurt-Jones EA, Stevenson MA, Chen LB, Finberg RW, Koo GC, Calderwood SK: HSP70 stimulates cytokine production through a CD14-dependant pathway, demonstrating its dual role as a chaperone and cytokine. *Nat Med* 6:435–442, 2000.
8. Asea A, Rehli M, Kabingu E, Boch JA, Bare O, Auron PE, Stevenson MA, Calderwood SK: Novel signal transduction pathway utilized by extracellular HSP70: role of Toll-like receptor (TLR) 2 and TLR4. *J Biol Chem* 277: 15028–15034, 2002.
9. Multhoff G: Heat shock protein 70 (HSP70): membrane location, export and immunological relevance. *Methods* 43:229–237, 2007.
10. Halliwell B, Gutteridge JMC: *Free Radicals in Biology and Medicine*. Oxford: Oxford University Press, 2007.
11. Andrades ME, Ritter C, Dal-Pizzol F: The role of free radicals in sepsis development. *Front Biosci (Elite Ed)* 1:277–287, 2009.
12. Dal-Pizzol F: Alternative activated macrophage: a new key for systemic inflammatory response syndrome and sepsis treatment? *Crit Care Med* 32: 1971–1972, 2004.
13. Dare AJ, Phillips AR, Hickey AJ, Mittal A, Loveday B, Thompson N, Windsor JA: A systematic review of experimental treatments for mitochondrial dysfunction in sepsis and multiple organ dysfunction syndrome. *Free Radic Biol Med* 47:1517–1525, 2009.
14. Silva EG, Behr GA, Zanotto-Filho A, Lorenzi R, Pasquali MA, Ravazolo LG, Bordignon CL Jr, Silva FA, Aboy AL, Bassani VL, et al.: Antioxidant activities and free radical scavenging potential of *Bauhinia microstachya* (RADDI) MACBR. (Caesalpinaceae) extracts linked to their polyphenol content. *Biol Pharm Bull* 30:1488–1496, 2007.
15. Draper HH, Hadley M: Malondialdehyde determination as index of lipid peroxidation. *Methods Enzymol* 186:421–431, 1990.
16. Levine RL, Garland D, Oliver CN, Amici A, Climent I, Lenz AG, Ahn BW, Shaltiel S, Stadtman ER: Determination of carbonyl content in oxidatively modified proteins. *Methods Enzymol* 186:464–478, 1990.
17. Rinaldi S, Landucci F, De Gaudio AR: Antioxidant therapy in critically septic patients. *Curr Drug Targets* 10:872–880, 2009.
18. Berger MM, Chiolero RL: Antioxidant supplementation in sepsis and systemic inflammatory response syndrome. *Crit Care Med* 35:S584–S590, 2007.
19. Bruemmer-Smith S, Stuber F, Schroeder S: Protective functions of intracellular heat-shock protein (HSP) 70-expression in patients with severe sepsis. *Intensive Care Med* 27:1835–1841, 2001.
20. Weiss YG, Bouwman A, Gehan B, Schears G, Raj N, Deutschman CS: Cecal ligation and double puncture impairs heat shock protein 70 (HSP-70) expression in the lungs of rats. *Shock* 13:19–23, 2000.
21. Schroeder S, Bischoff J, Lehmann LE, Hering R, von Spiegel T, Putensen C, Hoeft A, Stuber F: Endotoxin inhibits heat shock protein 70 (HSP70) expression in peripheral blood mononuclear cells of patients with severe sepsis. *Intensive Care Med* 25:52–57, 1999.
22. Hashiguchi N, Ogura H, Tanaka H, Koh T, Nakamori Y, Noborio M, Shiozaki T, Nishino M, Kuwagata Y, Shimazu T, et al.: Enhanced expression of heat shock proteins in activated polymorphonuclear leukocytes in patients with sepsis. *J Trauma* 51:1104–1109, 2001.
23. Wheeler DS, Fisher LE Jr, Catravas JD, Jacobs BR, Carcillo JA, Wong HR: Extracellular hsp70 levels in children with septic shock. *Pediatr Crit Care Med* 6:308–311, 2005.
24. Pittet JF, Lee H, Morabito D, Howard MB, Welch WJ, Mackersie RC: Serum levels of HSP72 measured early after trauma correlate with survival. *J Trauma* 52:611–617, discussion 617; 2002.
25. Pockley AG, Shepherd J, Corton JM: Detection of heat shock protein 70 (HSP70) and anti- HSP70 antibodies in the serum of normal individuals. *Immunol Invest* 27:367–377, 1998.
26. Rozhkova E, Yurinskaya M, Zatsepina O, Garbuz D, Karpov V, Surkov S, Murashev A, Ostrov V, Margulis B, Evgen'ev M, et al.: Exogenous mammalian extracellular HSP70 reduces endotoxin manifestations at the cellular and organism levels. *Ann N Y Acad Sci* 1197:94–107, 2010.
27. Kuo HT, Chen HW, Hsiao HH, Chen HC: Heat shock response protects human peritoneal mesothelial cells from dialysate-induced oxidative stress and mitochondrial injury. *Nephrol Dial Transplant* 24:1799–1809, 2009.
28. Basu S, Binder RJ, Suto R, Anderson KM, Srivastava PK: Necrotic but not apoptotic cell death releases heat shock proteins, which deliver a partial maturation signal to dendritic cells and activate the NF-kappa B pathway. *Int Immunol* 12:1539–1546, 2000.
29. Radons J, Multhoff G: Immunostimulatory functions of membrane-bound and exported heat shock protein 70. *Exerc Immunol Rev* 11:17–33, 2005.